Environmental Science & Technology
2024, Volume 58, Issue 1, Pages 207-218
https://doi.org/10.1021/acs.est.3c06684
https://archimer.ifremer.fr/doc/00868/98029/

Pearl Farming Micro-Nanoplastics Affect Oyster Physiology and Pearl Quality

Gardon Tony [1,*], Le Luyer Jeremy [1], Le Moullac Gilles [1], Soyez Claude [1], Lagarde Fabienne [2], Dehaut Alexandre [3], Paul-Pont Ika [4], Huvet Arnaud [4]

[1] Ifremer, ILM, IRD, University of French Polynesia, EIO, F-98719 Taravao, Tahiti, French Polynesia, France
[2] Institute of Molecules and Materials of Le Mans, IMMM−UMR CNRS 6283, University of Le Mans, Avenue Olivier Messiaen, 72085 Le Mans, France
[3] ANSES−LSA, Boulevard du Bassin Napoléon, 62200 Boulogne-sur-Mer, France
[4] University of Brest, Ifremer, CNRS, IRD, LEMAR, F-29280 Plouzané, France

* Corresponding author : Tony Gardon, email address : tony.gardon@ifremer.fr

Abstract :

Pearl farming is crucial for the economy of French Polynesia. However, rearing structures contribute significantly to plastic waste, and the widespread contamination of pearl farming lagoons by microplastics has raised concerns about risks to the pearl industry. This study aimed to evaluate the effects of micro-nanoplastics (MNPs, 0.4–200 μm) on the pearl oyster (Pinctada margaritifera) over a 5-month pearl production cycle by closely mimicking ecological scenarios. MNPs were produced from weathered plastic pearl farming gear and tested at environmentally relevant concentrations (0.025 and 1 μg L–1) to decipher biological and functional responses through integrative approaches. The significant findings highlighted the impacts of MNPs on oyster physiology and pearl quality, even at remarkably low concentrations. Exposure to MNPs induced changes in energy metabolism, predominantly driven by reduced assimilation efficiency of microalgae, leading to an alteration in gene expression patterns. A distinct gene expression module exhibited a strong correlation with physiological parameters affected by MNP conditions, identifying key genes as potential environmental indicators of nutritional-MNP stress in cultured oysters. The alteration in pearl biomineralization, evidenced by thinner aragonite crystals and the presence of abnormal biomineral concretions, known as keshi pearls, raises concerns about the potential long-term impact on the Polynesian pearl industry.

Graphical abstract

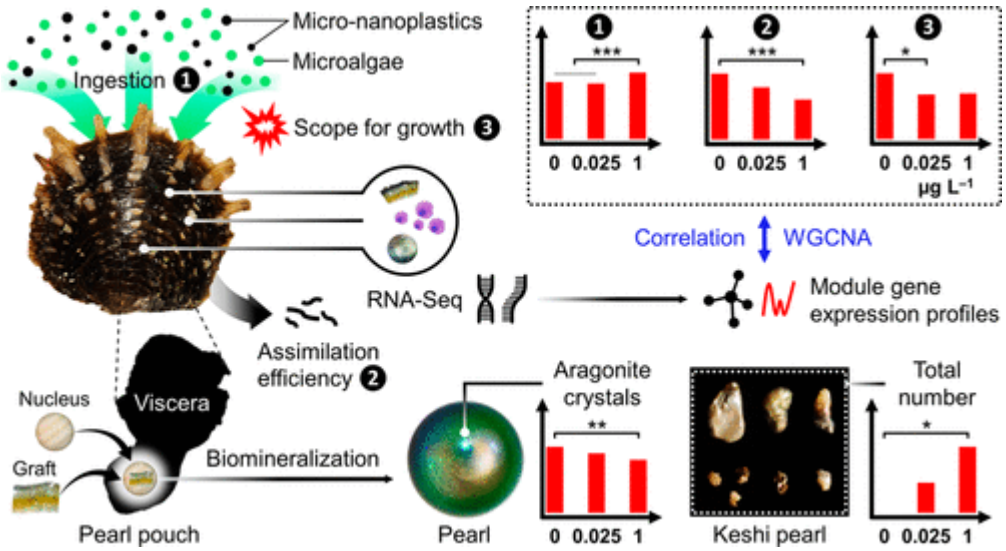

Keywords : pearl oyster, micro-nanoplastic exposure, environmental scenarios, ecophysiology, energy metabolism, functional genomics, pearl cycle

Introduction

Mounting volumes of plastic debris in the environment have become a global concern. With plastic production and consumption surpassing proper waste management capabilities, plastic waste accumulates in the environment, particularly in the ocean.[1] Plastic debris can remain in the marine environment for many years due to slow degradability.[2] Driven by various environmental factors,[3] larger plastic pieces break down into smaller fragments, of which 92% are microplastics (MPs) of 0.33–5 mm in size,[4] excluding consideration for smaller MPs and nanoplastics (NPs, <0.1 μm) that are as yet poorly quantified in nature.[5] Given their pervasive presence and small size, MPs have emerged as a worldwide issue, intensifying concerns about their ecological impacts.[6] MPs are prone to ingestion by a diverse range of organisms,[7] as evidenced by laboratory experiments on

filter-feeding species,[8,9] and by the presence of MPs in the digestive tracts of wild animals.[10,11] Experimental consumption of MP can lead to detrimental health effects, affecting functions such as respiration,[12] nutrition,[13] assimilation efficiency,[9] reproduction,[8] and growth.[14] Yet, most laboratory experiments have utilized single polymer type, usually spherical in shape (termed model particles), often at higher concentrations in terms of particle count per volume than real-world settings.[15,16] Although this type of study is necessary to understand the toxicity mechanisms at play,[17] it lacks ecological relevance regarding the real environmental MP exposure complexity, encompassing diverse particle shapes, sizes, polymer types, surface characteristics, chemical properties, and biological load, underscoring the challenges of investigating the actual ecological impact of MPs in aquatic ecosystems.[16,17] While, a handful of studies have tried to consider the complexity of *in situ* MP exposure,[18–20] a significant disparity persists between potential risks and actual risks associated with MPs,[16,21] largely due to limitations in replicating these conditions in laboratory settings.

In French Polynesia (FP), pearl farming ranks as the second most important economic resource, contributing to $22.3 million in 2020. The trade of pearls and mother-of-pearl is widespread across 28 island and atoll lagoons.[22] Nonetheless, pearl farming is linked to a distinct plastic source, as much of the equipment (*e.g.*, ropes, collectors, and buoys) is fashioned from synthetic materials that accumulate over time, potentially becoming sites for the release of MPs.[23] Recent monitoring in pearl farming lagoons revealed extensive MP contamination in both the seawater and cultured oysters.[24] The water column, a vital environment for cultivating pearl oysters (*Pinctada margaritifera*), emerged as a heavily contaminated compartment (14–716 MP m^{-3}); this means that *P. margaritifera* is exposed to substantial microscale MP pollution (2–125 MP g^{-1} dry weight).[24] Ropes and spat collectors—key plastic components in pearl farming, constructed from polyethylene (PE) and polypropylene (PP)—were identified as major contributors to the abundance

of small-sized (20–200 µm) and fragment-shaped MPs.[24] Consequently, pearl farming could inadvertently contribute to its own plastic pollution risk, potentially affecting pearl oysters and leading to broader repercussions on marine life and lagoon ecosystems.

Experimental exposure to polystyrene microbeads has already shown a dose-dependent (0.25, 2.5, and 25 µg L^{-1}) effect on energy balance,[9] and dose-specific transcriptomic disruption of gene expression[25] in *P. margaritifera*. In this study, we simulated more realistic scenarios by exposing pearl oysters to micro-nanoplastics (MNPs) from pearl farming equipment over a 5-month pearl production cycle. Three MNP concentrations were tested: 0 (control), 0.025, and 1 µg L^{-1}. We employed integrative approaches to assess the impacts of this exposure at individual, cellular, and molecular levels, while also evaluating crucial endpoints such as pearl quality. Demonstrating effects in a more realistic context aims to inform decision-making, stimulate changes in industry processes, and influence legislation by outlining government policies to mitigate this emerging risk to lagoon ecosystems and the sustainability of pearl farming.

Materials and Methods

Experimental animals. Pearl oysters were sampled on April 03, 2018, in a pearl farm located on Mangareva Island (23°06′34″S; 134°57′57″W) in the Gambier archipelago (23°07′S; 134°58′W, FP). A stock of 600 adult oysters (1.5–2 years old) was transferred (transfer authorization No. 643 issued by the Ministry of Marine Resources of FP) to the lagoon of Vairao (Ifremer marine concession No. 8120/MLD: 17°48′26.0″S, 149°18′14.4″W, Tahiti, FP) on April 04, 2018. All the experimental procedures comply with French law and with institutional guidelines.

Pearl farming MNPs. MNPs were produced from two widely used types of pearl farming plastic gear (*i.e.*, synthetic rope and spat collectors), collected from weathered structures of a pearl farm in Manihi atoll (14°24′10.4″S, 145°57′29.2″W), according to the methodological protocol of Gardon et al.[26] Based on FTIR and Py-GC-MS measurements, the synthetic rope (SR) and spat collector (SC) were made of PE and PP, respectively (Figure S1). These two polymers are the most commonly used plastic polymers worldwide and are often found in MPs sampled from pearl farming atolls.[24] The MNP size distribution ranged from 0.4 to 200 µm (Figure S2) following laser diffraction analysis (Beckman Coulter LS 130 particle laser diffractometer, Beckman Coulter, Inc., Brea, CA), matching the retention size range of *P. margaritifera* (*i.e.*, 2–200 µm).[27] MNPs produced from SR and SC were conserved separately in stock solutions, resuspended in filtered (1.2 µm) 70% ethanol at 1.5 g L^{-1} and stored at 4 °C.

MNP exposure. A total of 240 pearl oysters (height, 7.6 ± 0.3 cm; weight, 36.1 ± 5.5 g) were conditioned in duplicate in 6 rectangular 500 L tanks (4 donors and 36 receivers for a total of 40 pearl oysters per tank, 80 oysters per condition) supplied by natural seawater directly pumped and filtered (25 and 5 µm) from the lagoon at 26.5 ± 0.6 °C (pH 8.2, dissolved oxygen 6.8 ± 0.5 mg O_2 L^{-1}, salinity 35 psu), and kept under a 12 h light: 12 h dark cycle. The tanks were equipped with 2 air-lifts connected to the pressurized air circuit and 4 circulation pumps in order to maintain a homogeneous environment around the oysters. A mixed diet of two microalgae (*Tisochrysis lutea* [*T-iso*] and *Chaetoceros gracilis*), used as optimal food for *P. margaritifera* in laboratory settings,[27,28] was continuously supplied at a dry-weight-algae/dry-weight-oyster ratio of 7–8% (*i.e.*, 35–40 cells $µl^{-1}$, below the threshold for triggering pseudofeces production). Before exposure, pearl oysters were placed in a 500 L tank for calcein marking performed at 150 mg L^{-1} (calcein diluted in seawater) overnight to assess the shell growth rate (refer to the Supporting Information).[29]

After 2 weeks of acclimation, both types of MNPs (*i.e.*, SR and SC) were incorporated at equal weights (ratio SC/SR = ~5.2) and injected continuously at concentrations of 0 (control), 0.025 and 1 µg L^{-1}. The MNP concentrations tested in the present study were similar in terms of MP mass concentration to estimates from Gardon et al.[24] of concentrations that may occur in the pearl oyster living environment. The tested mass concentrations of 0.025 and 1 µg L^{-1} are both included within the range of 0.003–3 µg L^{-1} (for particle size ranging from 20 to 200 µm) extrapolated from *in situ* data points of 716 MP m^{-3} measured in the water column of the pearl farming atoll of Takaroa.[24] Here, we tested 0.4–200 µm MNPs at 0.025 µg L^{-1} (~2.8×10^{6} MNPs L^{-1}) in order to target a response window where no effect occur for MNP stress based on previously reported dose-effects (0.25, 2.5, and 25 µg L^{-1}) on oyster physiology,[9] and gene expression.[25] Thus, we reduced the previously lowest tested dose of 0.25 µg L^{-1} by a factor of 10 to achieve 0.025 µg L^{-1}. A 40-fold higher dose of 1 µg L^{-1} (~1.1×10^{8} MNPs L^{-1}) was also tested in order to overlap with previous tested concentrations and match the linear regression of extrapolated field data suggested by Lenz et al. (2016).[16] These two concentrations were therefore tested to get as close as possible to the "current" scenario (*i.e.*, number of particles per volume *vs.* mass concentration). The MNP mixture was incorporated in 5 µm-filtered seawater and distributed continuously from a solution prepared daily in six cylindrical-conical 50 L tanks (1 per replicate). To limit aggregation, MNP solutions were added with Tween® 20 at a final concentration of 0.0002% (which is below the nontoxic concentration, 0.0007% v/v),[30] and distributed in all tanks, including the control. Due to methodological limitations in detecting and accurately quantifying polydisperse MNPs (with 80-90% of particles <1 µm, Figure S2) in exposure media, especially at such low concentrations, adjustments in concentrations were made based on previous research. This research highlighted disparities between expected and actual concentrations in experimental tanks, indicating an exposure 13-15% lower than the theoretically distributed concentrations.[8,9] Consequently, an

exposure level 13% higher than the theoretical levels was implemented to compensate for particle loss and biomass-induced variations within the experimental design.

Experimental grafts. After 2 months of exposure, pearl oysters were removed from the water for processing for the graft step. Receiver oysters were half-opened with a prop, and donor oysters were sacrificed. Ten mantle grafts from each donor were sampled and transplanted to receivers (1 donor for 10 receivers). For each receiver, one graft and one nucleus (2.0 BU size, Ø ~0.6 mm, ~0.4 g weight; Imai Seikaku Co. Ltd., Japan) were both inserted into the pearl pouch by a transplant specialist to simulate a pearl production cycle. Each nucleus was previously weighed with a highly accurate balance with ± 0.0001 mg accuracy to assess pearl nacre deposition on the surface after harvesting at the end of the exposure. One nucleus transplanted to one of the 10 receivers per donor was a magnetized nucleus (*i.e.*, 4 per tank, 8 per treatment) for the assessment of pearl rotation in the pearl pouch (see Supporting Information).[31,32] Once the receivers were grafted, all pearl oysters were put back in their respective experimental tanks to continue MNP exposure over a 3-month period.

Ecophysiological measurement. At 2 weeks post-graft (2.5 months exposure), ten receiver oysters per treatment were placed individually in an ecophysiological measurement system (EMS) to monitor the clearance rate (ingestion) and oxygen consumption. Details of the EMS acquisition system are provided in the Supporting Information. Assimilation efficiency was measured after collecting feces in each hemispheric chamber and 50 ml of microalgae mixture administered during ecophysiological measurements.[33] Ecophysiological measurements were conducted during the 2.5- to 4-month exposure period, with each condition alternated between each run of 48-h data acquisition. A total of 120 pearl oysters were individually monitored in the EMS, with 40 oysters per treatment. After each run, the oysters were returned to their original experimental tank to

continue exposure until the end of the 5-month experiment, during which RNA-Seq and pearl quality analyses were conducted on the same individuals to explore potential connections.

Metabolic rates including ingestion, oxygen consumption, and assimilation efficiency, used to calculate the scope for growth (SFG), were computed following Chávez-Villalba et al.,[33] and describe in Gardon et al.[9] Detailed calculations are provided in the Supporting Information as Supplementary Methods.

Oyster sampling. Pearl products were collected at the end of the 5-month exposure period. Measurements of pearl quality traits were conducted on biomineral structures formed around the nucleus, with a specific emphasis on the microstructures of aragonite crystals (see Supporting Information). Keshi pearl production sometimes occurs after nucleus rejection and corresponds to the biomineralization of the remaining grafted piece of mantle and/or particles that may penetrate the pearl pouch before healing of the transplantation incision. An analysis of keshi pearls was carried out to determine the origin of these biomineral concretions, following the procedures outlined by Hermabessiere et al.[34] and Djouina et al.[35] (see Supporting Information). The visceral mass was then sampled, drained on absorbent paper and placed in 10% formalin seawater for 72 h before being transferred into 70% ethanol for histology analysis (see Supporting Information). A piece of mantle and a piece of pearl sac (in the case of pearl harvest) were also sampled from each pearl oyster, as well as hemocytes collected in the byssal gland with a needle (1 ml; 0.45 × 13 mm). These samples were placed in RNA later solution (500 µl) and stored at –80 °C for downstream transcriptomics. Each muscle from each pearl oyster was also sampled and frozen in liquid nitrogen before storage at –80 °C for energy reserve assessment by glycogen content (see Supporting Information).

RNA extraction and sequencing. Total RNA was extracted from mantle, hemocyte and pearl sac samples with TRIZOL Reagent (Life Technologies, USA) at a ratio of 1 ml per 100 mg tissue. RNA quantity and integrity were evaluated with a Nanodrop (NanoDrop Technologies Inc., USA) and a 2100 BioAnalyzer System (Agilent Technologies, USA). RNA was dried in RNA-stable solution (Thermo Fisher Scientific, USA) and shipped at ambient temperature to McGill sequencing platform services (Montreal, Canada). TruSeq RNA libraries were randomly multiplexed (N = 20 individuals per lane) and subjected to 100-bp paired-end sequencing on an Illumina NovaSeq 6000 system at the McGill Genome Quebec platform (Montreal, CA).

RNA-Seq data analysis. Raw reads were first filtered with Trimmomatic v0.38 with a minimum length (60 bp),[36] minimum quality (leading: 20; trailing: 20), and the presence of putative contaminants and remaining adaptors. Read quality was assessed before and after trimming with FastQC v0.11.8 and MultiQC v1.6.[37] Only high-quality paired-end reads were retained and mapped against the reference genome[38] using GSNAP v2018.07.04 with default parameters[39] but allowing a minimum mismatch value of 2 and a minimum read coverage of 90%. We used only properly paired and uniquely mapped reads for the downstream analysis.[39]

Differential gene expression was assessed through pairwise comparisons and Wald tests using the *DESeq2* v1.22.2 R package.[40] Genes were considered differentially expressed (DEGs) when the absolute value of $\log_2$FC was > 2 and the false discovery rate (FDR) was < 0.01. The *KOGMWU* package[41] was used to test for rank-based enrichment of eukaryotic orthologous groups (KOG) and Gene Ontology (GO) terms using EggNOG-mapper v2.0[42] in the mantle, hemocytes and pearl sac sequencing datasets. The KOG_MWU function calculates delta rank values for these 23 broad functional groups using $\log_2$FC values for the entire datasets. Functional responses to 0.025 and 1 µg L^{-1} MNPs were compared according to sample type to identify common and

divergent patterns. Supplementary comparisons were performed between sample types for each MNP condition to identify common responses among tissue samples.

Weighted gene coexpression network analysis (WGCNA), implemented in R (v4.1.2) and based on variance-stabilization (VST) data values, was used to identify modules of genes in mantle, pearl sac, and hemocytes, whose expression significantly correlated with conditions (control, 0.025, and 1 µg L^{-1}), MNP conditions (0.025 and 1 µg L^{-1}), and physiological and functional traits associated with the same individuals (except for hemocytes, where only 10 common oysters out of 29, representing 3–4 individuals per condition, due to sampling feasibility). A signed network was constructed using a soft threshold power of 13, a minimum module size of 50, and a module merging threshold of 25% dissimilarity. Module–trait relationships were computed by Pearson's correlation tests. Modules exhibiting a $r \geq 0.45$ and $P \leq 0.01$ were selected as modules of interest. Eigengene expression within each module was also statistically tested to identify significant differences between conditions. GO enrichment analysis for biological process (BP) and molecular function (MF) was performed on module genes using the Mann–Whitney *U* test implemented in the GOMWU framework using module kME input file, *P. margaritifera* annotations, *go.obo* database and a custom Perl script.

The Genes in WGCNA modules of interest were then overlapped with DEG list to identify potential links with differences between conditions, as well as associated physiological and functional trait relationships.

Statistical analysis. Data are presented as the mean with the 95% confidence interval of the mean (mean ± 1.96 standard error), except for frequency distributions, where data are presented as the mean ± standard deviation. Normality and homoscedasticity were tested with Shapiro–Wilk and Levene's tests, respectively. Data expressed in relative values were previously transformed by the arcsine square root function. Mean values of a single-response variable were compared using a

one-way ANOVA for the condition factor (α = 0.05). Tukey's post hoc test was used to evaluate the significance of differences between the averages of each group. When the assumptions of normality and homogeneity of variance were not met, even after data transformations (square root, logarithmic, and Box-Cox transformations), we used the nonparametric Kruskal–Wallis' (KW) test to compare the means of each condition. Dunn's post hoc test, employing the Bonferroni-adjusted *P*-values, was used for multiple comparisons and to assess the significance of differences between the means of each group. Frequency distributions were analyzed using Pearson's chi-squared test to determine if a difference occurred between conditions. Fisher's exact test was then used to compare conditions using a 2 × 2 contingency table. The results were considered significant at $P \leq 0.05$. All analyses were performed in the statistics software RStudio v4.1.2.

Results

Metabolic rates. MNP exposure led to a significantly higher ingestion rate in oysters exposed to 1 µg L^{-1} (12.4 ± 0.6 × 10^7 cells h^{-1} g^{-1}) than in oysters exposed to the control (10.7 ± 0.5 × 10^7 cells h^{-1} g^{-1}) and 0.025 µg L^{-1} (10.5 ± 0.6 × 10^7 cells h^{-1} g^{-1}) conditions (Tukey's HSD, $P < 0.001$) (Figure 1B). Furthermore, a significantly lower assimilation efficiency was observed in oysters exposed to 1 µg L^{-1} (26.1 ± 5.2%) than in control oysters (37.5 ± 3.4%; Tukey's HSD, $P < 0.001$), while only a downward trend was observed in oysters in the 0.025 µg L^{-1} condition (31.4 ± 3.3%; Tukey's HSD, $P = 0.100$) (Figure 1D). No significant difference was observed regarding oxygen consumption (ANOVA, $P = 0.420$), with a mean of 0.79 ± 0.08, 0.81 ± 0.07 and 0.85 ± 0.06 mg O_2 h^{-1} g^{-1} under control, 0.025 µg L^{-1} and 1 µg L^{-1} conditions, respectively (Figure 1C).

Scope for growth. Metabolic rate analysis revealed a mean energy balance (scope for growth) of 31.2 ± 3.9, 22.2 ± 4.7 and 22.6 ± 6.8 J h^{-1} g^{-1} for the control, 0.025 µg L^{-1} MNP and 1

µg L^{-1} MNP conditions, respectively (Figure 1E). The overall KW test was at the limit of significance ($P = 0.050$), and multiple comparisons revealed a slight significant difference in means between the control and 0.025 µg L^{-1} conditions (Dunn's test, $P = 0.048$) (Figure 1E).

Energy reserve and shell growth. The glycogen content analysis on pearl oyster muscle revealed a significantly lower energy reserve in the 0.025 µg L^{-1} (4.6 ± 0.8 µg mg^{-1}) condition compared with the control (8.1 ± 1.2 µg mg^{-1}) and 1 µg L^{-1} (7.9 ± 1.5 µg mg^{-1}) conditions (Tukey's HSD test, $P < 0.001$ and $P = 0.001$, respectively) (Figure 1F). No significant difference in shell growth was observed among conditions (ANOVA, $P = 0.321$, Figure 1G).

Harvest. The number of pearls collected at the end of the experiment showed statistically similar frequency distribution among conditions ($\chi^2 = 0.164$, $P = 0.921$). The mean percentages were 62.4% ± 12.8% ($N = 23$) for individuals producing pearls in the control condition, 59.7% ± 17.4% ($N = 27$) and 59.9% ± 11.4% ($N = 31$) for those in the 0.025 and 1 µg L^{-1} conditions, respectively (Figure 2A and B). However, a significant difference in the frequency distribution of keshi pearl production, involving pearl oysters that have rejected their nucleus (Figure 2A and C), emerged between the control and 1 µg L^{-1} conditions (Fisher's exact test, $P = 0.039$). The 0.025 µg L^{-1} condition showed an intermediate value that was not significantly different (Fisher's exact test, $P = 0.144$). Specifically, the 0.025 µg L^{-1} condition exhibited a mean of 9.9% ± 8.3% ($N = 4$) and the 1 µg L^{-1} condition showed 17.6% ± 9.1% ($N = 9$) of pearl oysters producing keshi pearls. Conversely, no keshi pearls were collected from the control condition ($N = 0$; Figure 2A).

Pearl quality traits. Pearl nacre deposition measured on the nucleus and composed of periostracum, calcite and aragonite crystals (Figure 2D) reached similar mean values of 80.2 ± 12.2 µg in the control condition, 85.4 ± 17.8 µg in the 0.025 µg L^{-1} condition, and 78.0 ± 21.1 µg in the 1 µg L^{-1} condition (KW test, $P = 0.717$). Similarly, no significant difference in biomineralization rate (thickness) was measured among conditions (ANOVA, $P = 0.430$), with values of 3.0 ± 0.5,

3.4 ± 0.7 and 2.9 ± 0.6 µm d^{-1} in the control, 0.025 and 1 µg L^{-1} conditions, respectively (Figure 2E). However, a significantly higher proportion of organic material in the coating on the nucleus (periostracum) was measured in the 0.025 µg L^{-1} condition (7.3 ± 6.5%) compared to the control (1.2 ± 1.9%) (Dunn's test, P = 0.025), while no difference was observed regarding calcite and aragonite crystals (KW test, P = 0.258 and P = 0.148, respectively) (Figure 2F). Focusing on aragonite crystals at the microstructure level, no significant difference in aragonite front spacing (Figure 2G and H) was measured on the pearl surface (KW test, P = 0.950), with a mean of 16.3 ± 1.9 µm in the control condition, 15.9 ± 1.7 µm in the 0.025 µg L^{-1} condition and 18.2 ± 3.9 µm in the 1 µg L^{-1} condition (Figure 2G). However, a significant difference in aragonite platelet thickness (Figure 2I and J) was measured (KW test, P = 0.010), with values of 491.9 ± 45.3, 442.4 ± 36.1 and 395.1 ± 18.5 nm in the control, 0.025 and 1 µg L^{-1} conditions, respectively, revealing a significantly lower value in the 1 µg L^{-1} condition compared to the control condition (Dunn's test, P = 0.002; Figure 2I).

Keshi pearl origin. Observation of keshi pearls under a stereomicroscope revealed the presence of a purple particle (~9 µm) embedded in the mineral surface microlayer of a keshi pearl (Figure 2K and L), displaying the characteristic color of weathered purple PE rope (Figure 2M and N). This superficial detection was uniquely observed in one keshi pearl produced from a pearl oyster exposed to 1 µg L^{-1} MNPs. The developed methodology did not enable the analysis and detection of a PE signature in this purple particle. Further details regarding the analysis of keshi pearls are presented in the Supporting Information.

RNA-Seq data. RNA sequencing of mantle (N = 29), hemocyte (N = 29), and pearl sac (N = 29) samples yielded means of 36.6 ± 4.5, 33.2 ± 3.3, and 34.4 ± 2.3 M raw reads per individual, respectively. After trimming, 95.2% of reads were recovered in mantle, hemocyte, and pearl sac samples and used for downstream analyses. The mapping rate reached 46.0 ± 1.1%, 36.1 ± 0.8%

and 42.2 ± 1.0% in mantle, hemocyte, and pearl sac samples, respectively, with no significant differences among conditions (ANOVA, $P = 0.609$, $P = 0.149$, and $P = 0.191$, respectively). Sequencing results and read survival after trimming and mapping are shown in Table S1.

Global gene expression patterns across tissues and conditions. The global sequencing results and retained reads were similar across conditions and tissues, as shown in Table S1. First, a hierarchical clustering analysis comparing the change in magnitude and direction of gene expression within each KOG class among datasets revealed that the patterns of the 0.025 and 1 µg L^{-1} conditions were mostly similar but tissue specific (Figure 3A–C). Indeed, *P. margaritifera* KOG functional enrichment correlated across conditions and tissues, with Pearson's *r* values of 0.74 ($P < 0.001$), 0.90 ($P < 0.001$) and 0.56 ($P = 0.004$) for the mantle, hemocytes and pearl sac, respectively (Figure 3A–C). No significant correlations in gene expression were detected among tissue samples from each MNP condition, except between mantle and pearl sac datasets for the 1 µg L^{-1} condition ($r = 0.59$, $P = 0.002$) (Figure S3).

In the mantle, individuals exposed to MNPs exhibited upregulation of genes involved in "energy production and conversion" (0.025 and 1 µg L^{-1}, $P_{adj} < 0.001$), which was the most significant enrichment, followed by "replication, recombination and repair" (0.025 µg L^{-1} MNPs, $P_{adj} = 0.049$; 1 µg L^{-1} MNPs, $P_{adj} = 0.016$). Regarding downregulated genes, the most significant enrichment common to both MNP conditions was associated with "cytoskeleton" (0.025 and 1 µg L^{-1}, $P_{adj} < 0.001$), although this KOG class was upregulated in hemocyte samples, followed by "signal transduction mechanisms" (0.025 and 1 µg L^{-1} MNPs, $P_{adj} < 0.001$, respectively) (Figure 3D). Hemocytes of exposed oysters also exhibited downregulation of genes associated with "nuclear structure" (0.025 µg L^{-1} MNPs, $P_{adj} = 0.047$; 1 µg L^{-1} MNPs, $P_{adj} < 0.001$), "RNA processing and modification" and "translation, ribosomal structure and biogenesis" (0.025 and 1 µg L^{-1} MNPs, $P_{adj} < 0.001$, respectively) (Figure 3D). Finally, in the pearl sac, individuals exposed

to MNP conditions exhibited common enrichment of upregulated genes involved in "chromatin structure and dynamics" (0.025 µg L^{-1} MNPs, P_{adj} = 0.009; 1 µg L^{-1} MNPs, P_{adj} = 0.031) (Figure 3D). Some unique patterns specific to MNP conditions were also observed, as shown in Figure 3D.

Gene coexpression modules associated with MNPs and physiological traits. The expression values of 23,610 genes in 29 mantle samples were used to construct the coexpression module by WGCNA. After clustering of module eigengenes (MEs) based on dissimilarity, a total of 10 modules (out of 26, Figure S4) were selected according to module-trait relationships ($r \geq 0.45$, $P \leq 0.01$) regarding correlations of ME expression with experimental conditions and physiological traits (Figures 4A and S5). Among the modules of interest, 5 modules were identified in cluster 1, 4 modules in cluster 2, and 1 module in cluster 3 (Figure 4A). The tan module (N = 718 genes; cluster 3) was identified as a key module showing a strong correlation with condition (r = 0.67, P < 0.001), specifically with 1 µg L^{-1} MNPs (r = 0.69, P < 0.001), and strong correlations with physiological traits such as ingestion (r = 0.54, P = 0.002) and assimilation (r = –0.45, P = 0.01) (Figure 4A). This module exhibited significantly higher ME expression in the 1 µg L^{-1} group than in both the control and 0.025 µg L^{-1} groups (Dunn's test, P = 0.007 and P = 0.014, respectively) (Figure 4B). The tan module was significantly enriched for "MAPK cascade", "omega-hydroxylase P450 pathway", "response to potassium ion" and "inorganic anion transport" (Figure 4C). Additional information regarding ME expression across the modules of interest and representative GO enrichments for modules displaying significant differences between conditions can be found in Figure 4B and C, as well as in the Supporting Information as Supplementary Results. Comprehensive details concerning all GO enrichments in BP and MF for the modules of interest are provided in Table S2.

Regarding the DEGs between the MNP conditions and the control conditions, a total of 438 DEGs were identified, with 88 DEGs *vs.* 0.025 µg L^{-1} MNPs and 405 DEGs *vs.* 1 µg L^{-1} MNPs;

of these DEGs, 55 were common to both MNP conditions (Figure 4D). A total of 24 and 64 up- and downregulated genes were found, respectively, from individuals treated under the 0.025 µg L^{-1} condition compared with the control and 246 and 159 up- and downregulated genes, respectively, from individuals treated under the 1 µg L^{-1} condition (Figure S6). Focusing on the tan module, a total of 82 DEGs (7 and 82 DEGs from 0.025 and 1 µg L^{-1} MNPs, respectively) were identified among the module genes, with 53 genes annotated according to UniProt entries (Table S4). All DEGs were upregulated, and 7 DEGs were common to both MNP conditions, of which 6 were annotated (Figure 4E and Table S4). Furthermore, by focusing on shared DEGs among sample types (N = 5 DEGs; Figure S7), a total of 4 DEGs were identified in the tan module (Figure 4E and Table S4), namely, *CYP2C8, CYP2J2* (cytochrome P450 transcripts), *HR4* (hormone receptor 4), and *SULT1B1* (sulfotransferase family 1B member 1), as being specific to the 1 µg L^{-1} condition (Figure S7). A complete list of DEG distribution among WGCNA modules in mantle samples is available in Table S3.

The WGCNA approach did not identify a module of interest with biomineralization-related genes in pearl sac samples, as no significant correlation was observed between conditions and pearl quality traits. Supplementary Results concerning WGCNA, DEGs analysis and GO enrichment in hemocyte (Figure S6 and S8–S9, and Table S4–S5) and pearl sac (Figure S6 and S10, and Table S6) samples are presented in the Supporting Information.

Discussion

Biochemical and physiological processes involved in the life cycle of heterotrophic organisms are closely dependent on (*i*) their ability to extract essential energy from their environment through food intake and (*ii*) the orchestration of energy management across various levels of biological

organization. The findings of this study reveal that experimental exposure to MNPs, aligned with *in situ* MP mass concentrations, alters pearl oyster energy metabolism, resulting in consequences across individual, cellular, and molecular levels, along with disruption of the harvest and impairment of pearl quality traits.

The SFG defines the energy needed for growth beyond maintenance, serving as an indicator of an individual's potential to thrive in their environment. The SFG is primarily influenced by ingestion and assimilation efficiency,[43] which impact energy gain in bivalves.[44] Here, the linear decrease in assimilation efficiency observed in individuals exposed to MNPs at a notably lower level of 1 μg L^{-1} indicates that the presence of MNPs altered microalgae assimilation for an equal water volume filtered by oysters. However, the highest MNP concentration triggered compensatory behavior, traduced by higher ingestion rates, in pearl oysters. Similar increases in food intake to counter energetic loss were previously observed in the Pacific oyster after a 2-month exposure to micro-PS.[8] Energy gain through compensatory behavior, however, is constrained by a lower assimilation rate at higher MNPs exposure, ultimately influencing the final SFG. A disbalanced energy budget without compensatory behavior results in lower reserve energy contents in oysters exposed to 0.025 μg L^{-1} MNPs compared to the control condition (–3.5 μg mg^{-1}) and 1 μg L^{-1} MNPs (–3.3 μg mg^{-1}). Early glycogen depletion is consistent with its role as a rapidly mobilizable metabolic fuel to meet bivalves' sudden energy demands.[45] How recurrent mobilization of reserves without physiological compensation might lead to long-term detrimental effects on individual's fitness remains to be determined.[46]

Molecular approaches employing dose-increasing exposure reveal tissue-specific responses that are largely conserved across MNPs concentrations but may diverge in terms of response intensity. Notably, the mantle's upregulated genes related to "energy production and conversion" highlight a hypothesized bioenergetic response to protect cells from oxidative stress.[47] Highest

MNPs concentration only triggers mitogen-activated protein kinase (MAPK) cascade together with stress response mechanisms, encompassing the response to potassium ions and the ω-hydroxylase P450 pathway. MAPK pathways (p38, JNK, and ERK) relay signals from various stimuli, triggering physiological responses including proliferation, differentiation, development, inflammation, stress, and apoptosis.[48] MAPK activation is linked to reactive oxygen species (ROS) production in micro-PS-exposed marine copepods.[49] Activation of potassium channels, linked to ATP hydrolysis for energy production, is proposed as an early oxidative stress response.[50] Meanwhile, cytochrome P450 ω-hydroxylases play a vital role in xenobiotic detoxification and lipid metabolism.[51] Indeed, MPs are known to reduce lipid digestion by forming large lipid-MP heteroaggregates and reducing lipase activity.[52] Conversely, moderated exposure also reveals unique gene signature enrichments in pairwise differential expression analysis, such as "carbohydrate transport and metabolism", observed in oysters exposed at 0.025 µg L^{-1}. This enrichment is key to understanding the observed low glycogen levels in oyster muscle. A depletion of cellular energy stores (carbohydrates, lipids and proteins) has previously been demonstrated in mussels exposed to micro-PS.[45] Convergent signals both biochemical on the glycogen content and molecular on the expression levels of genes involved in the metabolism of glycogen and wholly carbohydrates constitute a strong element of support for this energy hypothesis. This immediate stress response likely precedes the suggested secondary cellular homeostasis response in the 1 µg L^{-1} condition, engaging a plethora of genes that restore equilibrium under new environmental regime.[53] This distinction is accentuated by the notable disparity in the total number of DEGs, which were nearly five times more abundant in the mantle of individuals exposed to 1 µg L^{-1} MNPs (N = 405) compared to those exposed to 0.025 µg L^{-1} MNPs (N = 88). This reinforces the concept of a dose-specific transcriptomic disruption in energy metabolism, as previously suggested.[25] The physiological and molecular signs seen in pearl oysters exposed to both MNP conditions indicate

hallmarks of "*pejus*" conditions, characterized by reduced fitness but positive growth and reproduction.[46] However, the more pronounced molecular disorders observed in the 1 µg L^{-1} condition appear to reflect *P. margaritifera*'s gradual transition from "*pejus*" to "*pessimum*" conditions, representing a high degree of stress.[46] Notably, certain distinct patterns, such as "secondary metabolite biosynthesis, transport, and catabolism", enriched among upregulated genes in the 1 µg L^{-1} condition, may illustrate an energy metabolism shift linked to defense mechanisms. Secondary metabolites (SMs) are typically produced to serve crucial roles in an organism's interaction with its environment. These modifications of central metabolite precursors (*e.g.*, carbohydrates, lipids, and amino acids) enhance acclimation to environmental constraints.[54] While some animal SMs originate internally, most are diet-derived,[55] often through plant consumption.[56] Ingested SMs, whether directly or *via* MPs following adsorption,[57] can influence metabolic rates, nutrient digestibility, and energy expenditure based on type and quantity.[58] Moreover, animals exploit SMs as a strategy to counter challenges that disturb homeostasis due to their bioactive attributes, like antioxidants countering oxidative damage.[58] Further investigation is essential to comprehend SM origins and their role in *P. margaritifera* homeostasis. This requires consideration of interactions between microalgae-derived chemicals and MNPs, which could significantly explain both direct and indirect MNP effects on the environment and biodiversity.

Pearl quality assessment revealed significant effects of MNP exposure on pearl nacre microstructure, particularly impacting aragonite crystals and resulting in thinner aragonite platelets at 1 µg L^{-1} MNPs. Interestingly, depositing thick aragonite crystal layers early in the culturing process, followed by thinner layers near the pearl's surface in the later phase before harvest, could be advantageous for luster and color.[59] However, this effect was observed early, after a 3-month experimental cycle under MNP exposure. In contrast, natural pearl production spans over 18 months, raising questions about the long-term effects of MNPs on pearl quality. This is particularly

noteworthy as Japanese farmers harvest pearls in December, when water temperatures approach the upper limits of tolerance for oysters, since low temperatures induce a reduction in platelet thickness and pearl growth in *P. fucata*.[60] This outcome suggests that the thinner aragonite platelets observed in the present study at 1 µg L^{-1} MNPs may result from the energy metabolism disorder,[61,62] and that the presence of MNPs in pearl farming lagoons could potentially lead to the production of lower-quality pearls without lengthening the production cycle. Additionally, the harvest conducted after experimental exposure revealed that pearl oysters, which had rejected their nucleus post-grafting, yielded significantly more keshi pearls at 1 µg L^{-1} than oysters in the control condition exhibiting no keshi pearl. It's therefore possible that MNPs triggered keshi pearl production through the potential translocation of MNPs across epithelial membranes,[63] and/or external MNP intrusion *via* the incision created on the pearl pouch by the operator before receiver oyster healing. Indeed, small plastic particles can be embedded into shells during biomineralization.[64] While PE-PP particles were not detected within the mineral matrix of keshi pearls, microscopy revealed a particle with the expected size, shape, and color—a distinct purple akin to the purple PE rope used for MNP production and exposure. Despite the occasional value represented by keshi pearls, the presence of MNPs in the pearl pouch could potentially interfere with the biomineralization processes of pearl production, warranting further research.

In conclusion, this study demonstrated that mimicking the *in situ* conditions of MNP exposure can adversely influence various facets of energy metabolism in *P. margaritifera*. This interference affects energy assimilation, conversion, and increases energy costs for basal maintenance.[46] At a concentration of 1 µg L^{-1} MNPs, a compensatory effect on food intake was observed, potentially balancing the reduced energy intake due to digestive disruptions in molecular functions related to lipid metabolism. No such mechanism was seen at 0.025 µg L^{-1} MNPs, thus explaining the energy budget. It's important to note that stronger impacts might emerge at lower

doses, a significant consideration for comprehending plastic pollution effects on ecosystems. Stress is exacerbated by food availability.[65] Given the oligotrophic nature of lagoon ecosystems, far from the nonlimiting food supply we applied experimentally, stronger effects could arise under natural conditions. This is especially pertinent considering the presence of multiple stressors, such as temperature and acidification linked to global change, which could profoundly impact marine organisms when combined with MNP exposure.[66] This study underscores the risk posed by MNPs within the environmental exposure spectrum (exposome) confronting pearl oysters, their related economy, and lagoon ecosystems in French Polynesia.

Associated content

Supporting Information

The Supporting Information is available in attached file.

Supplementary Methods and Results encompassing ecophysiological and functional parameters, along with transcriptomic approaches. Supplementary Figures (S1 to S10) and Tables (S1 to S6) including details about polymer identification of MNP, particle size distribution, and RNA-Seq data analysis (PDF).

Data Availability

RNA-Seq data were deposited into the European Bioinformatics Institute–European Nucleotide Archive (EBI–ENA) databank under the project ID PRJEB63073. Additional data are presented in the main text of this article and the Supporting Information file.

Author information

Author Contributions

T.G., G.L.M., and A.H. designed and supervised the research. T.G., J.L.L., C.S., F.L., and A.D. conducted the research. T.G. and J.L.L. analyzed the data. T.G. visualized the data and drafted the original manuscript, which was reviewed by J.L.L., A.D., I.P.P., and A.H., and edited by T.G. All authors discussed the data and approved the manuscript.

Notes

The authors declare no competing financial interest.

Acknowledgments

The authors thank L. Bish from Ifremer for providing microalgae throughout the 5-month experiment. Appreciation is also expressed to G. Duflos, C. Himber and M. Colin from Anses, M. Kazour from the LOG and K. Mahé from Ifremer for participation in keshi pearl analyses. The Ifremer Bioinformatics Core Facility (SeBiMER; https://ifremer-bioinformatics.github.io/) receives acknowledgment for providing technical help and scientific support for bioinformatics analysis. We extend our gratitude to the *Pôle de Calcul et de Données Marines* (PCDM; https://wwz.ifremer.fr/en/Research-Technology/Research-Infrastructures/Digital-infrastructures/Computation-Centre) for providing computing support and storage resources through DATARMOR.

The present study was supported by the MICROLAG project funded by the French Polynesian government under *Direction des Ressources Marines* (to T.G.), by a doctoral research grant No. 09793 from Ifremer (to T.G.), and by the European Union, the European Regional Development Fund (ERDF), the French State, the French Region Hauts-de-France and Ifremer under the framework of the project CPER MARCO 2015–2020 (to A.D.).

References

(1) Lebreton, L.; Andrady, A. Future Scenarios of Global Plastic Waste Generation and Disposal. *Palgrave Commun.* **2019**, *5* (1), 1–11. https://doi.org/10.1057/s41599-018-0212-7.

(2) Thompson, R. C. Lost at Sea: Where Is All the Plastic? *Science* **2004**, *304* (5672), 838–838. https://doi.org/10.1126/science.1094559.

(3) Andrady, A. L. Microplastics in the Marine Environment. *Mar. Pollut. Bull.* **2011**, *62* (8), 1596–1605. https://doi.org/10.1016/j.marpolbul.2011.05.030.

(4) Eriksen, M.; Lebreton, L. C. M.; Carson, H. S.; Thiel, M.; Moore, C. J.; Borerro, J. C.; Galgani, F.; Ryan, P. G.; Reisser, J. Plastic Pollution in the World's Oceans: More than 5 Trillion Plastic Pieces Weighing over 250,000 Tons Afloat at Sea. *PLoS ONE* **2014**, *9* (12), e111913. https://doi.org/10.1371/journal.pone.0111913.

(5) Schwaferts, C.; Niessner, R.; Elsner, M.; Ivleva, N. P. Methods for the Analysis of Submicrometer- and Nanoplastic Particles in the Environment. *TrAC Trends Anal. Chem.* **2019**, *112*, 52–65. https://doi.org/10.1016/j.trac.2018.12.014.

(6) Rochman, C. M.; Browne, M. A.; Underwood, A. J.; van Franeker, J. A.; Thompson, R. C.; Amaral-Zettler, L. A. The Ecological Impacts of Marine Debris: Unraveling the Demonstrated Evidence from What Is Perceived. *Ecology* **2016**, *97* (2), 302–312. https://doi.org/10.1890/14-2070.1.

(7) Galloway, T. S.; Cole, M.; Lewis, C. Interactions of Microplastic Debris throughout the Marine Ecosystem. *Nat. Ecol. Evol.* **2017**, *1* (5), 0116. https://doi.org/10.1038/s41559-017-0116.

(8) Sussarellu, R.; Suquet, M.; Thomas, Y.; Lambert, C.; Fabioux, C.; Pernet, M. E. J.; Le Goïc, N.; Quillien, V.; Mingant, C.; Epelboin, Y.; Corporeau, C.; Guyomarch, J.; Robbens, J.; Paul-Pont, I.; Soudant, P.; Huvet, A. Oyster Reproduction Is Affected by Exposure to Polystyrene Microplastics. *Proc. Natl. Acad. Sci.* **2016**, *113* (9), 2430–2435. https://doi.org/10.1073/pnas.1519019113.

(9) Gardon, T.; Reisser, C.; Soyez, C.; Quillien, V.; Le Moullac, G. Microplastics Affect Energy Balance and Gametogenesis in the Pearl Oyster *Pinctada Margaritifera*. *Environ. Sci. Technol.* **2018**, *52* (9), 5277–5286. https://doi.org/10.1021/acs.est.8b00168.

(10) Leslie, H. A.; Brandsma, S. H.; van Velzen, M. J. M.; Vethaak, A. D. Microplastics En Route: Field Measurements in the Dutch River Delta and Amsterdam Canals, Wastewater Treatment Plants, North Sea Sediments and Biota. *Environ. Int.* **2017**, *101*, 133–142. https://doi.org/10.1016/j.envint.2017.01.018.

(11) Bessa, F.; Barría, P.; Neto, J. M.; Frias, J. P. G. L.; Otero, V.; Sobral, P.; Marques, J. C. Occurrence of Microplastics in Commercial Fish from a Natural Estuarine Environment. *Mar. Pollut. Bull.* **2018**, *128*, 575–584. https://doi.org/10.1016/j.marpolbul.2018.01.044.

(12) Watts, A. J. R.; Urbina, M. A.; Goodhead, R.; Moger, J.; Lewis, C.; Galloway, T. S. Effect of Microplastic on the Gills of the Shore Crab *Carcinus Maenas*. *Environ. Sci. Technol.* **2016**, *50* (10), 5364–5369. https://doi.org/10.1021/acs.est.6b01187.

(13) Cole, M.; Lindeque, P.; Fileman, E.; Halsband, C.; Galloway, T. S. The Impact of Polystyrene Microplastics on Feeding, Function and Fecundity in the Marine Copepod *Calanus Helgolandicus*. *Environ. Sci. Technol.* **2015**, *49* (2), 1130–1137. https://doi.org/10.1021/es504525u.

(14) Watts, A. J. R.; Urbina, M. A.; Corr, S.; Lewis, C.; Galloway, T. S. Ingestion of Plastic Microfibers by the Crab *Carcinus Maenas* and Its Effect on Food Consumption and Energy Balance. *Environ. Sci. Technol.* **2015**, *49* (24), 14597–14604. https://doi.org/10.1021/acs.est.5b04026.

(15) Phuong, N. N.; Zalouk-Vergnoux, A.; Poirier, L.; Kamari, A.; Châtel, A.; Mouneyrac, C.; Lagarde, F. Is There Any Consistency between the Microplastics Found in the Field and Those Used in Laboratory Experiments? *Environ. Pollut.* **2016**, *211*, 111–123. https://doi.org/10.1016/j.envpol.2015.12.035.

(16) Lenz, R.; Enders, K.; Nielsen, T. G. Microplastic Exposure Studies Should Be Environmentally Realistic. *Proc. Natl. Acad. Sci.* **2016**, *113* (29), E4121–E4122. https://doi.org/10.1073/pnas.1606615113.

(17) Paul-Pont, I.; Tallec, K.; Gonzalez-Fernandez, C.; Lambert, C.; Vincent, D.; Mazurais, D.; Zambonino-Infante, J.-L.; Brotons, G.; Lagarde, F.; Fabioux, C.; Soudant, P.; Huvet, A. Constraints and Priorities for Conducting Experimental Exposures of Marine Organisms to Microplastics. *Front. Mar. Sci.* **2018**, *5*, 252. https://doi.org/10.3389/fmars.2018.00252.

(18) Revel, M.; Lagarde, F.; Perrein-Ettajani, H.; Bruneau, M.; Akcha, F.; Sussarellu, R.; Rouxel, J.; Costil, K.; Decottignies, P.; Cognie, B.; Châtel, A.; Mouneyrac, C. Tissue-Specific Biomarker Responses in the Blue Mussel *Mytilus* Spp. Exposed to a Mixture of Microplastics at Environmentally Relevant Concentrations. *Front. Environ. Sci.* **2019**, *7*, 33. https://doi.org/10.3389/fenvs.2019.00033.

(19) Pannetier, P.; Morin, B.; Le Bihanic, F.; Dubreil, L.; Clérandeau, C.; Chouvellon, F.; Van Arkel, K.; Danion, M.; Cachot, J. Environmental Samples of Microplastics Induce Significant Toxic Effects in Fish Larvae. *Environ. Int.* **2020**, *134*, 105047. https://doi.org/10.1016/j.envint.2019.105047.
(20) Schür, C.; Zipp, S.; Thalau, T.; Wagner, M. Microplastics but Not Natural Particles Induce Multigenerational Effects in *Daphnia Magna*. *Environ. Pollut.* **2020**, *260*, 113904. https://doi.org/10.1016/j.envpol.2019.113904.
(21) Koelmans, A. A.; Besseling, E.; Foekema, E.; Kooi, M.; Mintenig, S.; Ossendorp, B. C.; Redondo-Hasselerharm, P. E.; Verschoor, A.; van Wezel, A. P.; Scheffer, M. Risks of Plastic Debris: Unravelling Fact, Opinion, Perception, and Belief. *Environ. Sci. Technol.* **2017**, *51* (20), 11513–11519. https://doi.org/10.1021/acs.est.7b02219.
(22) Siu, D. Les exportations de produits perliers, fortement impactées par la Covid-19 en 2020. *Inst. Stat. Polynésie Fr.* **2021**, No. 1274, 4.
(23) Andréfouët, S.; Thomas, Y.; Lo, C. Amount and Type of Derelict Gear from the Declining Black Pearl Oyster Aquaculture in Ahe Atoll Lagoon, French Polynesia. *Mar. Pollut. Bull.* **2014**, *83* (1), 224–230. https://doi.org/10.1016/j.marpolbul.2014.03.048.
(24) Gardon, T.; El Rakwe, M.; Paul-Pont, I.; Le Luyer, J.; Thomas, L.; Prado, E.; Boukerma, K.; Cassone, A.-L.; Quillien, V.; Soyez, C.; Costes, L.; Crusot, M.; Dreanno, C.; Le Moullac, G.; Huvet, A. Microplastics Contamination in Pearl-Farming Lagoons of French Polynesia. *J. Hazard. Mater.* **2021**, *419*, 126396. https://doi.org/10.1016/j.jhazmat.2021.126396.
(25) Gardon, T.; Morvan, L.; Huvet, A.; Quillien, V.; Soyez, C.; Le Moullac, G.; Le Luyer, J. Microplastics Induce Dose-Specific Transcriptomic Disruptions in Energy Metabolism and Immunity of the Pearl Oyster *Pinctada Margaritifera*. *Environ. Pollut.* **2020**, *266*, 115180. https://doi.org/10.1016/j.envpol.2020.115180.
(26) Gardon, T.; Paul-Pont, I.; Le Moullac, G.; Soyez, C.; Lagarde, F.; Huvet, A. Cryogrinding and Sieving Techniques as Challenges towards Producing Controlled Size Range Microplastics for Relevant Ecotoxicological Tests. *Environ. Pollut.* **2022**, *315*, 120383. https://doi.org/10.1016/j.envpol.2022.120383.
(27) Pouvreau, S.; Jonquières, G.; Buestel, D. Filtration by the Pearl Oyster, *Pinctada Margaritifera*, under Conditions of Low Seston Load and Small Particle Size in a Tropical Lagoon Habitat. *Aquaculture* **1999**, *176* (3–4), 295–314. https://doi.org/10.1016/S0044-8486(99)00102-7.
(28) Vahirua-Lechat, I.; Laure, F.; LeCoz, J. R.; Bianchini, J. P.; Bellais, M.; Le Moullac, G. Changes in Fatty Acid and Sterol Composition during Oogenesis in the Pearl Oyster *Pinctada Margaritifera*. *Aquac. Res.* **2008**, *39* (16), 1739–1746. https://doi.org/10.1111/j.1365-2109.2008.02050.x.
(29) Linard, C.; Gueguen, Y.; Moriceau, J.; Soyez, C.; Hui, B.; Raoux, A.; Cuif, J. P.; Cochard, J.-C.; Le Pennec, M.; Le Moullac, G. Calcein Staining of Calcified Structures in Pearl Oyster *Pinctada Margaritifera* and the Effect of Food Resource Level on Shell Growth. *Aquaculture* **2011**, *313* (1), 149–155. https://doi.org/10.1016/j.aquaculture.2011.01.008.
(30) Khosrovyan, A.; Kahru, A. Virgin and UV-Weathered Polyamide Microplastics Posed No Effect on the Survival and Reproduction of *Daphnia Magna*. *PeerJ* **2022**, *10*, e13533. https://doi.org/10.7717/peerj.13533.
(31) Gueguen, Y.; Czorlich, Y.; Mastail, M.; Le Tohic, B.; Defay, D.; Lyonnard, P.; Marigliano, D.; Gauthier, J.-P.; Bari, H.; Lo, C.; Chabrier, S.; Le Moullac, G. Yes, It Turns: Experimental Evidence of Pearl Rotation during Its Formation. *R. Soc. Open Sci.* **2015**, *2* (7), 150144. https://doi.org/10.1098/rsos.150144.
(32) Le Moullac, G.; Schuck, L.; Chabrier, S.; Belliard, C.; Lyonnard, P.; Broustal, F.; Soyez, C.; Saulnier, D.; Brahmi, C.; Ky, C.-L.; Beliaeff, B. Influence of Temperature and Pearl Rotation on Biomineralization in the Pearl Oyster, *Pinctada Margaritifera*. *J. Exp. Biol.* **2018**, *221* (18), jeb186858. https://doi.org/10.1242/jeb.186858.
(33) Chávez-Villalba, J.; Soyez, C.; Aurentz, H.; Le Moullac, G. Physiological Responses of Female and Male Black-Lip Pearl Oysters *(Pinctada Margaritifera)* to Different Temperatures and Concentrations of Food. *Aquat. Living Resour.* **2013**, *26* (3), 263–271. https://doi.org/10.1051/alr/2013059.
(34) Hermabessiere, L.; Himber, C.; Boricaud, B.; Kazour, M.; Amara, R.; Cassone, A.-L.; Laurentie, M.; Paul-Pont, I.; Soudant, P.; Dehaut, A.; Duflos, G. Optimization, Performance, and Application of a Pyrolysis-GC/MS Method for the Identification of Microplastics. *Anal. Bioanal. Chem.* **2018**, *410* (25), 6663–6676. https://doi.org/10.1007/s00216-018-1279-0.
(35) Djouina, M.; Vignal, C.; Dehaut, A.; Caboche, S.; Hirt, N.; Waxin, C.; Himber, C.; Beury, D.; Hot, D.; Dubuquoy, L.; Launay, D.; Duflos, G.; Body-Malapel, M. Oral Exposure to Polyethylene Microplastics Alters Gut Morphology, Immune Response, and Microbiota Composition in Mice. *Environ. Res.* **2022**, *212*, 113230. https://doi.org/10.1016/j.envres.2022.113230.
(36) Bolger, A. M.; Lohse, M.; Usadel, B. Trimmomatic: A Flexible Trimmer for Illumina Sequence Data. *Bioinformatics* **2014**, *30* (15), 2114–2120. https://doi.org/10.1093/bioinformatics/btu170.

(37) Ewels, P.; Magnusson, M.; Lundin, S.; Käller, M. MultiQC: Summarize Analysis Results for Multiple Tools and Samples in a Single Report. *Bioinformatics* **2016**, *32* (19), 3047–3048. https://doi.org/10.1093/bioinformatics/btw354.
(38) Le Luyer, J.; Auffret, P.; Quillien, V.; Leclerc, N.; Reisser, C.; Vidal-Dupiol, J.; Ky, C.-L. Whole Transcriptome Sequencing and Biomineralization Gene Architecture Associated with Cultured Pearl Quality Traits in the Pearl Oyster, *Pinctada Margaritifera*. *BMC Genomics* **2019**, *20* (1), 111. https://doi.org/10.1186/s12864-019-5443-5.
(39) Wu, T. D.; Reeder, J.; Lawrence, M.; Becker, G.; Brauer, M. J. GMAP and GSNAP for Genomic Sequence Alignment: Enhancements to Speed, Accuracy, and Functionality. In *Statistical Genomics: Methods and Protocols*; Mathé, E., Davis, S., Eds.; Methods in Molecular Biology; Springer New York: New York, NY, 2016; pp 283–334. https://doi.org/10.1007/978-1-4939-3578-9_15.
(40) Love, M. I.; Huber, W.; Anders, S. Moderated Estimation of Fold Change and Dispersion for RNA-Seq Data with DESeq2. *Genome Biol.* **2014**, *15* (12), 550. https://doi.org/10.1186/s13059-014-0550-8.
(41) Dixon, G. B.; Davies, S. W.; Aglyamova, G. V.; Meyer, E.; Bay, L. K.; Matz, M. V. Genomic Determinants of Coral Heat Tolerance across Latitudes. *Science* **2015**, *348* (6242), 1460–1462. https://doi.org/10.1126/science.1261224.
(42) Huerta-Cepas, J.; Forslund, K.; Coelho, L. P.; Szklarczyk, D.; Jensen, L. J.; von Mering, C.; Bork, P. Fast Genome-Wide Functional Annotation through Orthology Assignment by eggNOG-Mapper. *Mol. Biol. Evol.* **2017**, *34* (8), 2115–2122. https://doi.org/10.1093/molbev/msx148.
(43) Albentosa, M.; Viñas, L.; Besada, V.; Franco, A.; González-Quijano, A. First Measurements of the Scope for Growth (SFG) in Mussels from a Large Scale Survey in the North-Atlantic Spanish Coast. *Sci. Total Environ.* **2012**, *435–436*, 430–445. https://doi.org/10.1016/j.scitotenv.2012.07.025.
(44) Hawkins, A.; James, M.; Hickman, R.; Hatton, S.; Weatherhead, M. Modelling of Suspension-Feeding and Growth in the Green-Lipped Mussel *Perna Canaliculus* Exposed to Natural and Experimental Variations of Seston Availability in the Marlborough Sounds, New Zealand. *Mar. Ecol. Prog. Ser.* **1999**, *191*, 217–232. https://doi.org/10.3354/meps191217.
(45) Shang, Y.; Wang, X.; Chang, X.; Sokolova, I. M.; Wei, S.; Liu, W.; Fang, J. K. H.; Hu, M.; Huang, W.; Wang, Y. The Effect of Microplastics on the Bioenergetics of the Mussel *Mytilus Coruscus* Assessed by Cellular Energy Allocation Approach. *Front. Mar. Sci.* **2021**, *8*, 754789. https://doi.org/10.3389/fmars.2021.754789.
(46) Sokolova, I. M. Energy-Limited Tolerance to Stress as a Conceptual Framework to Integrate the Effects of Multiple Stressors. *Integr. Comp. Biol.* **2013**, *53* (4), 597–608. https://doi.org/10.1093/icb/ict028.
(47) Crawford, D. R.; Wang, Y.; Schools, G. P.; Kochheiser, J.; Davies, K. J. Down-Regulation of Mammalian Mitochondrial RNAs during Oxidative Stress. *Free Radic. Biol. Med.* **1997**, *22* (3), 551–559. https://doi.org/10.1016/s0891-5849(96)00380-2.
(48) Zhang, W.; Liu, H. T. MAPK Signal Pathways in the Regulation of Cell Proliferation in Mammalian Cells. *Cell Res.* **2002**, *12* (1), 9–18. https://doi.org/10.1038/sj.cr.7290105.
(49) Jeong, C.-B.; Kang, H.-M.; Lee, M.-C.; Kim, D.-H.; Han, J.; Hwang, D.-S.; Souissi, S.; Lee, S.-J.; Shin, K.-H.; Park, H. G.; Lee, J.-S. Adverse Effects of Microplastics and Oxidative Stress-Induced MAPK/Nrf2 Pathway-Mediated Defense Mechanisms in the Marine Copepod *Paracyclopina Nana*. *Sci. Rep.* **2017**, *7* (41323). https://doi.org/10.1038/srep41323.
(50) Udensi, U. K.; Tchounwou, P. B. Potassium Homeostasis, Oxidative Stress, and Human Disease. *Int. J. Clin. Exp. Physiol.* **2017**, *4* (3), 111–122. https://doi.org/10.4103/ijcep.ijcep_43_17.
(51) Ni, K.-D.; Liu, J.-Y. The Functions of Cytochrome P450 ω-Hydroxylases and the Associated Eicosanoids in Inflammation-Related Diseases. *Front. Pharmacol.* **2021**, *12*, 716801. https://doi.org/10.3389/fphar.2021.716801.
(52) Tan, H.; Yue, T.; Xu, Y.; Zhao, J.; Xing, B. Microplastics Reduce Lipid Digestion in Simulated Human Gastrointestinal System. *Environ. Sci. Technol.* **2020**, *54* (19), 12285–12294. https://doi.org/10.1021/acs.est.0c02608.
(53) Kültz, D. Molecular and Evolutionary Basis of the Cellular Stress Response. *Annu. Rev. Physiol.* **2005**, *67*, 225–257. https://doi.org/10.1146/annurev.physiol.67.040403.103635.
(54) Pott, D. M.; Osorio, S.; Vallarino, J. G. From Central to Specialized Metabolism: An Overview of Some Secondary Compounds Derived From the Primary Metabolism for Their Role in Conferring Nutritional and Organoleptic Characteristics to Fruit. *Front. Plant Sci.* **2019**, *10*, 835. https://doi.org/10.3389/fpls.2019.00835.
(55) Torres, J. P.; Schmidt, E. W. The Biosynthetic Diversity of the Animal World. *J. Biol. Chem.* **2019**, *294* (46), 17684–17692. https://doi.org/10.1074/jbc.REV119.006130.

(56) Chomel, M.; Guittonny-Larchevêque, M.; Fernandez, C.; Gallet, C.; DesRochers, A.; Paré, D.; Jackson, B. G.; Baldy, V. Plant Secondary Metabolites: A Key Driver of Litter Decomposition and Soil Nutrient Cycling. *J. Ecol.* **2016**, *104* (6), 1527–1541. https://doi.org/10.1111/1365-2745.12644.
(57) Kim, S. W.; Liang, Y.; Lozano, Y. M.; Rillig, M. C. Microplastics Reduce the Negative Effects of Litter-Derived Plant Secondary Metabolites on Nematodes in Soil. *Front. Environ. Sci.* **2021**, *9*, 790560. https://doi.org/10.3389/fenvs.2021.790560.
(58) Forbey, J. S.; Harvey, A. L.; Huffman, M. A.; Provenza, F. D.; Sullivan, R.; Tasdemir, D. Exploitation of Secondary Metabolites by Animals: A Response to Homeostatic Challenges. *Integr. Comp. Biol.* **2009**, *49* (3), 314–328. https://doi.org/10.1093/icb/icp046.
(59) Muhammad, G.; Atsumi, T.; Sunardi; Komaru, A. Nacre Growth and Thickness of Akoya Pearls from Japanese and Hybrid *Pinctada Fucata* in Response to the Aquaculture Temperature Condition in Ago Bay, Japan. *Aquaculture* **2017**, *477*, 35–42. https://doi.org/10.1016/j.aquaculture.2017.04.032.
(60) Muhammad, G.; Atsumi, T.; Komaru, A. The Influence of Water Temperature, Salinity and Food Availability on Nacre Deposition Rates in Shells and Pearls of Japanese and Hybrid Pearl Oyster, *Pinctada Fucata* (Gould, 1850). *Aquaculture* **2020**, *528*, 735512. https://doi.org/10.1016/j.aquaculture.2020.735512.
(61) Joubert, C.; Linard, C.; Le Moullac, G.; Soyez, C.; Saulnier, D.; Teaniniuraitemoana, V.; Ky, C. L.; Gueguen, Y. Temperature and Food Influence Shell Growth and Mantle Gene Expression of Shell Matrix Proteins in the Pearl Oyster *Pinctada Margaritifera*. *PLoS ONE* **2014**, *9* (8), e103944. https://doi.org/10.1371/journal.pone.0103944.
(62) Le Pabic, L.; Parrad, S.; Sham Koua, M.; Nakasai, S.; Saulnier, D.; Devaux, D.; Ky, C.-L. Culture Site Dependence on Pearl Size Realization in *Pinctada Margaritifera* in Relation to Recipient Oyster Growth and Mantle Graft Biomineralization Gene Expression Using the Same Donor Phenotype. *Estuar. Coast. Shelf Sci.* **2016**, *182*, 294–303. https://doi.org/10.1016/j.ecss.2016.03.009.
(63) Al-Sid-Cheikh, M.; Rowland, S. J.; Stevenson, K.; Rouleau, C.; Henry, T. B.; Thompson, R. C. Uptake, Whole-Body Distribution, and Depuration of Nanoplastics by the Scallop *Pecten Maximus* at Environmentally Realistic Concentrations. *Environ. Sci. Technol.* **2018**, *52* (24), 14480–14486. https://doi.org/10.1021/acs.est.8b05266.
(64) Han, Z.; Jiang, T.; Xie, L.; Zhang, R. Microplastics Impact Shell and Pearl Biomineralization of the Pearl Oyster Pinctada Fucata. *Environ. Pollut.* **2021**, 118522. https://doi.org/10.1016/j.envpol.2021.118522.
(65) Cominassi, L.; Moyano, M.; Claireaux, G.; Howald, S.; Mark, F. C.; Zambonino-Infante, J.-L.; Peck, M. A. Food Availability Modulates the Combined Effects of Ocean Acidification and Warming on Fish Growth. *Sci. Rep.* **2020**, *10* (1), 2338. https://doi.org/10.1038/s41598-020-58846-2.
(66) Wen, B.; Zhang, N.; Jin, S.-R.; Chen, Z.-Z.; Gao, J.-Z.; Liu, Y.; Liu, H.-P.; Xu, Z. Microplastics Have a More Profound Impact than Elevated Temperatures on the Predatory Performance, Digestion and Energy Metabolism of an Amazonian Cichlid. *Aquat. Toxicol.* **2018**, *195*, 67–76. https://doi.org/10.1016/j.aquatox.2017.12.010.

Figures

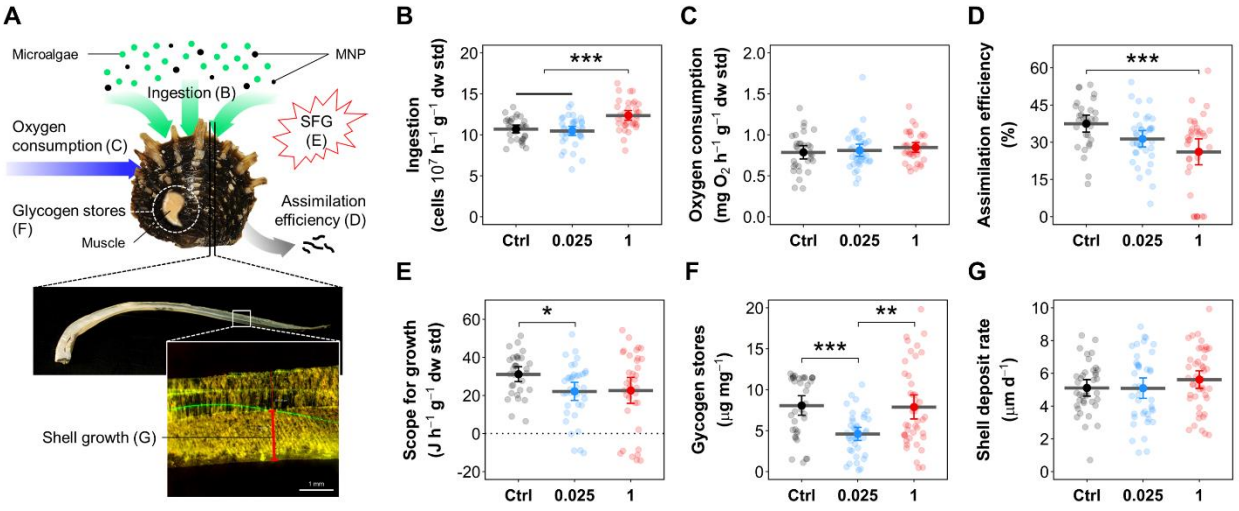

Figure 1. Physiological parameters of *P. margaritifera* exposed to micro-nanoplastics. (A) Schematic of the monitored ecophysiological parameters. (B to G) Boxplots showing the effect of MNP exposure on (B) ingestion rate, (C) oxygen consumption, (D) assimilation efficiency, (E) scope for growth (SFG), (F) glycogen stores and (G) shell growth. Data are expressed as the mean with the 95% confidence interval ($31 \leq N \leq 46$). Asterisks indicate statistically significant differences between conditions ("*", $P < 0.05$; "**", $P < 0.01$; "***", $P < 0.001$).

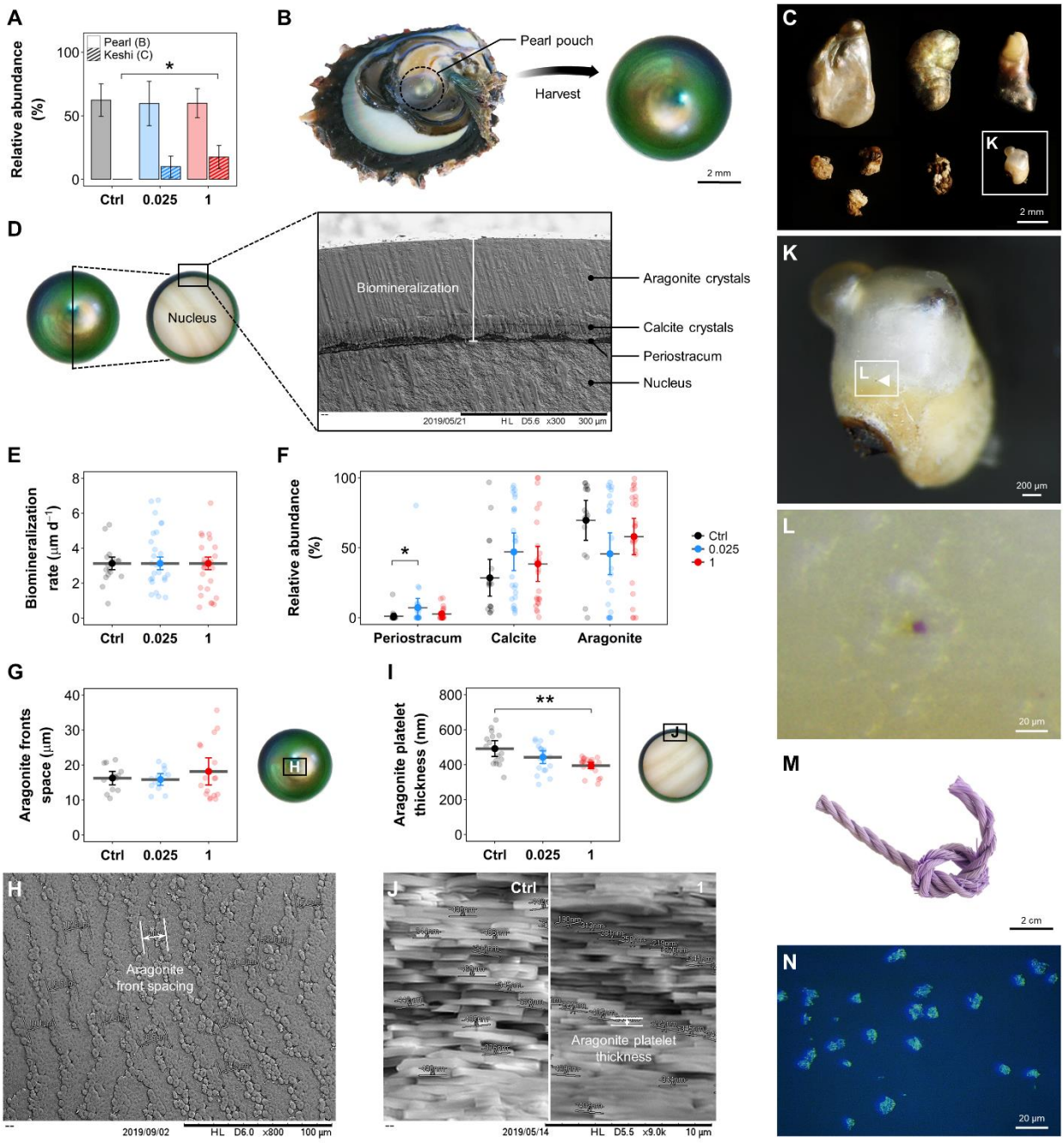

Figure 2. Functional results following a 3-month pearl production cycle under micro-nanoplastics exposure. (A) Histograms of the frequency distribution of collected (B) pearls and (C) keshi pearls showing different morphotypes. Pearl quality assessment was based on (D) biomineral secretion produced on the nucleus for 3 months, which was used to obtain (E) the biomineralization rate and

(F) the relative abundance of pearl nacre deposition structures composed of periostracum, calcite and aragonite crystals. The aragonite crystal microstructure was also characterized by measuring (G and H) the space between aragonite fronts on the pearl surface and (I and J) the platelet thickness on the pearl cross-section using SEM. (J) Two pooled SEM images illustrate comparison in aragonite platelet thickness between the control (left) and 1 µg L^{-1} MNPs (right) conditions. (K and L) Observation of a particle with a purple color identified in the mineral surface microlayer of a keshi pearl. (M and N) Pictures of the weathered purple synthetic rope used to produce PE micro-nanoplastics in the present study. Data are expressed as the mean with the 95% confidence interval of the mean ($17 \leq N \leq 25$), except for A, which shows the mean ± standard deviation. Asterisks indicate statistically significant differences between conditions ("*", $P < 0.05$; "**", $P < 0.01$).

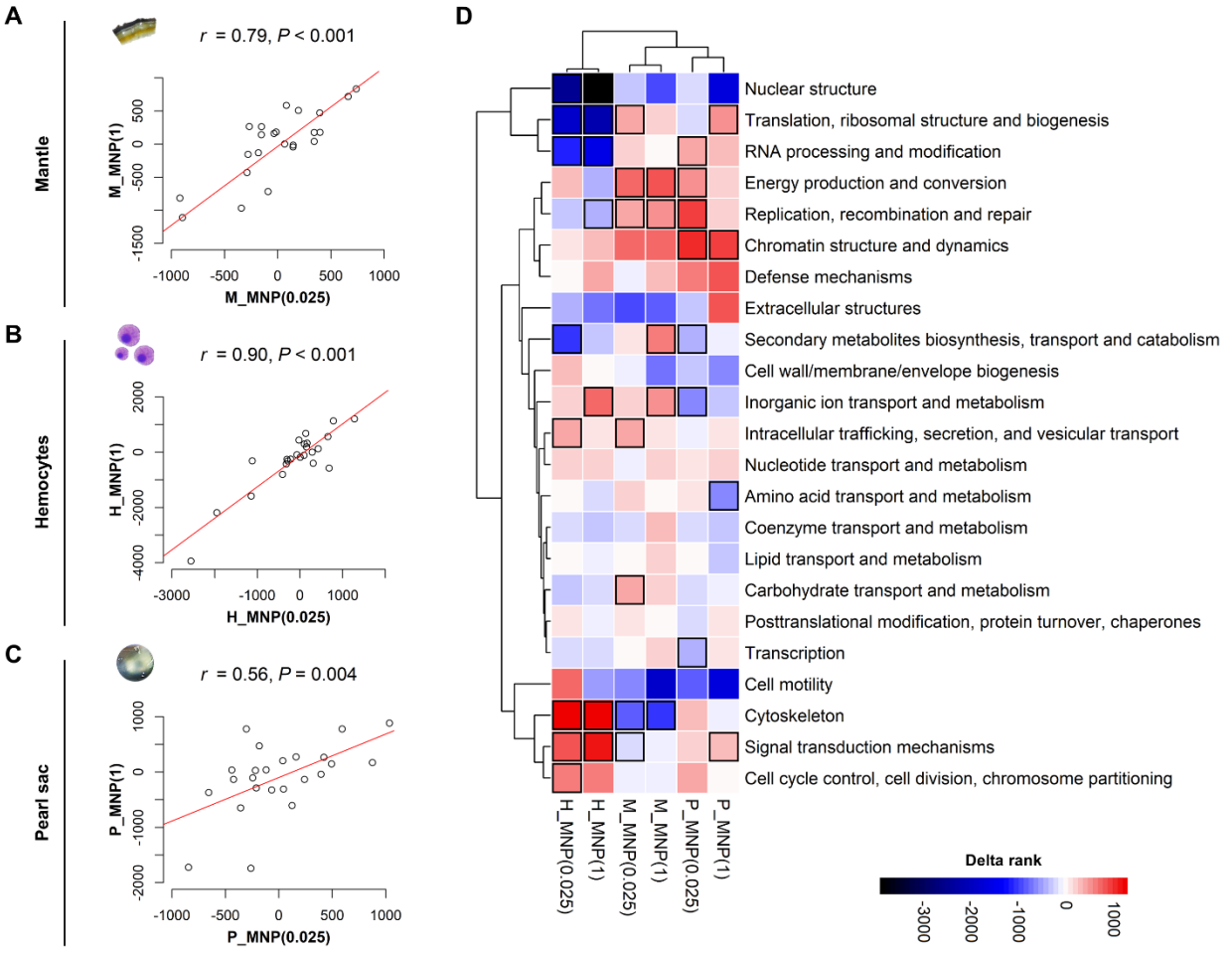

Figure 3. Hierarchical clustering analysis of KOG enrichments in the *P. margaritifera* transcriptome following micro-nanoplastics exposure. Pearson's correlations of KOG delta rank values in the (A) mantle, (B) hemocytes and (C) pearl sac of *P. margaritifera* exposed to 0.025 and 1 µg L^{-1} MNPs. (D) Shared KOG term enrichments (rows) among up- or downregulated genes (delta rank heatmap) under MNP conditions across tissues (columns; M: mantle, H: hemocytes or P: pearl sac). KOG categories in bolded squares denote statistically significant enrichments (FDR-adjusted $P < 0.05$).

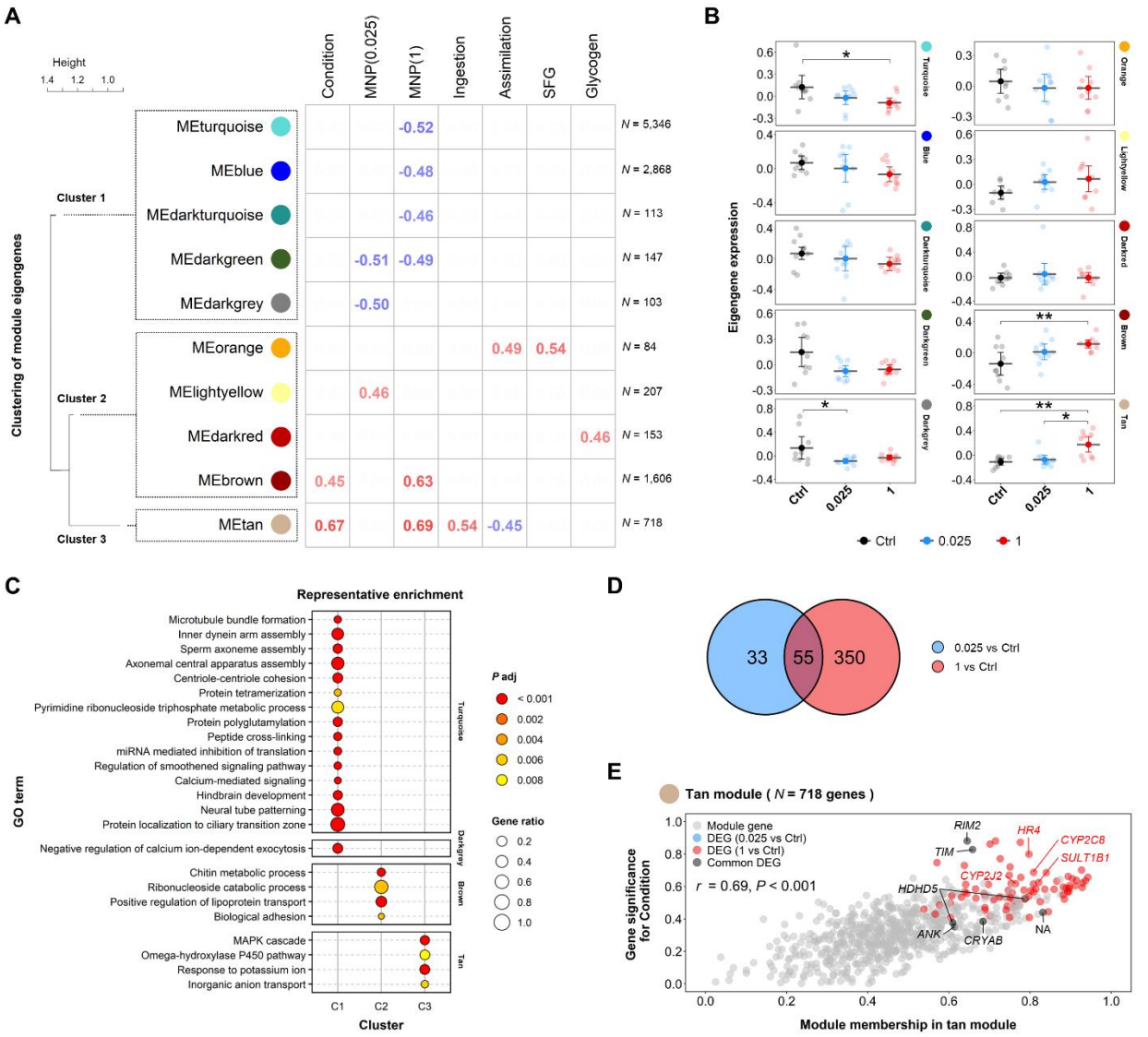

Figure 4. Transcriptomic responses in the mantle of *P. margaritifera* after a 5-month exposure to micro-nanoplastics. (A) Heatmap of identified modules (*y*-axis) and functionally enriched pathways in relation to experimental traits ($|r| \geq 0.45$, $P \leq 0.01$; *x*-axis) from WGCNA. The clustering tree of module eigengenes (MEs) on the left is based on a merging threshold of 100% dissimilarity initially established at 25% for network construction. The numbers on the right of the heatmap represent the number of genes identified in each module. (B) Eigengene expression for selected WGCNA modules significantly correlated with experimental conditions and/or

physiological traits in response to MNP exposure ("*", $P < 0.05$; "**", $P < 0.01$). Data are expressed as the mean with the 95% confidence interval ($N = 9–10$). (C) Representative functional enrichment analysis of module genes identified in the turquoise, darkgrey, brown and tan modules based on an adjusted *P* value cutoff ($P < 0.01$) and cut-height (0.8) of the GO terms tree to obtain "independent groups". The dendrograms depict the sharing of genes between categories; the fractions correspond to genes with $P < 0.05$ relative to the total number of genes within the category. (D) Venn diagram of differentially expressed genes (DEGs) in both MNP conditions compared to the control ($|\log_2 FC| > 2$; FDR < 0.01). (E) Scatterplot of gene significance for condition *vs.* module membership in the tan module illustrating module-trait associations. Gray genes represent module genes; blue and red genes represent DEGs specific to 0.025 and 1 µg L^{-1} MNPs, respectively, with labeled red genes ($N = 4$) identified as common DEGs with other tissues (hemocytes and pearl sac) in the 1 µg L^{-1} condition, including *CYP2J2* and *CYP2C8* (cytochrome P450 family 2 subfamily J member 2 and subfamily C member 8, respectively), *HR4* (hormone receptor 4) and *SULT1B1* (sulfotransferase family 1B member 1); labeled black genes represent common DEGs in both MNP conditions ($N = 7$, of which 6 were annotated), including 2 transcript variants of *HDHD5* (haloacid dehalogenase-like hydrolase domain containing 5), *RIM2* (replication in mitochondria 2), *CRYAB* (crystallin alpha B), *TIM* (timeless) and *ANK* (ankyrin).

SUPPORTING INFORMATION

Pearl Farming Micro-Nanoplastics Affect Oyster Physiology and Pearl Quality

Tony Gardon,[a,*] Jérémy Le Luyer,[a] Gilles Le Moullac,[a] Claude Soyez,[a] Fabienne Lagarde,[b] Alexandre Dehaut,[c] Ika Paul-Pont,[d] and Arnaud Huvet[d]

[a] Ifremer, ILM, IRD, University of French Polynesia, EIO, F-98719, Taravao, Tahiti, French Polynesia, France.

[b] Institute of Molecules and Materials of Le Mans, IMMM – UMR CNRS 6283, University of Le Mans, Avenue Olivier Messiaen, 72085, Le Mans, France.

[c] ANSES – LSA, Boulevard du Bassin Napoléon, 62200, Boulogne-sur-Mer, France.

[d] University of Brest, Ifremer, CNRS, IRD, LEMAR, F-29280, Plouzané, France.

* Corresponding author: Tony Gardon

E-mail: tony.gardon@ifremer.fr; ORCID ID: 0000-0002-5761-0526

This PDF file includes:

- Supplementary Methods
- Supplementary Results
- Supplementary Figures and Tables:
    - Total Figures: 10
    - Total Tables: 6

Total pages: 63

Table of contents

Supplementary Methods

Shell nacre deposition. At the end of the experiment, the shells of dissected oysters were sawn with a "Swap Top" Trim Saw machine, which included a diamond Trim Saw Blade (Thin Cut) IC-40961. The shell edges were then polished for 5 s with various grades of water sandpaper sheets. The shell sections were examined under a Leitz Dialux 22 compound fluorescence microscope equipped with an I3-filter block and an optical micrometer. Shell growth was measured by evaluating the thickness of deposits on the ventral side of the shell, from the surface to the calcein mark, with an optical micrometer.[1] The shell deposit rate (SDR) was calculated by dividing the thickness of the deposits by the time that had elapsed since marking. SDR is expressed in µm d^{-1}.

Pearl rotation. Pearl rotation was conducted in receiver oysters transplanted with a magnetized nucleus. The magnetized nucleus was produced by piercing the bead and including a bar magnet inside (length 0.5 mm; Ø 0.15 mm) before filling the holes with dental resin. Pearl rotation was then monitored in the pearl pouch of pearl oysters with a magnetometer placed in the derivation of the studied treatment tank as described in Le Moullac et al.[2] The magnetometer was made of a half-sphere in acrylic glass (Ø 20 cm) on which were set 25 magnetic sensors spread across the convex surface at different angles (0°, 30°, 60° and 90°) to the base (where the grafted oyster was located). The human–machine interface (HMI), called "magneto" (VEGA Industrie, Avrainville, France), was composed of a microcontroller that uses internal software to collect, process and transfer data to the software (magneto-magnetometer interface 1.0) that produces visualized data from a real-time sensor. Data were processed with a MATLAB® system and converted into 3D coordinates for calculation of pearl movement kinetics. The mean angular speed of rotation (min^{-1}) was recorded for 48 h.

Ecophysiological measurement system. The ecophysiological measurement system (EMS) consisted of eleven hemispheric open-flow chambers in transparent Altuglas®. One oyster was placed in each chamber, and the eleventh chamber was occupied by an empty oyster shell to be used as a control.[3] Experimental conditions for *in vivo* exposure were replicated in the EMS during measurements. The flow rates in the chambers were constant at 12 L h^{-1}. Each chamber was

equipped with a two-way electromagnetic valve activated by an automaton. The released water was analyzed for 3 min using a fluorometer (10-AUTM, Turner Designs, Sunnyvale, CA) to measure microalgae fluorescence and an oximeter (OXI 538/CellOX® 325, WTW, Weilheim, Germany) to measure dissolved oxygen. Data were recorded with acquisition software (computer programming by National Instruments™) for 3 min per chamber by alternating measurements in chambers with and without (control) oysters. Oysters remained in the chambers for at least 48 h; measurements of each oyster were taken every 24 min until 120 measurements of the clearance rate and oxygen consumption had been recorded.[3]

Ingestion and respiration. The ingestion rate (IR) is an indicator of feeding activity,[3] and is defined as the quantity of microalgae cleared per unit of time. IR was calculated as follows:

$$\mathrm{IR} = \mathrm{V} \times (\mathrm{C1} - \mathrm{C2}) \quad (1)$$

where C1 is the fluorescence level of the control chamber, C2 is the fluorescence of the experimental chamber containing one oyster, and V is the constant water flow rate (12 L h^{-1}).[3]

The oxygen consumption rate (OC) was measured (mg O_2 h^{-1}) by calculating the differences in OC between the control and experimental chambers:

$$\mathrm{OC} = \mathrm{V} \times (\mathrm{O1} - \mathrm{O2}) \quad (2)$$

where O1 is the oxygen level in the control chamber, O2 is the oxygen level in the experimental chamber, and V is the water flow rate.[3]

IR and OC were estimated, and an average was calculated for each oyster. The values were converted to a standard animal basis (1 g, dry weight) using the following formula:

$$Ys = \left(\frac{Ws}{We}\right)^{b} \times Ye \quad (3)$$

where Y*s* is the physiological activity of a standard oyster, W*s* is the dry weight of a standard oyster (1 g), W*e* is the dry weight of the specimen, Y*e* is the measured physiological activity, and *b* is the

allometric coefficient of a given activity.[3] The average *b* allometric coefficients were 0.66 for IR and 0.75 for OC.[4]

Assimilation efficiency. The assimilation efficiency (AE) of organic matter was assessed by analyzing microalgae and feces according to the method of Conover (1966) and as described by Chávez-Villalba et al.[3] Biodeposits of each individual were treated by filtration on a GF/C filter (1.2 µm porosity, Ø 47 mm) previously burned at 450 °C and weighed. The filters were then dried at 60 °C for 24 h to obtain the dry weight of biodeposits (DW) and then burned at 450 °C for 4 h to obtain the weight of the mineral matter (W_{MM}). The weight of organic matter (W_{OM}) biodeposits is the difference between the DW and W_{MM}. The W_{OM} of the food ration was calculated by filtering 50 ml of the microalgae mixture, followed by treatment of biodeposits according to the procedure described for organic waste. After conversion of the W_{OM} biodeposits and W_{OM} microalgae to relative values, AE (%) was calculated as:

$$\mathrm{AE} = \frac{\mathrm{OM}m - \mathrm{OM}b}{(100 - \mathrm{OM}b) \times \mathrm{OM}m} \quad (4)$$

where AE is the assimilation efficiency, OM*m* (%) is the microalgae organic matter value (0.87 for *Tisochrysis lutea* and 0.6 for *Chaetoceros gracilis*) and Om*b* (%) is the waste organic matter (biodeposits).[3]

Energy budget. Ecophysiology data were converted into energy values to define the scope for growth (SFG):

$$\mathrm{SFG} = (\mathrm{IR} \times \mathrm{AE}) - \mathrm{OC} \quad (5)$$

where IR is the ingestion rate, AE is the assimilation efficiency, and OC is the oxygen consumption.[3] We used 20.3 J for 1 mg of particulate organic matter and 14.1 J for 1 mg O_2.[5]

Pearl quality trait measurements. The collected pearls were weighed with a balance with ± 0.0001 mg accuracy to measure the weight of pearl nacre deposited on the nucleus surface by subtracting the initial weight of the grafted nucleus. The pearls were then sawn into two equal parts

with a “Swap Top” Trim Saw machine (Inland, Middlesex, UK), which included a diamond Trim Saw Blade (Thin Cut) IC-40961. One part was first fragmented into pieces using a hammer and screwdriver before 1 min of sonication in a 30% ethanol bath at 30 kHz to dissociate small particles from fragments. The fragments were then fixed with a carbon tab onto an aluminum stub (Ø 12.5 mm, Agar Scientific Ltd., UK) to analyze the mineralized portion of the nacre on the nucleus (S1), while the second part was directly fixed flat on another stub for pearl surface analysis (S2). The samples were metallized with a 15 nm layer of gold on their surface using a Rotary Pumped Coater (Quorum Technologies, Q150R ES model) and observed at 15 kV (in charge-up reduction mode) using a Hitachi TM 3030 scanning electron microscope (SEM). Images (300×) of fractured pearl (S1) were captured to measure the thickness of the periostracum (an organic coating on the nucleus), calcite and aragonite crystals. The biomineralization rate (*i.e.*, total thickness of the periostracum, calcite and aragonite crystals) was calculated by dividing the thickness of deposits by the time that had elapsed since grafting (expressed in µm d^{-1}). Focusing on the aragonite crystal microstructure, the thickness of platelets (S1) and the spacing of their organization into growth fronts on the pearl surface (S2) were measured ($1{,}064 \leq N \leq 2{,}454$ and $759 \leq N \leq 959$ per condition for S1 and S2, respectively) in high-magnification images (9,000× and 800×, respectively).

Keshi pearl analysis. Keshi pearls that displayed particles in the nacre layers under direct illumination were examined using an Olympus SZX16 stereomicroscope equipped with a UC90 camera. The surface was gently sanded using fine sandpapers (P1200 and Silicon Carbide 800/2400) commonly utilized for sclerochronological studies. µ-Raman analyses were conducted on a Horiba XploRA PLUS V1.2, following the procedure outlined by Hermabessiere et al.,[6] while Pyrolysis-GC-MS (Py-GC-MS) analyses were performed using a Shimadzu QP2010-Plus device, following the optimized method detailed in the same article. Analysis of intact keshi pearls involved dissolving them in 98% sulfuric acid, allowing observation of the residual particles under a stereomicroscope. Selected fragments collected post-observation underwent analysis using a Perkin Elmer Spotlight™ 400 FTIR spectrometer equipped with an MCT detector linked to a Spectrum 3 MIR spectrometer. The procedure followed was in accordance with Djouina et al.,[7] with a variation in the number of accumulations, which was set to 10 for this study.

Histological analysis. The fixed gonads were dehydrated through a graded series of ethanol, embedded in paraffin, sectioned into 3 µm slices on a rotary microtome, stained using hematoxylin and eosin and finally mounted on glass microscope slides. Gametogenesis was evaluated for each individual through the identification of regression signs (*i.e.*, epithelial detachment or advanced regression stage).

Glycogen content. Glycogen levels in muscle were measured in triplicate with a Glycogen Colorimetric/Fluorometric Assay Kit (BioVision©, Milpitas, CA, USA) following the manufacturer's instructions. Briefly, 10 mg of thawed muscle was diluted with 200 µl of distilled water, then boiled at 100 °C for 10 min and centrifuged at 13,000 rpm for 5 min. The supernatants were hydrolyzed by incubation with a hydrolysis enzyme mixture for 30 min at room temperature. To avoid glucose background readings, a glucose control without the addition of a hydrolysis enzyme mixture was used to determine the level of glucose present in the samples, and thus, the glucose background was subtracted from the glycogen readings. Subsequently, the samples were incubated with a reaction mixture for the oxidation reaction, and the resulting-colored product was evaluated for optical density (OD) at 570 nm.

Supplementary Results

Pearl rotation. The mean angular speed of pearl rotation in the pearl sac of *P. margaritifera* was similar among conditions (ANOVA, $P = 0.355$), with values of 5.9 ± 2.6, 4.0 ± 1.5 and 6.5 ± 1.3 deg min^{-1} in the control, 0.025 and 1 µg L^{-1} conditions, respectively.

Gametogenesis. All pearl oysters were of the male sex, except one individual of the female sex in the control condition. No sign of abnormal gametogenesis was observed by gonad cross-section histology analysis, regardless of condition.

Keshi pearl origin. Following a gentle sanding step, the purple particle (~9 µm) embedded in the mineral surface microlayer of the keshi pearl was tentatively identified using µ-Raman; however, it remained within a thin mineral layer and was subsequently lost during further sanding. Consequently, this approach failed to detect a PE signature corresponding to MNPs derived from

weathered purple rope. To overcome losses due to sanding, the particles were initially analyzed as a whole using Py-GC-MS, yet the mass spectrometry signals were not workable. In a subsequent attempt, a keshi pearl was dissolved using 98% sulfuric acid, after confirming its harmlessness for both PE and PP fragments. Employing this technique, several black fragments were observed and provisionally identified using μ-FTIR, although none of them matched the signature of PP spat collector.

Gene coexpression modules associated with MNPs and physiological traits. *Mantle module functional enrichment.* Among the modules of interest, 5 modules (cluster 1) were characterized by reduced expression under MNP conditions compared to control conditions, with the darkgrey (N = 103 genes) and turquoise (N = 5,346 genes) modules showing significantly lower ME expression at 0.025 (Dunn's test, P = 0.043) and 1 (Dunn's test, P = 0.023) μg L^{-1} MNPs, respectively. In the darkgrey module, GO enrichment analysis for BP highlighted "negative regulation of calcium ion-dependent exocytosis" (GO:0045955, $P_{adj} < 0.001$). The turquoise module exhibited several representative enrichments (N = 15 GO) associated with cell organization and biogenesis, metabolism, development and signal transduction. Four modules were also identified in cluster 2, with the brown module (N = 1,606 genes) showing significantly higher ME expression at 1 μg L^{-1} MNPs than under the control conditions (Tukey's HSD test, P = 0.006). The most significant enrichments identified in this module were "chitin metabolic process" (GO:0006030, $P_{adj} < 0.001$), "positive regulation of lipoprotein transport" (GO:0140077, $P_{adj} < 0.001$), "ribonucleoside catabolic process" (GO:0042454, $P_{adj} = 0.006$) and "biological adhesion" (GO:0022610, $P_{adj} = 0.005$).

Hemocyte module functional enrichment. A coexpression module was constructed by WGCNA of the expression values of 24,910 genes in 29 hemocyte samples. Overall, 12 modules were detected (Figure S8), and a total of 3 modules of interest were selected according to module-trait relationships ($r \geq 0.45$, $P \leq 0.01$), with 727, 1,020 and 2,092 genes in the magenta, pink and red modules, respectively (Figure S9). None of these 3 modules were related to condition, but the magenta module exhibited a strong correlation with 0.025 μg L^{-1} MNPs (r = –0.67, $P < 0.001$) and 1 μg L^{-1} MNPs (r = –0.52, P = 0.004), and there was a significant difference in ME expression between the control condition and both 0.025 and 1 μg L^{-1} conditions (Tukey's HSD test, P = 0.022 and P = 0.017, respectively) (Figure S9). This module was significantly enriched for "maturation

of LSU-rRNA from tricistronic rRNA transcript" (GO:0002108, $P_{adj} < 0.001$), "cytoplasmic translation" (GO:0002181, $P_{adj} < 0.001$), "ribosomal small subunit assembly" (GO:0000028, $P_{adj} < 0.001$) and "establishment of protein localization to endoplasmic reticulum" (GO:0072599, $P_{adj} = 0.006$) (Figure S9). Details for all GO enrichments in BP and MF are provided for the magenta, pink and red modules in Table S4.

A total of 204 DEGs were identified under MNP conditions compared to the control conditions, with 132 DEGs *vs.* 0.025 µg L^{-1} MNPs and 110 DEGs *vs.* 1 µg L^{-1} MNPs, of which 38 were common DEGs (Figure S9). A total of 73 and 59 up- and downregulated genes, respectively, were found in individuals under the 0.025 µg L^{-1} condition compared with the control condition, and 55 and 55 up- and downregulated genes, respectively, in the 1 µg L^{-1} condition compared to the control condition (Figure S6). A complete list of DEG distribution among WGCNA modules in hemocyte samples is available in Table S5.

Pearl sac module functional enrichment. A coexpression module was constructed by WGCNA of the expression values of 28,116 genes in 29 pearl sac samples. Overall, 11 modules were detected (Figure S9), but no modules were selected according to module-trait relationships ($r \geq 0.45$, $P \leq 0.01$).

A total of 146 DEGs were identified in MNP conditions compared to the control condition, with 80 DEGs *vs.* 0.025 µg L^{-1} MNPs and 73 DEGs *vs.* 1 µg L^{-1} MNPs, with 7 common DEGs. We found a total of 22 and 58 up- and downregulated genes, respectively, in individuals treated under the 0.025 µg L^{-1} condition compared with individuals treated under the control condition and 44 and 29 up- and downregulated genes, respectively, in the 1 µg L^{-1} condition (Figure S6). A complete list of DEGs in the pearl sac is available in Table S6.

Supplementary Figures and Tables

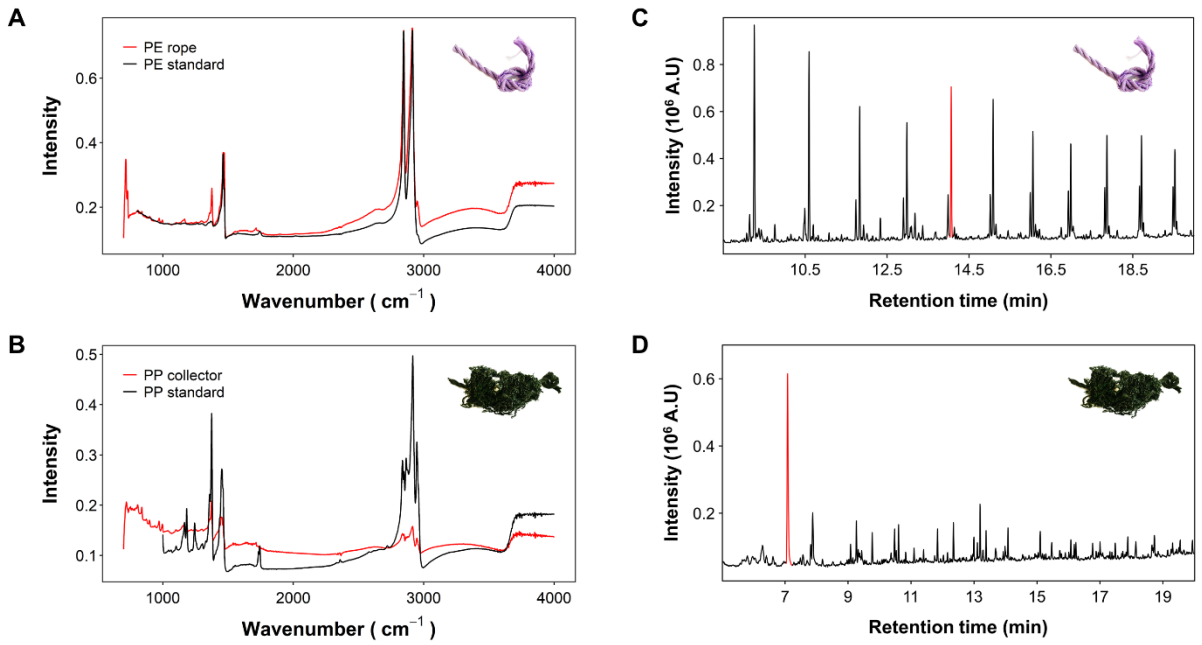

Figure S1. Polymer identification by FTIR and Py-GC-MS in both plastic pearl farming gear used for micro-nanoplastic production. (A) FTIR identification of polyethylene (PE) for the synthetic rope and (B) polypropylene (PP) for the spat collector. (C) Synthetic rope analyzed by Py-GC-MS with the specific pattern of PE including the 1,13 tetradecadiene specific marker in red and (D) the pyrogram of spat collector with the specific detection of 2,4 dimethyl-1-heptene in red.

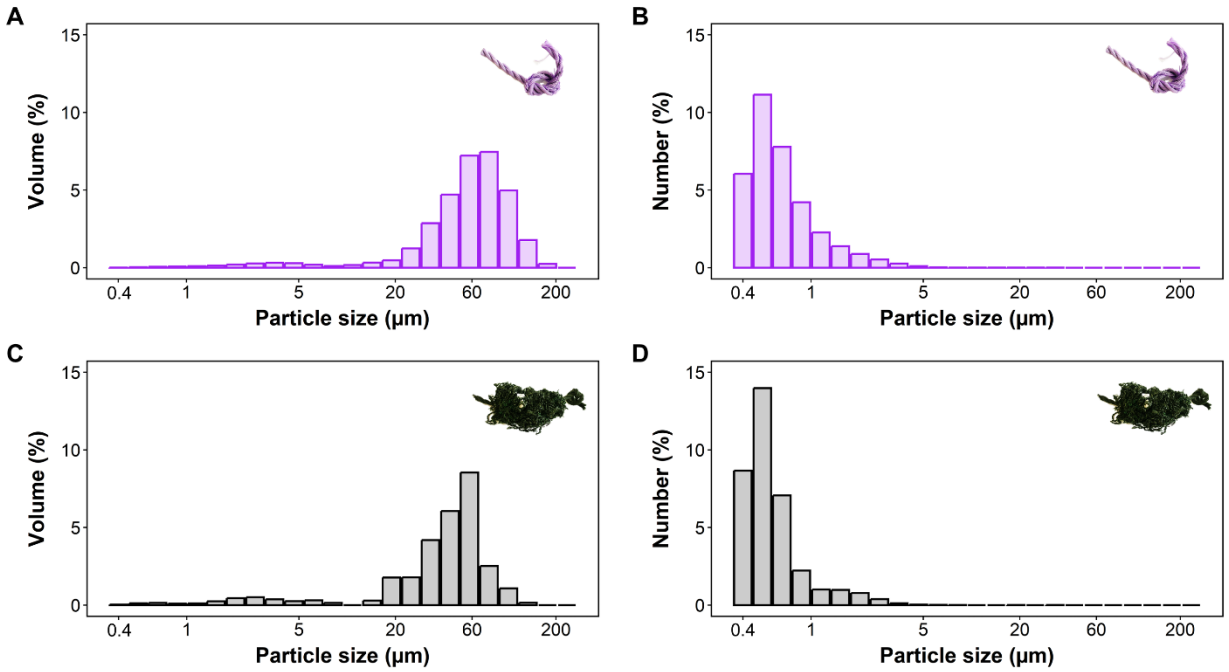

Figure S2. Particle size distribution of micro-nanoplastics by laser diffraction analysis. Bar plots show the differences in volume and number of particle sizes made from (A and B) rope and (C and D) spat collector.

Table S1. Sequencing results and reads survival after trimming and mapping.

Sample	Individual	Condition (µg L^{-1})	Input read pairs	Reads survival	Reads mapped
Mantle	1	0 (control)	2.97×10^7	2.81×10^7	1.35×10^7
Mantle	2	0 (control)	7.84×10^7	7.45×10^7	3.91×10^7
Mantle	3	0 (control)	3.60×10^7	3.42×10^7	1.43×10^7
Mantle	4	0 (control)	2.82×10^7	2.68×10^7	1.40×10^7
Mantle	5	0 (control)	3.37×10^7	3.19×10^7	1.42×10^7
Mantle	6	0 (control)	5.24×10^7	5.01×10^7	2.20×10^7
Mantle	7	0 (control)	5.19×10^7	4.96×10^7	2.46×10^7
Mantle	8	0 (control)	3.10×10^7	2.92×10^7	1.46×10^7
Mantle	9	0 (control)	2.50×10^7	2.39×10^7	1.15×10^7
Mantle	10	0.025	2.69×10^7	2.55×10^7	1.26×10^7
Mantle	11	0.025	2.96×10^7	2.81×10^7	1.20×10^7
Mantle	12	0.025	3.79×10^7	3.60×10^7	1.73×10^7
Mantle	13	0.025	2.89×10^7	2.76×10^7	1.40×10^7
Mantle	14	0.025	2.71×10^7	2.59×10^7	1.14×10^7
Mantle	15	0.025	2.87×10^7	2.73×10^7	1.34×10^7
Mantle	16	0.025	4.22×10^7	4.02×10^7	1.93×10^7
Mantle	17	0.025	3.34×10^7	3.18×10^7	1.56×10^7
Mantle	18	0.025	4.62×10^7	4.40×10^7	2.07×10^7
Mantle	19	0.025	4.21×10^7	4.00×10^7	2.12×10^7
Mantle	20	1	2.77×10^7	2.65×10^7	1.29×10^7
Mantle	21	1	3.74×10^7	3.56×10^7	1.80×10^7
Mantle	22	1	5.87×10^7	5.58×10^7	2.48×10^7
Mantle	23	1	2.78×10^7	2.65×10^7	1.39×10^7
Mantle	24	1	3.95×10^7	3.76×10^7	1.97×10^7
Mantle	25	1	4.03×10^7	3.82×10^7	1.76×10^7
Mantle	26	1	4.52×10^7	4.31×10^7	2.28×10^7
Mantle	27	1	1.69×10^7	1.60×10^7	7.18×10^6
Mantle	28	1	2.75×10^7	2.62×10^7	1.32×10^7
Mantle	29	1	2.99×10^7	2.85×10^7	1.40×10^7
Hemocytes	1	0 (control)	2.72×10^7	2.59×10^7	1.01×10^7
Hemocytes	2	0 (control)	4.22×10^7	3.94×10^7	1.38×10^7
Hemocytes	3	0 (control)	8.63×10^6	8.24×10^6	2.75×10^6
Hemocytes	4	0 (control)	1.71×10^7	1.64×10^7	6.41×10^6
Hemocytes	5	0 (control)	3.21×10^7	3.06×10^7	1.15×10^7
Hemocytes	6	0 (control)	3.21×10^7	3.00×10^7	1.13×10^7
Hemocytes	7	0 (control)	3.05×10^7	2.88×10^7	1.19×10^7
Hemocytes	8	0.025	3.50×10^7	3.31×10^7	1.24×10^7
Hemocytes	9	0.025	3.12×10^7	2.99×10^7	1.17×10^7
Hemocytes	10	0.025	4.08×10^7	3.89×10^7	1.53×10^7
Hemocytes	11	0.025	3.86×10^7	3.67×10^7	1.51×10^7
Hemocytes	12	0.025	3.11×10^7	2.97×10^7	1.23×10^7

Table S1 (*continued*)

Hemocytes	13	0.025	3.69×10^7	3.53×10^7	1.29×10^7
Hemocytes	14	0.025	3.58×10^7	3.42×10^7	1.13×10^7
Hemocytes	15	0.025	3.44×10^7	3.29×10^7	1.35×10^7
Hemocytes	16	0.025	2.08×10^7	1.99×10^7	8.11×10^6
Hemocytes	17	0.025	2.41×10^7	2.30×10^7	9.38×10^6
Hemocytes	18	0.025	4.22×10^7	4.02×10^7	1.47×10^7
Hemocytes	19	1	4.02×10^7	3.84×10^7	1.48×10^7
Hemocytes	20	1	3.55×10^7	3.37×10^7	1.32×10^7
Hemocytes	21	1	2.76×10^7	2.63×10^7	9.54×10^6
Hemocytes	22	1	5.31×10^7	5.06×10^7	1.93×10^7
Hemocytes	23	1	3.06×10^7	2.90×10^7	1.07×10^7
Hemocytes	24	1	4.29×10^7	4.10×10^7	1.65×10^7
Hemocytes	25	1	3.33×10^7	3.17×10^7	1.13×10^7
Hemocytes	26	1	4.33×10^7	4.14×10^7	1.53×10^7
Hemocytes	27	1	4.02×10^7	3.83×10^7	1.36×10^7
Hemocytes	28	1	3.27×10^7	3.12×10^7	1.12×10^7
Hemocytes	29	1	2.41×10^7	2.28×10^7	8.51×10^6
Pearl sac	1	0 (control)	2.68×10^7	2.56×10^7	1.11×10^7
Pearl sac	2	0 (control)	3.14×10^7	2.99×10^7	1.34×10^7
Pearl sac	3	0 (control)	3.34×10^7	3.18×10^7	1.56×10^7
Pearl sac	4	0 (control)	3.80×10^7	3.63×10^7	1.61×10^7
Pearl sac	5	0 (control)	3.40×10^7	3.24×10^7	1.41×10^7
Pearl sac	6	0 (control)	3.13×10^7	2.98×10^7	1.36×10^7
Pearl sac	7	0 (control)	3.66×10^7	3.49×10^7	1.63×10^7
Pearl sac	8	0 (control)	2.42×10^7	2.30×10^7	9.55×10^6
Pearl sac	9	0 (control)	3.89×10^7	3.72×10^7	1.66×10^7
Pearl sac	10	0 (control)	4.55×10^7	4.34×10^7	1.89×10^7
Pearl sac	11	0.025	3.47×10^7	3.31×10^7	1.62×10^7
Pearl sac	12	0.025	3.22×10^7	3.07×10^7	1.31×10^7
Pearl sac	13	0.025	4.47×10^7	4.25×10^7	1.88×10^7
Pearl sac	14	0.025	3.22×10^7	3.05×10^7	1.34×10^7
Pearl sac	15	0.025	3.05×10^7	2.92×10^7	1.23×10^7
Pearl sac	16	0.025	5.59×10^7	5.35×10^7	2.61×10^7
Pearl sac	17	0.025	3.20×10^7	3.05×10^7	1.44×10^7
Pearl sac	18	0.025	3.36×10^7	3.21×10^7	1.32×10^7
Pearl sac	19	0.025	3.06×10^7	2.90×10^7	1.25×10^7
Pearl sac	20	0.025	3.59×10^7	3.43×10^7	1.67×10^7
Pearl sac	21	1	3.43×10^7	3.24×10^7	1.29×10^7
Pearl sac	22	1	3.29×10^7	3.13×10^7	1.32×10^7
Pearl sac	23	1	3.83×10^7	3.62×10^7	1.49×10^7
Pearl sac	24	1	3.92×10^7	3.73×10^7	1.59×10^7
Pearl sac	25	1	3.35×10^7	3.18×10^7	1.46×10^7
Pearl sac	26	1	3.25×10^7	3.10×10^7	1.31×10^7

Table S1 (*continued*)

Pearl sac	27	1	2.83×10^7	2.70×10^7	1.11×10^7
Pearl sac	28	1	2.95×10^7	2.81×10^7	1.38×10^7
Pearl sac	29	1	2.65×10^7	2.53×10^7	1.09×10^7

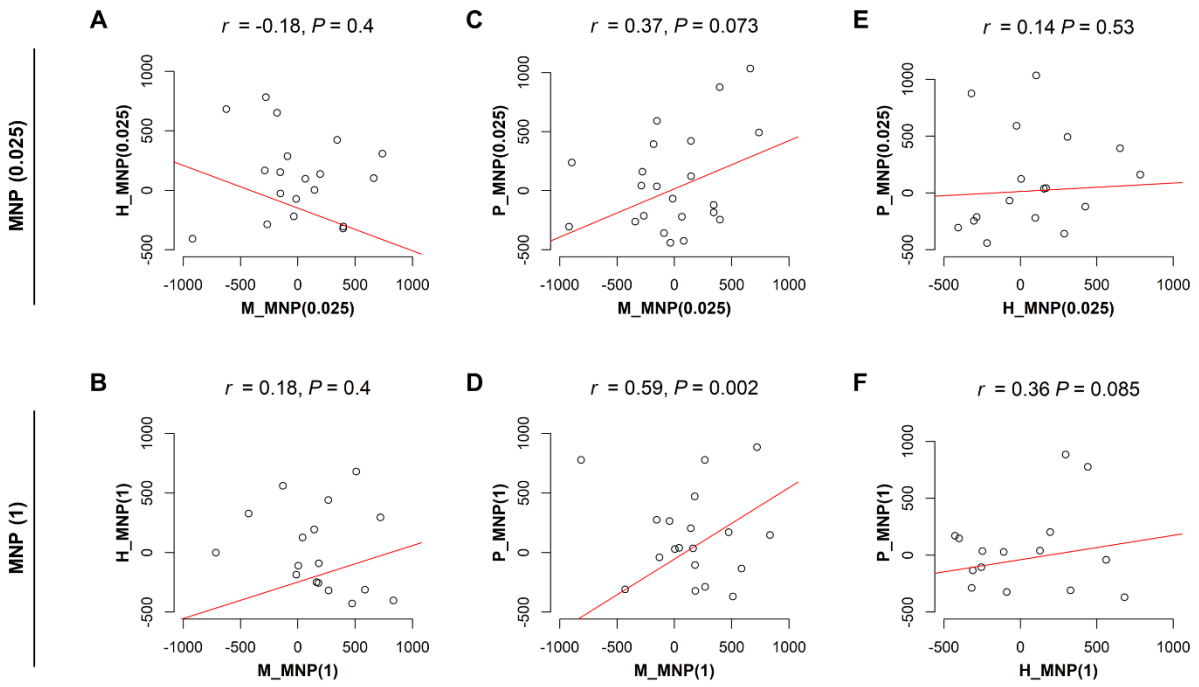

Figure S3. Correlations of eukaryotic orthologous group (KOG) expressions between tissues sampled in *P. margaritifera* after a 5-month exposure to 0.025 and 1 µg L^{-1} micro-nanoplastics. Pearson's correlations of KOG delta rank values between mantle and hemocytes (A–B), mantle and pearl sac (C–D), and hemocytes, and pearl sac (E–F) in 0.025 and 1 µg MNPs L^{-1}, respectively.

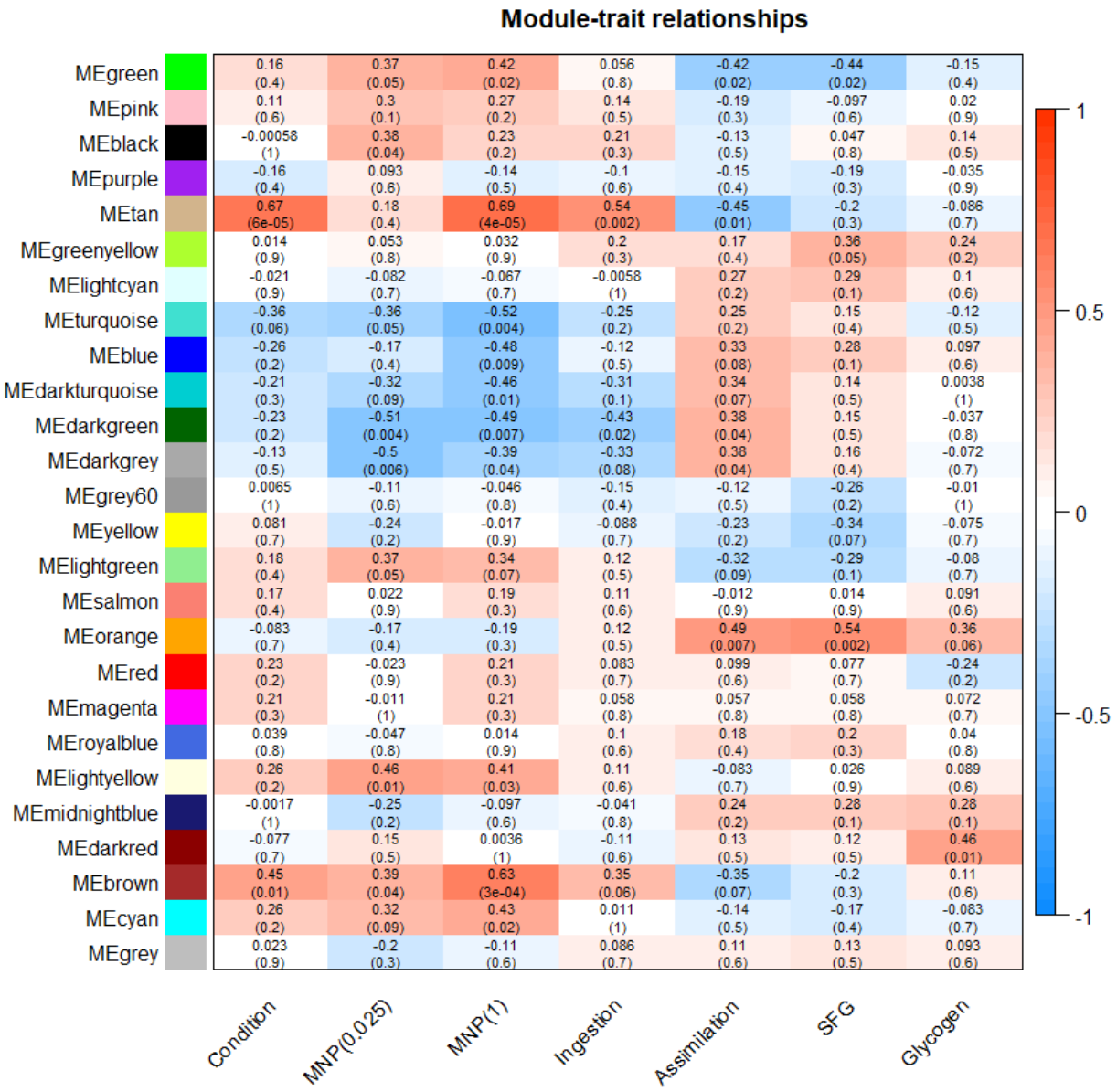

Figure S4. WGCNA module identification on mantle samples sequencing dataset. Correlation analysis of the identified modules according to conditions (control and MNP conditions), single MNP condition (0.025 or 1 µg L^{-1}) and to physiological traits of individuals showing significant effects in response to MNP exposure (*i.e.*, ingestion, assimilation efficiency, scope for growth, and glycogen stores).

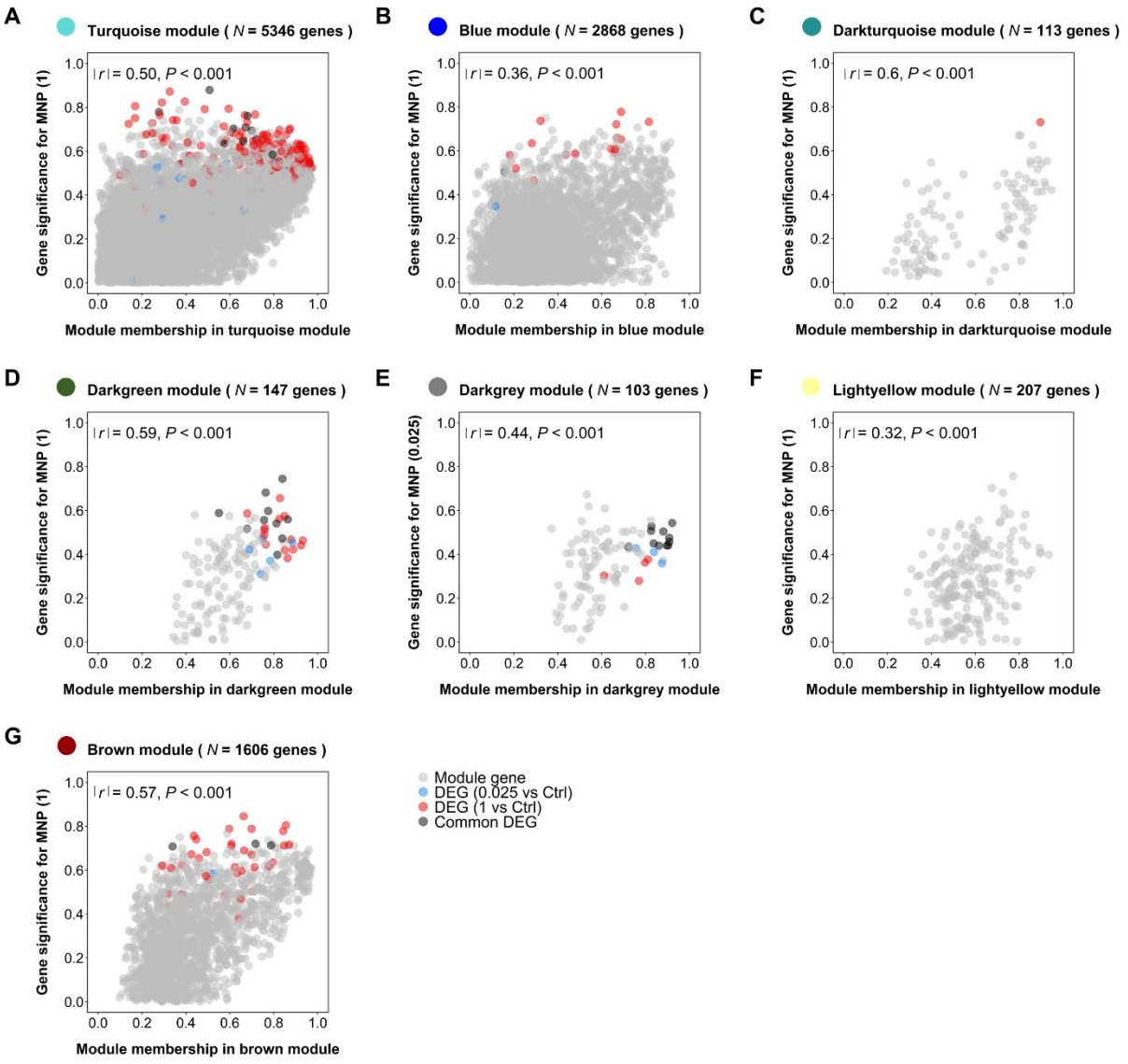

Figure S5. Gene significance for MNP conditions showing the best correlation *vs.* module membership in modules of interest illustrating module-trait associations from WGCNA on mantle samples sequencing dataset. Scatterplots of module genes in (A) turquoise, (B) blue, (C) darkturquoise, (D) darkgreen, (E) darkgrey, (F) lightyellow and (G) brown modules. Gray genes represent module genes; blue and red genes represent DEGs specific to 0.025 µg MNPs L^{-1} and 1 MNPs µg L^{-1}, respectively, and black genes represent common DEGs to both MNP conditions. DEGs identified in each module genes are detailed in Table S3.

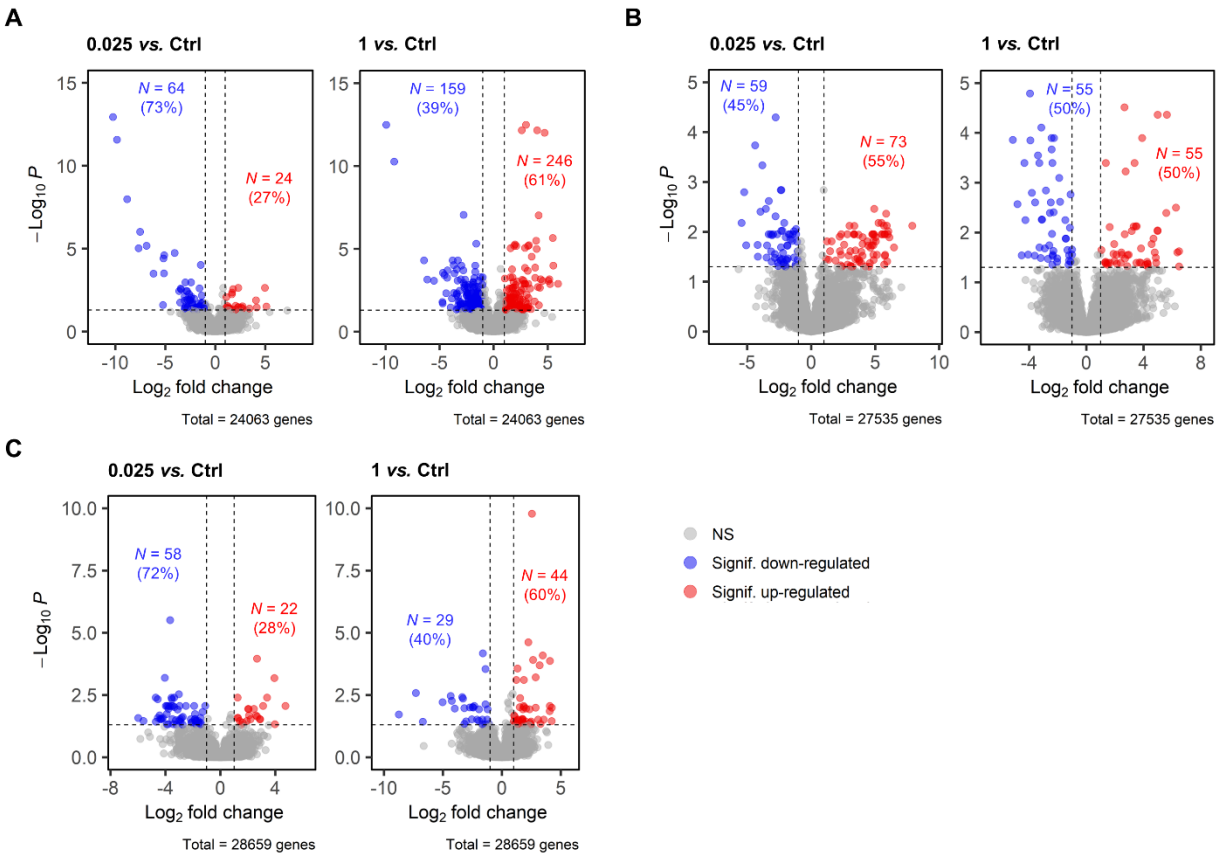

Figure S6. Differentially expressed genes between MNP conditions and the control in mantle, hemocytes, and pearl sac of *P. margaritifera* after a 5-month exposure to micro-nanoplastics. Volcano plot showing expression of differentially expressed genes between MNP conditions (0.025 and 1 µg L^{-1}) compared to the control ($|\log_2 FC| > 2$; FDR < 0.01) with a $P_{adj} < 0.05$ used as the threshold to judge the significance of the difference in gene expression in (A) mantle (B) hemocytes and (C) pearl sac. Blue plots represent downregulated genes; red plots represent upregulated genes and gray plots represent genes with no significant difference.

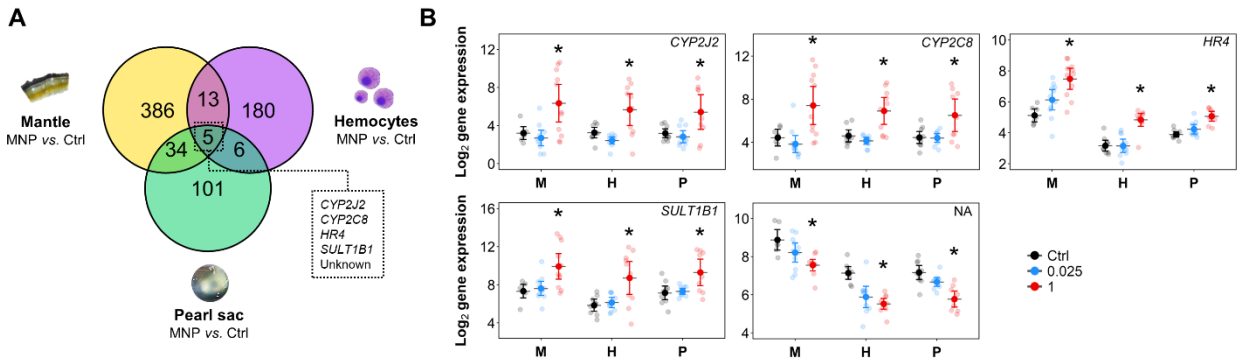

Figure S7. Differentially expressed genes across *P. margaritifera* tissues after a 5-month exposure to micro-nanoplastics. (A) Venn diagram of shared differentially expressed genes (DEGs) in mantle, hemocyte and pearl sac samples identified in both MNP conditions compared to the control ($|\log_2 FC| > 2$; FDR < 0.01). (B) Boxplots of gene expression associated with DEGs common to the tissue samples, including *CYP2J2* and *CYP2C8* (cytochrome P450 family 2 subfamily J member 2 and subfamily C member 8, respectively), *HR4* (hormone receptor 4), *SULT1B1* (sulfotransferase family 1B member 1) and an unannotated gene (NA). Significant differences between the control and MNP conditions ($|\log_2 FC| > 2$; FDR < 0.01) are represented by an asterisk ("*"). Data are expressed as the mean with the 95% confidence interval ($7 \leq N \leq 12$). M: mantle; H: hemocytes; P: pearl sac.

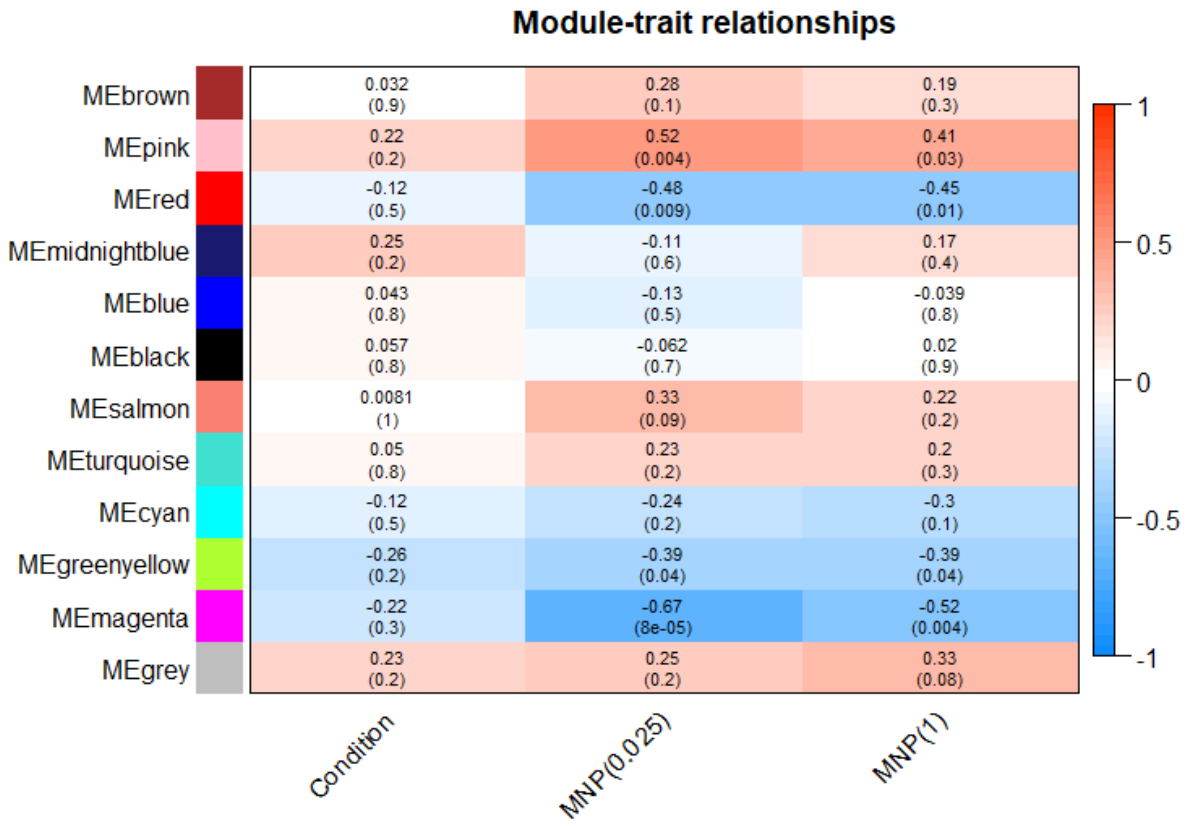

Figure S8. WGCNA module identification on hemocyte samples sequencing dataset. Correlation analysis of the identified modules according to conditions (control and MNP conditions) and single MNP condition (0.025 or 1 µg L^{-1}).

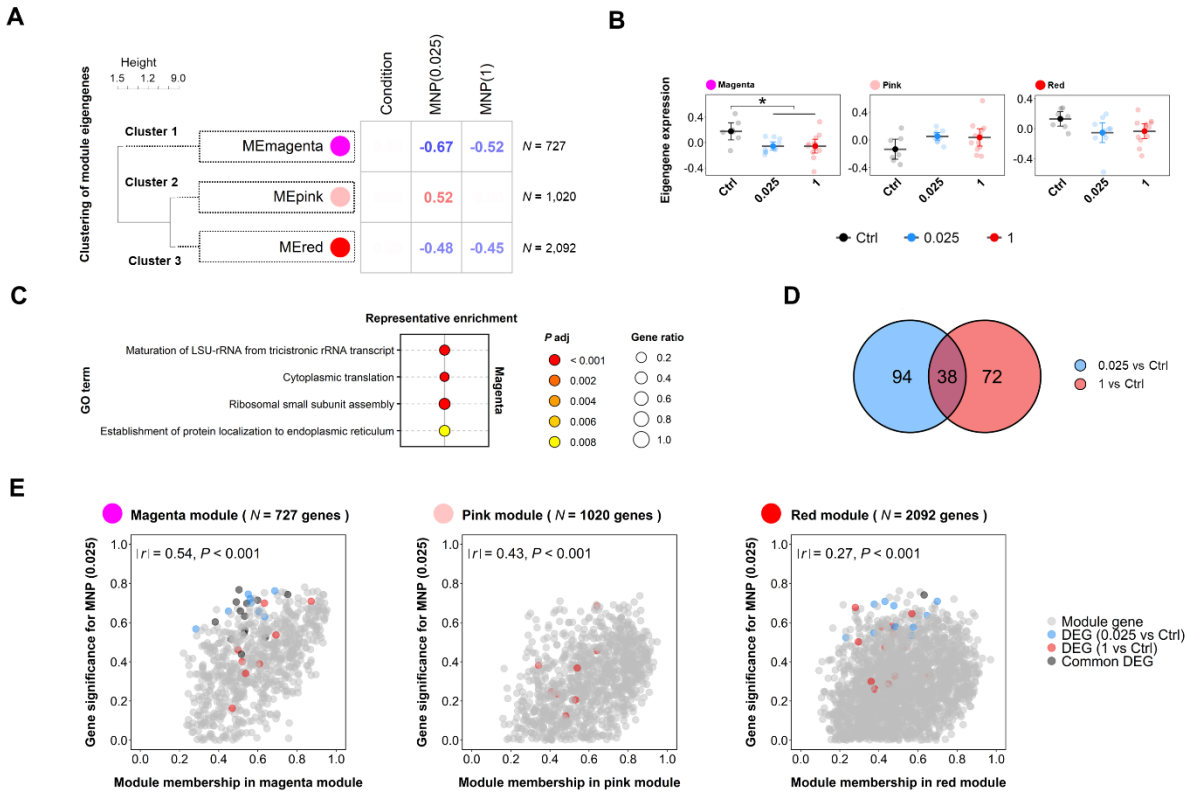

Figure S9. Transcriptomic responses in the hemocytes of *P. margaritifera* after a 5-month exposure to micro-nanoplastics. (A) Heatmap of identified modules (*y*-axis) and functionally enriched pathways in relation to experimental traits ($|\boldsymbol{r}| \geq 0.45$, $P \leq 0.01$; *x*-axis) from WGCNA. The clustering tree of module eigengenes (MEs) on the left is based on a merging threshold of 100% dissimilarity initially established at 25% for network construction. The numbers on the right of the heatmap represent the number of genes identified in each module. (B) Eigengene expression for selected WGCNA modules significantly correlated with experimental conditions and/or physiological traits in response to MNP exposure ("*", $P < 0.05$; "**", $P < 0.01$). Data are expressed as the mean with the 95% confidence interval (N = 7–12). (C) Representative functional enrichment analysis of module genes identified in the magenta module based on an adjusted *P* value cutoff ($P < 0.01$) and cut-height (0.8) of the GO terms tree to obtain "independent groups". The dendrograms depict the sharing of genes between categories; the fractions correspond to genes with $P < 0.05$ relative to the total number of genes within the category. (D) Venn diagram of differentially expressed genes (DEGs) in both MNP conditions compared to the control ($|\log_2 FC| > 2$; FDR < 0.01). (E) Scatterplots of gene significance for condition *vs.* module membership in the

in magenta, pink and red modules illustrating module-trait associations. Gray genes represent module genes; blue and red genes represent DEGs specific to 0.025 and 1 μg L^{-1} MNPs, respectively. DEGs identified in each module genes are detailed in Table S5.

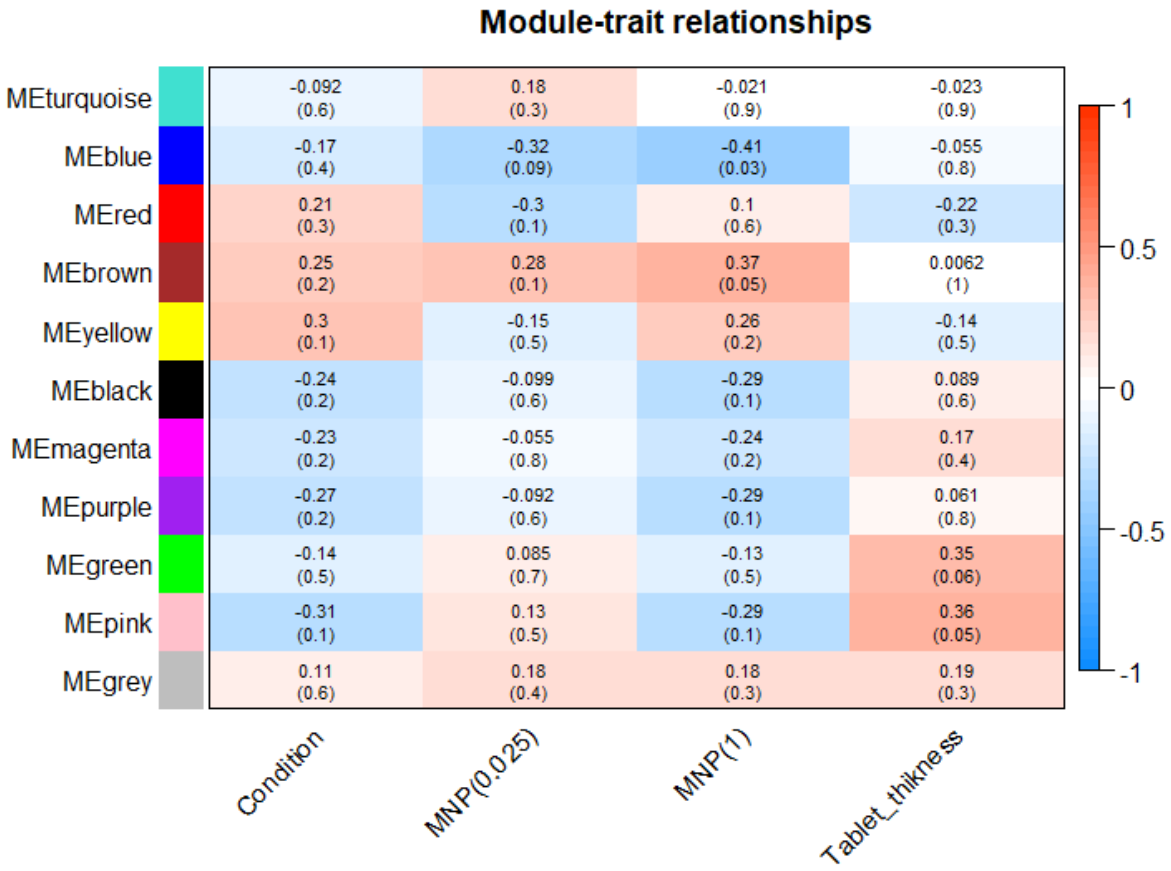

Figure S10. WGCNA module identification on pearl sac samples sequencing dataset. Correlation analysis of the identified modules according to conditions (control and MNP conditions), single MNP condition (0.025 or 1 µg L^{-1}), and pearl quality traits of individuals showing significant effects in response to MNP exposure (*i.e.*, aragonite platelet thickness).

Table S2. Gene Ontology (GO) enrichments in molecular function (MF) and biological process (BP) of module genes of interest (turquoise, darkgrey, brown, and tan modules) identified in mantle samples from WGCNA.

GO ID	GO term	Level	Nseqs	P_{adj}
● Turquoise module				
MF				
GO:0045505	dynein intermediate chain binding	2	47	< 0.001
GO:0003774	motor activity	2	149	< 0.001
GO:0003777	microtubule motor activity	2	84	< 0.001
GO:0015631	tubulin binding	4	288	< 0.001
GO:0008017	microtubule binding	2	205	< 0.001
GO:0008092	cytoskeletal protein binding	3	859	< 0.001
GO:0030371	translation repressor activity	2	43	< 0.001
GO:0045504	dynein heavy chain binding	2	19	< 0.001
GO:0005509	calcium ion binding	5	845	< 0.001
GO:0030234	enzyme regulator activity	2	775	0.0015
GO:0004550	nucleoside diphosphate kinase activity	5	17	0.0017
GO:0003735	structural constituent of ribosome	2	134	0.0020
GO:0001103	RNA polymerase II repressing transcription factor binding	2	20	0.0025
GO:0045503	dynein light chain binding	3	13	0.0027
GO:0004826	phenylalanine-tRNA ligase activity	2	8	0.0028
GO:0004096	catalase activity	2	10	0.0033
GO:0003723	RNA binding	3	1325	0.0043
GO:0032027	myosin light chain binding	2	7	0.0053
GO:0015038	glutathione disulfide oxidoreductase activity	2	10	0.0060
GO:0070410	co-SMAD binding	2	25	0.0074
GO:0004708	MAP kinase kinase activity	5	11	0.0097
GO:0043015	gamma-tubulin binding	2	24	0.0118
GO:0098772	molecular function regulator	1	1264	0.0119
GO:0003810	protein-glutamine gamma-glutamyltransferase activity	2	22	0.0123
GO:0005272	sodium channel activity	2	44	0.0134
GO:0004198	calcium-dependent cysteine-type endopeptidase activity	6	22	0.0164
GO:0016881	acid-amino acid ligase activity	4	22	0.0221
GO:0017022	myosin binding	4	75	0.0232
GO:0032036	myosin heavy chain binding	2	5	0.0241
GO:0050145	nucleoside monophosphate kinase activity	2	23	0.0268
GO:0070739	protein-glutamic acid ligase activity	2	10	0.0285
GO:0016887	ATPase activity	2	549	0.0300
GO:0005248	voltage-gated sodium channel activity	3	11	0.0335
GO:0097371	MDM2/MDM4 family protein binding	2	6	0.0362
GO:0004653	polypeptide N-acetylgalactosaminyltransferase activity	2	16	0.0449

Table S2 (*continued*)

BP				
GO:0000226	microtubule cytoskeleton organization	4	362	< 0.001
GO:0003006	developmental process involved in reproduction	2	686	< 0.001
GO:0003341	cilium movement	2	141	< 0.001
GO:0003352	regulation of cilium movement	2	23	< 0.001
GO:0003356	regulation of cilium beat frequency	4	12	< 0.001
GO:0006928	movement of cell or subcellular component	2	1001	< 0.001
GO:0007010	cytoskeleton organization	4	725	< 0.001
GO:0007017	microtubule-based process	2	680	< 0.001
GO:0007018	microtubule-based movement	3	343	< 0.001
GO:0007224	smoothened signaling pathway	3	59	< 0.001
GO:0007288	sperm axoneme assembly	3	22	< 0.001
GO:0007389	pattern specification process	2	368	< 0.001
GO:0008543	fibroblast growth factor receptor signaling pathway	7	70	< 0.001
GO:0008589	regulation of smoothened signaling pathway	3	73	< 0.001
GO:0010457	centriole-centriole cohesion	2	11	< 0.001
GO:0010586	miRNA metabolic process	3	48	< 0.001
GO:0018095	protein polyglutamylation	3	22	< 0.001
GO:0018149	peptide cross-linking	2	28	< 0.001
GO:0018200	peptidyl-glutamic acid modification	2	37	< 0.001
GO:0019722	calcium-mediated signaling	2	119	< 0.001
GO:0021532	neural tube patterning	3	6	< 0.001
GO:0021591	ventricular system development	3	32	< 0.001
GO:0021915	neural tube development	4	58	< 0.001
GO:0022402	cell cycle process	2	750	< 0.001
GO:0022412	cellular process involved in reproduction in multicellular organism	2	294	< 0.001
GO:0022414	reproductive process	1	1077	< 0.001
GO:0030030	cell projection organization	3	814	< 0.001
GO:0030902	hindbrain development	2	15	< 0.001
GO:0031023	microtubule organizing center organization	3	63	< 0.001
GO:0031503	protein-containing complex localization	2	150	< 0.001
GO:0032886	regulation of microtubule-based process	4	192	< 0.001
GO:0035295	tube development	2	213	< 0.001
GO:0035721	intraciliary retrograde transport	6	19	< 0.001
GO:0035735	intraciliary transport involved in cilium assembly	2	18	< 0.001
GO:0035845	photoreceptor cell outer segment organization	3	11	< 0.001
GO:0036158	outer dynein arm assembly	4	30	< 0.001
GO:0036159	inner dynein arm assembly	8	22	< 0.001
GO:0040011	locomotion	1	674	< 0.001
GO:0044458	motile cilium assembly	2	19	< 0.001
GO:0045494	photoreceptor cell maintenance	2	51	< 0.001
GO:0045724	positive regulation of cilium assembly	2	22	< 0.001
GO:0046599	regulation of centriole replication	6	23	< 0.001

Table S2 (*continued*)

GO:0048598	embryonic morphogenesis	2	326	< 0.001
GO:0048609	multicellular organismal reproductive process	2	443	< 0.001
GO:0048793	pronephros development	5	20	< 0.001
GO:0050678	regulation of epithelial cell proliferation	3	176	< 0.001
GO:0060287	epithelial cilium movement involved in determination of left/right asymmetry	3	11	< 0.001
GO:0060429	epithelium development	4	168	< 0.001
GO:0060438	trachea development	2	9	< 0.001
GO:0060562	epithelial tube morphogenesis	2	96	< 0.001
GO:0060632	regulation of microtubule-based movement	2	41	< 0.001
GO:0061512	protein localization to cilium	5	39	< 0.001
GO:0070286	axonemal dynein complex assembly	2	51	< 0.001
GO:0070925	organelle assembly	2	481	< 0.001
GO:0072089	stem cell proliferation	2	45	< 0.001
GO:0097499	protein localization to non-motile cilium	6	11	< 0.001
GO:0097711	ciliary basal body-plasma membrane docking	3	38	< 0.001
GO:0120036	plasma membrane bounded cell projection organization	2	590	< 0.001
GO:1902017	regulation of cilium assembly	6	46	< 0.001
GO:1902115	regulation of organelle assembly	2	137	< 0.001
GO:1902117	positive regulation of organelle assembly	2	51	< 0.001
GO:1904158	axonemal central apparatus assembly	4	9	< 0.001
GO:1904491	protein localization to ciliary transition zone	6	9	< 0.001
GO:1905515	non-motile cilium assembly	2	56	< 0.001
GO:0009653	anatomical structure morphogenesis	2	1184	0.0012
GO:0007051	spindle organization	2	117	0.0017
GO:1903047	mitotic cell cycle process	3	502	0.0017
GO:0051865	protein autoubiquitination	9	98	0.0018
GO:0030154	cell differentiation	2	1247	0.0022
GO:0051302	regulation of cell division	2	102	0.0032
GO:0007166	cell surface receptor signaling pathway	2	1153	0.0033
GO:0021756	striatum development	2	16	0.0033
GO:0003002	regionalization	2	236	0.0034
GO:0010838	positive regulation of keratinocyte proliferation	2	14	0.0035
GO:1902855	regulation of non-motile cilium assembly	2	11	0.0035
GO:0001822	kidney development	2	125	0.0036
GO:0060296	regulation of cilium beat frequency involved in ciliary motility	2	8	0.0036
GO:0060830	ciliary receptor clustering involved in smoothened signaling pathway	3	5	0.0037
GO:0035148	tube formation	3	115	0.0037
GO:0050680	negative regulation of epithelial cell proliferation	2	84	0.0039
GO:1902116	negative regulation of organelle assembly	3	31	0.0043
GO:0035239	tube morphogenesis	3	252	0.0043
GO:0010564	regulation of cell cycle process	5	438	0.0047
GO:0090394	negative regulation of excitatory postsynaptic potential	3	9	0.0047
GO:1903441	protein localization to ciliary membrane	5	9	0.0050

Table S2 (*continued*)

GO:0051262	protein tetramerization	2	85	0.0051
GO:1902412	regulation of mitotic cytokinesis	2	5	0.0059
GO:0071599	otic vesicle development	2	7	0.0059
GO:0060041	retina development in camera-type eye	2	42	0.0061
GO:0009888	tissue development	2	459	0.0061
GO:0072178	nephric duct morphogenesis	2	5	0.0062
GO:0046602	regulation of mitotic centrosome separation	2	7	0.0079
GO:0051640	organelle localization	2	363	0.0079
GO:0021670	lateral ventricle development	2	8	0.0080
GO:0030916	otic vesicle formation	5	6	0.0082
GO:0030216	keratinocyte differentiation	3	32	0.0088
GO:0007507	heart development	4	175	0.0089
GO:0045880	positive regulation of smoothened signaling pathway	2	37	0.0089
GO:0048646	anatomical structure formation involved in morphogenesis	2	648	0.0091
GO:0008283	cell population proliferation	2	370	0.0108
GO:1902857	positive regulation of non-motile cilium assembly	3	8	0.0109
GO:0034453	microtubule anchoring	2	26	0.0109
GO:0019236	response to pheromone	4	7	0.0114
GO:0009953	dorsal/ventral pattern formation	2	73	0.0120
GO:2000177	regulation of neural precursor cell proliferation	5	90	0.0122
GO:0006432	phenylalanyl-tRNA aminoacylation	3	7	0.0129
GO:0070986	left/right axis specification	2	21	0.0131
GO:0048839	inner ear development	3	34	0.0133
GO:0031122	cytoplasmic microtubule organization	2	47	0.0134
GO:0008544	epidermis development	3	42	0.0136
GO:0048731	system development	2	457	0.0163
GO:0032465	regulation of cytokinesis	2	65	0.0168
GO:0032053	ciliary basal body organization	4	7	0.0169
GO:0018243	protein O-linked glycosylation via threonine	3	12	0.0211
GO:2000574	regulation of microtubule motor activity	2	10	0.0215
GO:0009141	nucleoside triphosphate metabolic process	2	75	0.0217
GO:0035610	protein side chain deglutamylation	2	5	0.0248
GO:1901068	guanosine-containing compound metabolic process	3	40	0.0276
GO:0031424	keratinization	2	11	0.0277
GO:0007281	germ cell development	3	121	0.0279
GO:2000027	regulation of animal organ morphogenesis	5	72	0.0280
GO:0009887	animal organ morphogenesis	3	439	0.0297
GO:0120034	positive regulation of plasma membrane bounded cell projection assembly	2	91	0.0318
GO:0046548	retinal rod cell development	7	10	0.0327
GO:0042733	embryonic digit morphogenesis	4	42	0.0338
GO:0007286	spermatid development	2	42	0.0350
GO:0045185	maintenance of protein location	2	107	0.0351
GO:0070121	Kupffer's vesicle development	3	11	0.0352

Table S2 (*continued*)

GO:0030856	regulation of epithelial cell differentiation	5	84	0.0354
GO:0046039	GTP metabolic process	4	28	0.0356
GO:0002467	germinal center formation	4	11	0.0363
GO:0060831	smoothened signaling pathway involved in dorsal/ventral neural tube patterning	2	5	0.0364
GO:0007160	cell-matrix adhesion	4	73	0.0365
GO:0048666	neuron development	2	120	0.0372
GO:0003170	heart valve development	2	11	0.0381
GO:0010837	regulation of keratinocyte proliferation	4	37	0.0408
GO:0003254	regulation of membrane depolarization	3	35	0.0410
GO:0048562	embryonic organ morphogenesis	4	79	0.0444
GO:1903546	protein localization to photoreceptor outer segment	2	6	0.0453
GO:0031589	cell-substrate adhesion	2	115	0.0484
GO:0051457	maintenance of protein location in nucleus	3	27	0.0495
GO:0002250	adaptive immune response	2	49	0.0497
● **Darkgrey module**				
MF				
GO:0030492	hemoglobin binding	3	15	< 0.001
GO:0017075	syntaxin-1 binding	2	18	< 0.001
GO:0000182	rDNA binding	7	5	< 0.001
GO:0098695	inositol 1,4,5-trisphosphate receptor activity involved in regulation of postsynaptic cytosolic calcium levels	2	5	< 0.001
GO:0015086	cadmium ion transmembrane transporter activity	3	6	< 0.001
GO:1905394	retromer complex binding	3	6	< 0.001
GO:0019238	cyclohydrolase activity	2	6	< 0.001
GO:0005544	calcium-dependent phospholipid binding	3	53	< 0.001
GO:0005375	copper ion transmembrane transporter activity	3	7	< 0.001
GO:0015093	ferrous iron transmembrane transporter activity	2	7	< 0.001
GO:1990226	histone methyltransferase binding	4	7	< 0.001
GO:0004040	amidase activity	4	7	< 0.001
GO:0015926	glucosidase activity	2	33	< 0.001
GO:0004096	catalase activity	3	10	< 0.001
GO:0005220	inositol 1,4,5-trisphosphate-sensitive calcium-release channel activity	5	10	< 0.001
GO:0005381	iron ion transmembrane transporter activity	3	10	< 0.001
GO:0008422	beta-glucosidase activity	2	10	< 0.001
GO:0031994	insulin-like growth factor I binding	2	10	< 0.001
GO:0001968	fibronectin binding	3	11	< 0.001
GO:0005384	manganese ion transmembrane transporter activity	3	11	< 0.001
GO:0016857	racemase and epimerase activity, acting on carbohydrates and derivatives	4	11	< 0.001
GO:0019855	calcium channel inhibitor activity	2	11	< 0.001
GO:0050662	obsolete coenzyme binding	-1	11	< 0.001
GO:0001786	phosphatidylserine binding	2	45	< 0.001
GO:0004622	lysophospholipase activity	2	13	0.0012

Table S2 (*continued*)

GO:0042301	phosphate ion binding	2	13	0.0012
GO:0000149	SNARE binding	2	103	0.0017
GO:0035251	UDP-glucosyltransferase activity	2	14	0.0023
GO:0030276	clathrin binding	2	53	0.0032
GO:0046982	protein heterodimerization activity	3	189	0.0053
GO:0005509	calcium ion binding	2	845	0.0054
GO:0001085	RNA polymerase II transcription factor binding	3	16	0.0067
GO:0003951	NAD+ kinase activity	2	16	0.0067
GO:0090599	alpha-glucosidase activity	2	16	0.0067
GO:0016854	racemase and epimerase activity	2	17	0.0104
GO:0005520	insulin-like growth factor binding	4	19	0.0236
GO:0019905	syntaxin binding	4	69	0.0275
GO:0001103	RNA polymerase II repressing transcription factor binding	3	20	0.0312
GO:0043023	ribosomal large subunit binding	4	20	0.0314
GO:0008131	primary amine oxidase activity	3	21	0.0393
BP				
GO:0017158	regulation of calcium ion-dependent exocytosis	2	33	< 0.001
GO:0045920	negative regulation of exocytosis	2	22	< 0.001
GO:0045955	negative regulation of calcium ion-dependent exocytosis	2	11	< 0.001
GO:1903306	negative regulation of regulated secretory pathway	3	15	< 0.001
GO:2000301	negative regulation of synaptic vesicle exocytosis	3	7	0.0143
GO:0023061	signal release	2	104	0.0200
GO:0061792	secretory granule maturation	2	8	0.0227
GO:1903233	regulation of calcium ion-dependent exocytosis of neurotransmitter	5	8	0.0227
GO:0014049	positive regulation of glutamate secretion	4	9	0.0308
GO:0031339	negative regulation of vesicle fusion	2	9	0.0308
GO:1903305	regulation of regulated secretory pathway	4	101	0.0357
GO:0045956	positive regulation of calcium ion-dependent exocytosis	2	14	0.0375
GO:0099550	trans-synaptic signaling, modulating synaptic transmission	2	14	0.0375
GO:0014048	regulation of glutamate secretion	3	13	0.0382
GO:0032252	secretory granule localization	5	12	0.0406
GO:0048172	regulation of short-term neuronal synaptic plasticity	2	19	0.0460
● **Brown module**				
MF				
GO:0140318	protein transporter activity	2	25	< 0.001
GO:0001517	N-acetylglucosamine 6-O-sulfotransferase activity	5	6	< 0.001
GO:0008273	calcium, potassium:sodium antiporter activity	4	7	< 0.001
GO:0031994	insulin-like growth factor I binding	2	10	< 0.001
GO:0005452	inorganic anion exchanger activity	2	11	< 0.001
GO:0070012	oligopeptidase activity	3	7	< 0.001
GO:0016843	amine-lyase activity	2	5	< 0.001
GO:0015297	antiporter activity	5	72	< 0.001

Table S2 (*continued*)

GO:0005534	galactose binding	2	5	< 0.001
GO:0004567	beta-mannosidase activity	2	5	< 0.001
GO:0004104	cholinesterase activity	2	5	< 0.001
GO:0048037	obsolete cofactor binding	-1	13	< 0.001
GO:0005520	insulin-like growth factor binding	4	19	0.0010
GO:0008447	L-ascorbate oxidase activity	2	6	0.0012
GO:0008061	chitin binding	2	46	0.0015
GO:0030492	hemoglobin binding	3	15	0.0023
GO:0015347	sodium-independent organic anion transmembrane transporter activity	2	11	0.0051
GO:0030165	PDZ domain binding	2	71	0.0057
GO:0022821	potassium ion antiporter activity	4	17	0.0101
GO:0004089	carbonate dehydratase activity	3	30	0.0120
GO:0008191	metalloendopeptidase inhibitor activity	4	30	0.0121
GO:1905172	RISC complex binding	2	7	0.0121
GO:0016840	carbon-nitrogen lyase activity	3	25	0.0246
GO:0005125	cytokine activity	5	52	0.0274
GO:0016742	hydroxymethyl-, formyl- and related transferase activity	2	13	0.0274
GO:0047631	ADP-ribose diphosphatase activity	3	8	0.0364
GO:0070883	pre-miRNA binding	3	8	0.0388
GO:0070008	serine-type exopeptidase activity	2	14	0.0469
GO:0004553	hydrolase activity, hydrolyzing O-glycosyl compounds	2	179	0.0486
BP				
GO:0000272	polysaccharide catabolic process	3	55	< 0.001
GO:0005975	carbohydrate metabolic process	2	484	< 0.001
GO:0006022	aminoglycan metabolic process	2	151	< 0.001
GO:0006030	chitin metabolic process	3	42	< 0.001
GO:0006814	sodium ion transport	2	101	< 0.001
GO:0015672	monovalent inorganic cation transport	6	221	< 0.001
GO:0032526	response to retinoic acid	2	44	< 0.001
GO:0033280	response to vitamin D	2	15	< 0.001
GO:0048806	genitalia development	3	25	< 0.001
GO:0048878	chemical homeostasis	4	756	< 0.001
GO:0097242	amyloid-beta clearance	2	41	< 0.001
GO:1901135	carbohydrate derivative metabolic process	2	773	< 0.001
GO:0042592	homeostatic process	2	1074	0.0024
GO:0006812	cation transport	2	569	0.0025
GO:0006044	N-acetylglucosamine metabolic process	2	11	0.0042
GO:0015701	bicarbonate transport	8	16	0.0043
GO:0042454	ribonucleoside catabolic process	7	12	0.0056
GO:0035277	spiracle morphogenesis, open tracheal system	2	8	0.0058
GO:0044321	response to leptin	2	16	0.0067
GO:0014015	positive regulation of gliogenesis	4	40	0.0069
GO:0003002	regionalization	3	236	0.0100

Table S2 (*continued*)

GO:0061642	chemoattraction of axon	3	13	0.0103
GO:0045056	transcytosis	4	22	0.0105
GO:0030001	metal ion transport	6	416	0.0108
GO:0097186	amelogenesis	3	5	0.0113
GO:0030206	chondroitin sulfate biosynthetic process	5	17	0.0115
GO:0070445	regulation of oligodendrocyte progenitor proliferation	4	14	0.0150
GO:1903510	mucopolysaccharide metabolic process	2	67	0.0191
GO:0007600	sensory perception	3	315	0.0196
GO:0050918	positive chemotaxis	2	24	0.0200
GO:0007389	pattern specification process	2	368	0.0205
GO:0098609	cell-cell adhesion	2	354	0.0206
GO:0002532	production of molecular mediator involved in inflammatory response	2	7	0.0207
GO:0046621	negative regulation of organ growth	3	33	0.0208
GO:0035461	vitamin transmembrane transport	2	31	0.0210
GO:0043174	nucleoside salvage	2	8	0.0212
GO:0010817	regulation of hormone levels	2	380	0.0217
GO:1901136	carbohydrate derivative catabolic process	2	188	0.0306
GO:0009256	10-formyltetrahydrofolate metabolic process	2	5	0.0307
GO:0007435	salivary gland morphogenesis	3	17	0.0328
GO:0009653	anatomical structure morphogenesis	2	1184	0.0331
GO:0014013	regulation of gliogenesis	2	58	0.0333
GO:0048608	reproductive structure development	2	142	0.0336
GO:0034404	nucleobase-containing small molecule biosynthetic process	2	71	0.0379
GO:0035725	sodium ion transmembrane transport	2	37	0.0391
GO:0044282	small molecule catabolic process	2	415	0.0397
GO:0032729	positive regulation of interferon-gamma production	3	10	0.0439
GO:0061052	negative regulation of cell growth involved in cardiac muscle cell development	2	14	0.0453
GO:0006826	iron ion transport	2	50	0.0453
GO:0055072	iron ion homeostasis	4	67	0.0463
GO:1901077	regulation of relaxation of muscle	4	5	0.0465
GO:0001568	blood vessel development	2	78	0.0478
GO:0043652	engulfment of apoptotic cell	2	21	0.0494
GO:0043649	dicarboxylic acid catabolic process	3	23	0.0494
GO:0033273	response to vitamin	2	53	0.0494
● **Tan module**				
MF				
GO:0015106	bicarbonate transmembrane transporter activity	3	17	< 0.001
GO:0005310	dicarboxylic acid transmembrane transporter activity	2	20	< 0.001
GO:0003700	DNA-binding transcription factor activity	2	497	< 0.001
GO:0016725	oxidoreductase activity, acting on CH or CH2 groups	2	25	< 0.001
GO:0140030	modification-dependent protein binding	2	150	< 0.001
GO:0036435	K48-linked polyubiquitin modification-dependent protein binding	3	5	< 0.001

Table S2 (*continued*)

GO:0008401	retinoic acid 4-hydroxylase activity	3	18	< 0.001
GO:1990405	protein antigen binding	2	5	< 0.001
GO:0003858	3-hydroxybutyrate dehydrogenase activity	2	12	< 0.001
GO:0016880	acid-ammonia (or amide) ligase activity	2	6	0.0012
GO:0015349	thyroid hormone transmembrane transporter activity	5	6	0.0016
GO:0140110	transcription regulator activity	1	804	0.0016
GO:0098770	FBXO family protein binding	3	6	0.0018
GO:0008391	arachidonic acid monooxygenase activity	3	43	0.0019
GO:0008392	arachidonic acid epoxygenase activity	5	32	0.0019
GO:0034185	apolipoprotein binding	2	41	0.0021
GO:1901682	sulfur compound transmembrane transporter activity	2	43	0.0021
GO:0031593	polyubiquitin modification-dependent protein binding	2	43	0.0022
GO:0070530	K63-linked polyubiquitin modification-dependent protein binding	3	14	0.0036
GO:0000981	DNA-binding transcription factor activity, RNA polymerase II-specific	3	328	0.0053
GO:0047485	protein N-terminus binding	2	75	0.0078
GO:0061578	Lys63-specific deubiquitinase activity	2	8	0.0118
GO:0005436	sodium:phosphate symporter activity	2	8	0.0146
GO:0016964	alpha-2 macroglobulin receptor activity	2	8	0.0214
GO:0032451	demethylase activity	2	40	0.0250
GO:0016500	protein-hormone receptor activity	3	18	0.0374
GO:0015297	antiporter activity	5	72	0.0378
GO:0022853	active ion transmembrane transporter activity	2	282	0.0378
GO:0070491	repressing transcription factor binding	5	43	0.0378
GO:0101020	estrogen 16-alpha-hydroxylase activity	2	30	0.0378
GO:0030226	apolipoprotein receptor activity	2	9	0.0407
GO:0001046	core promoter sequence-specific DNA binding	3	19	0.0444
BP				
GO:0000185	activation of MAPKKK activity	2	16	< 0.001
GO:0035864	response to potassium ion	2	11	< 0.001
GO:1900744	regulation of p38MAPK cascade	4	28	< 0.001
GO:0009612	response to mechanical stimulus	3	156	0.0050
GO:1900745	positive regulation of p38MAPK cascade	2	20	0.0056
GO:0015698	inorganic anion transport	3	80	0.0063
GO:0071850	mitotic cell cycle arrest	2	14	0.0071
GO:0097267	omega-hydroxylase P450 pathway	2	12	0.0083
GO:0031399	regulation of protein modification process	3	962	0.0100
GO:0044092	negative regulation of molecular function	2	586	0.0125
GO:0071260	cellular response to mechanical stimulus	3	51	0.0125
GO:0002931	response to ischemia	3	33	0.0136
GO:0031400	negative regulation of protein modification process	4	333	0.0143
GO:1901700	response to oxygen-containing compound	2	828	0.0154
GO:0008645	hexose transmembrane transport	2	13	0.0175
GO:0043086	negative regulation of catalytic activity	3	406	0.0176

Table S2 (*continued*)

GO:0009751	response to salicylic acid	2	7	0.0182
GO:0019369	arachidonic acid metabolic process	2	59	0.0184
GO:0019373	epoxygenase P450 pathway	2	30	0.0190
GO:0071479	cellular response to ionizing radiation	2	56	0.0194
GO:0042573	retinoic acid metabolic process	7	22	0.0217
GO:0046328	regulation of JNK cascade	4	82	0.0313
GO:0006805	xenobiotic metabolic process	2	108	0.0343
GO:0009719	response to endogenous stimulus	2	638	0.0351
GO:0002933	lipid hydroxylation	4	14	0.0352
GO:0042759	long-chain fatty acid biosynthetic process	3	14	0.0352
GO:0070988	demethylation	2	51	0.0353
GO:0002683	negative regulation of immune system process	2	171	0.0355
GO:0043405	regulation of MAP kinase activity	2	155	0.0357
GO:2000515	negative regulation of CD4-positive, alpha-beta T cell activation	2	5	0.0364
GO:0070371	ERK1 and ERK2 cascade	2	11	0.0366
GO:0000122	negative regulation of transcription by RNA polymerase II	2	448	0.0372
GO:0060216	definitive hemopoiesis	4	12	0.0375
GO:0045582	positive regulation of T cell differentiation	4	21	0.0379
GO:0046330	positive regulation of JNK cascade	2	50	0.0383
GO:0010996	response to auditory stimulus	2	9	0.0387
GO:0042126	nitrate metabolic process	4	6	0.0388
GO:0045621	positive regulation of lymphocyte differentiation	2	29	0.0404
GO:1905939	regulation of gonad development	2	5	0.0407
GO:0060349	bone morphogenesis	2	25	0.0410
GO:1902916	positive regulation of protein polyubiquitination	3	17	0.0413
GO:0006357	regulation of transcription by RNA polymerase II	2	1086	0.0415
GO:0031401	positive regulation of protein modification process	2	608	0.0420
GO:0001676	long-chain fatty acid metabolic process	6	85	0.0422
GO:0120254	olefinic compound metabolic process	3	91	0.0431
GO:0021895	cerebral cortex neuron differentiation	3	6	0.0435
GO:0007098	centrosome cycle	3	32	0.0438
GO:0046636	negative regulation of alpha-beta T cell activation	5	8	0.0445
GO:0051172	negative regulation of nitrogen compound metabolic process	5	1344	0.0450
GO:0017144	drug metabolic process	3	73	0.0456
GO:1901537	positive regulation of DNA demethylation	2	6	0.0458

Table S3. Differentially expressed genes (DEGs) across MNP conditions (0.025 and 1 µg L^{-1}) compared with the control condition identified in modules of interest from WGCNA performed on mantle samples sequencing dataset.

MNP condition	Sharing DEG	Sequencing gene ID	Log_2FC	P_{adj}	Uniprot *sp.*	Uniprot ID
● Turquoise module						
0.025 / Ctrl	Non-common	evm.TU.scaffold2282size117561.2	-3.47	2.63E-03	NA	NA
0.025 / Ctrl	Non-common	evm.TU.scaffold7792size68911.4	-3.42	2.84E-03	MOUSE	*NCAM2*
0.025 / Ctrl	Common	evm.TU.scaffold460size299527.3	-3.06	4.13E-02	ACRMI	*CADN*
0.025 / Ctrl	Common	evm.TU.scaffold1472size116207.6	-2.89	3.70E-03	METSE	*CALM*
0.025 / Ctrl	Common	evm.TU.scaffold10887size56046.3	-2.82	3.70E-03	RAT	*LR74A*
0.025 / Ctrl	Non-common	evm.TU.scaffold556size242659.10	-2.81	1.18E-02	MYTGA	*PLCL*
0.025 / Ctrl	Common	evm.TU.scaffold10132size55633.1	-2.53	1.26E-02	XENLA	*ZMY10*
0.025 / Ctrl	Common	evm.TU.scaffold5130size104591.3	-2.52	1.34E-02	NA	NA
0.025 / Ctrl	Common	evm.TU.scaffold7826size43469.2	-2.43	1.10E-03	BLAGE	*GST1*
0.025 / Ctrl	Common	evm.TU.scaffold1520size200124.4	-2.39	7.76E-03	XENLA	*CRHBP*
0.025 / Ctrl	Non-common	evm.TU.scaffold670size250180.11	-2.37	2.20E-02	NEMVE	*CIAO1*
0.025 / Ctrl	Non-common	evm.TU.scaffold13117size21283.1	-2.30	2.15E-02	PINMG	*PLSP*
0.025 / Ctrl	Non-common	evm.TU.scaffold3650size121286.1	-2.27	4.13E-02	MOUSE	*SO4C1*
0.025 / Ctrl	Non-common	evm.TU.scaffold538size272809.12	-2.14	4.88E-02	HUMAN	*CHIT1*
0.025 / Ctrl	Common	evm.TU.scaffold2782size126472.5	-2.08	1.07E-02	HUMAN	*ANR50*
0.025 / Ctrl	Non-common	evm.TU.scaffold2782size126472.1	-1.90	3.49E-02	HUMAN	*LR74A*
0.025 / Ctrl	Common	evm.TU.scaffold274size189192.2	-1.87	4.41E-02	PIG	*GGLO*
0.025 / Ctrl	Non-common	evm.TU.scaffold1550size128617.3	-1.62	3.57E-02	CAEEL	*PDE5*
0.025 / Ctrl	Non-common	evm.TU.scaffold1520size200124.2	-1.57	2.53E-03	NA	NA
0.025 / Ctrl	Common	evm.TU.scaffold813size224748.4	-1.51	2.74E-02	NA	NA
0.025 / Ctrl	Common	evm.TU.scaffold1174size268520.11	-1.47	1.86E-02	NA	NA
0.025 / Ctrl	Common	evm.TU.scaffold486size164273.5	-1.44	9.80E-05	NA	NA
0.025 / Ctrl	Common	evm.TU.scaffold410size171622.1	-1.39	2.01E-02	DROME	*GC76C*
0.025 / Ctrl	Non-common	evm.TU.scaffold6926size48685.2	-1.35	4.63E-02	HUMAN	*CBPC2*
0.025 / Ctrl	Non-common	evm.TU.scaffold392size205118.3	-1.34	6.85E-03	DROME	*CPO*
0.025 / Ctrl	Non-common	evm.TU.scaffold13755size19307.2	-1.30	3.38E-02	HUMAN	*MRM1*
0.025 / Ctrl	Common	evm.TU.scaffold1280size446155.31	-1.28	3.49E-02	XENLA	*CE152*
0.025 / Ctrl	Common	evm.TU.scaffold1523size134303.2	-1.27	1.79E-02	MOUSE	*RSPO2*
0.025 / Ctrl	Common	evm.TU.scaffold2120size147150.8	-1.22	3.61E-02	NA	NA
0.025 / Ctrl	Non-common	evm.TU.scaffold7149size67001.1	-1.18	4.15E-02	NA	NA
0.025 / Ctrl	Common	evm.TU.scaffold4715size154169.2	-1.17	3.32E-02	MOUSE	*NIM1*
0.025 / Ctrl	Non-common	evm.TU.scaffold8450size40129.2	-1.11	3.97E-02	CAEEL	*CEX2*
0.025 / Ctrl	Non-common	evm.TU.scaffold5824size123299.3	-1.03	2.52E-02	HUMAN	*HERC1*
1 / Ctrl	Non-common	evm.TU.scaffold3605size77135.2	-4.68	2.86E-04	NA	NA
1 / Ctrl	Non-common	evm.TU.scaffold11951size25182.10	-3.68	4.66E-03	NA	NA
1 / Ctrl	Non-common	evm.TU.scaffold5027size97772.4	-3.42	4.63E-02	ACRMI	*MLRP2*

Table S3 (*continued*)

1 / Ctrl	Non-common	evm.TU.scaffold5957size328954.4	-3.40	1.75E-04	NA	NA
1 / Ctrl	Non-common	evm.TU.scaffold7195size65380.3	-3.32	8.34E-04	NA	NA
1 / Ctrl	Non-common	evm.TU.scaffold1500size115322.2	-3.29	4.11E-02	BOVIN	*CD63*
1 / Ctrl	Common	evm.TU.scaffold460size299527.3	-3.12	1.47E-02	ACRMI	*CADN*
1 / Ctrl	Non-common	evm.TU.scaffold3500size108302.6	-3.08	2.23E-02	NA	NA
1 / Ctrl	Non-common	evm.TU.scaffold8287size40987.2	-3.06	2.09E-02	EPHMU	*CAS4*
1 / Ctrl	Common	evm.TU.scaffold1472size116207.6	-3.02	7.02E-04	METSE	*CALM*
1 / Ctrl	Non-common	evm.TU.scaffold5009size125620.3	-3.01	4.14E-02	HUMAN	*PFD2*
1 / Ctrl	Non-common	evm.TU.scaffold2994size85130.2	-2.95	4.32E-02	NA	NA
1 / Ctrl	Non-common	evm.TU.scaffold12753size22481.4	-2.87	1.98E-02	NA	NA
1 / Ctrl	Non-common	evm.TU.scaffold3542size77893.2	-2.80	1.98E-04	NA	NA
1 / Ctrl	Non-common	evm.TU.scaffold1634size311462.7	-2.79	3.65E-02	NA	NA
1 / Ctrl	Common	evm.TU.scaffold5130size104591.3	-2.78	1.17E-03	NA	NA
1 / Ctrl	Non-common	evm.TU.scaffold7224size46994.4	-2.77	9.15E-08	HUMAN	*HEBP2*
1 / Ctrl	Non-common	evm.TU.scaffold6290size68442.3	-2.73	2.18E-02	BRAFL	*FUCO*
1 / Ctrl	Common	evm.TU.scaffold10887size56046.3	-2.71	2.30E-03	RAT	*LR74A*
1 / Ctrl	Common	evm.TU.scaffold10132size55633.1	-2.71	1.69E-03	XENLA	*ZMY10*
1 / Ctrl	Common	evm.TU.scaffold1520size200124.4	-2.63	7.28E-04	XENLA	*CRHBP*
1 / Ctrl	Non-common	evm.TU.scaffold9515size85861.3	-2.62	3.94E-02	CAEEL	*ARF12*
1 / Ctrl	Non-common	evm.TU.scaffold4607size257860.4	-2.58	1.57E-03	NEOPA	*XYNB*
1 / Ctrl	Non-common	evm.TU.scaffold1007size132311.14	-2.52	4.14E-03	NA	NA
1 / Ctrl	Non-common	evm.TU.scaffold1320size225772.10	-2.49	6.86E-03	CHICK	*MOXD1*
1 / Ctrl	Non-common	evm.TU.scaffold3098size175394.6	-2.47	6.07E-03	BOVIN	*SE6L2*
1 / Ctrl	Non-common	evm.TU.scaffold646size212683.7	-2.42	4.49E-03	NA	NA
1 / Ctrl	Non-common	evm.TU.scaffold3856size74363.3	-2.41	2.07E-03	BOVIN	*TEKT3*
1 / Ctrl	Non-common	evm.TU.scaffold10440size30953.1	-2.40	5.19E-03	NA	NA
1 / Ctrl	Non-common	evm.TU.scaffold1323size145704.4	-2.39	2.18E-02	NA	NA
1 / Ctrl	Non-common	evm.TU.scaffold3246size246367.21	-2.39	2.30E-03	MOUSE	*LMX1B*
1 / Ctrl	Non-common	evm.TU.scaffold4870size90196.3	-2.38	4.27E-02	DROME	*HIL*
1 / Ctrl	Non-common	evm.TU.scaffold76size343677.22	-2.36	1.00E-02	NA	NA
1 / Ctrl	Non-common	evm.TU.scaffold1680size293446.12	-2.32	4.32E-02	NA	NA
1 / Ctrl	Non-common	evm.TU.scaffold3930size73502.1	-2.27	1.01E-02	XENTR	*ANKR1*
1 / Ctrl	Common	evm.TU.scaffold274size189192.2	-2.27	1.57E-03	PIG	*GGLO*
1 / Ctrl	Non-common	evm.TU.scaffold4646size66185.1	-2.27	4.86E-03	HUMAN	*DTHD1*
1 / Ctrl	Non-common	evm.TU.scaffold1203size265927.9	-2.25	1.23E-02	MOUSE	*STMN2*
1 / Ctrl	Non-common	evm.TU.scaffold2679size89875.3	-2.13	3.66E-02	DROME	*PERC*
1 / Ctrl	Non-common	evm.TU.scaffold5224size119327.1	-2.13	2.21E-02	HUMAN	*CG031*
1 / Ctrl	Non-common	evm.TU.scaffold2440size155032.13	-2.10	1.04E-02	THACU	*LAC3*
1 / Ctrl	Non-common	evm.TU.scaffold11153size28117.2	-2.05	1.47E-02	RAT	*TGM1*
1 / Ctrl	Non-common	evm.TU.scaffold628size555846.12	-2.00	4.45E-02	NA	NA
1 / Ctrl	Non-common	evm.TU.scaffold213size200314.6	-1.99	4.22E-02	NA	NA
1 / Ctrl	Non-common	evm.TU.scaffold2654size138451.1	-1.99	4.74E-03	CAEEL	*CPLX1*
1 / Ctrl	Non-common	evm.TU.scaffold3765size102138.2	-1.99	1.64E-02	MOUSE	*ASB16*

Table S3 (*continued*)

1 / Ctrl	Non-common	evm.TU.scaffold4017size72682.1	-1.98	1.34E-02	NA	NA
1 / Ctrl	Non-common	evm.TU.scaffold3979size95817.2	-1.97	3.00E-02	HUMAN	*MOT12*
1 / Ctrl	Non-common	evm.TU.scaffold12597size42776.3	-1.96	4.35E-03	MOUSE	*RSPH1*
1 / Ctrl	Non-common	evm.TU.scaffold7734size44023.2	-1.95	1.57E-03	NA	NA
1 / Ctrl	Non-common	evm.TU.scaffold1538size192633.5	-1.94	1.44E-02	CAEEL	*UNC22*
1 / Ctrl	Non-common	evm.TU.scaffold9079size64000.2	-1.92	4.27E-02	HUMAN	*DYH7*
1 / Ctrl	Non-common	evm.TU.scaffold188size206906.5	-1.90	3.11E-02	LYMST	*MYOM*
1 / Ctrl	Non-common	evm.TU.scaffold7991size81123.4	-1.89	3.49E-02	NA	NA
1 / Ctrl	Non-common	evm.TU.scaffold695size399694.13	-1.89	1.64E-02	NA	NA
1 / Ctrl	Non-common	evm.TU.scaffold14873size16104.1	-1.88	2.00E-02	NA	NA
1 / Ctrl	Non-common	evm.TU.scaffold7907size43009.11	-1.87	1.03E-03	NA	NA
1 / Ctrl	Non-common	evm.TU.scaffold1198size224948.9	-1.86	3.29E-02	VILV2	*POL*
1 / Ctrl	Non-common	evm.TU.scaffold2908size86298.2	-1.85	3.69E-02	NA	NA
1 / Ctrl	Non-common	evm.TU.scaffold3889size73985.2	-1.84	4.23E-02	MACFA	*DZAN1*
1 / Ctrl	Non-common	evm.TU.scaffold336size211905.15	-1.82	3.10E-02	HUMAN	*FCN1*
1 / Ctrl	Non-common	evm.TU.scaffold1906size173792.7	-1.82	2.21E-03	HUMAN	*WSB1*
1 / Ctrl	Non-common	evm.TU.scaffold2120size147150.9	-1.78	5.93E-04	DROYA	*PER*
1 / Ctrl	Common	evm.TU.scaffold7826size43469.2	-1.78	2.31E-02	BLAGE	*GST1*
1 / Ctrl	Non-common	evm.TU.scaffold2158size160354.12	-1.75	3.89E-02	NA	NA
1 / Ctrl	Non-common	evm.TU.scaffold1026size247016.2	-1.75	4.16E-02	BOVIN	*LEG9*
1 / Ctrl	Common	evm.TU.scaffold2782size126472.5	-1.75	2.61E-02	HUMAN	*ANR50*
1 / Ctrl	Non-common	evm.TU.scaffold5090size62038.6	-1.75	3.51E-02	NA	NA
1 / Ctrl	Non-common	evm.TU.scaffold1027size182162.1	-1.74	9.15E-03	NA	NA
1 / Ctrl	Non-common	evm.TU.scaffold3256size155363.1	-1.73	2.34E-02	SCHAM	*ANNU*
1 / Ctrl	Non-common	evm.TU.scaffold11396size27145.2	-1.73	3.29E-02	NA	NA
1 / Ctrl	Non-common	evm.TU.scaffold5050size86062.2	-1.72	4.31E-02	MOUSE	*PXDN*
1 / Ctrl	Non-common	evm.TU.scaffold637size177620.6	-1.71	7.44E-03	STRPU	*FBP1*
1 / Ctrl	Common	evm.TU.scaffold813size224748.4	-1.70	1.82E-03	NA	NA
1 / Ctrl	Non-common	evm.TU.scaffold31size304358.11	-1.70	2.23E-02	HUMAN	*NWD2*
1 / Ctrl	Non-common	evm.TU.scaffold2120size147150.7	-1.68	1.04E-04	NA	NA
1 / Ctrl	Non-common	evm.TU.scaffold2148size296962.7	-1.66	3.78E-02	XENLA	*TEKT4*
1 / Ctrl	Non-common	evm.TU.scaffold6434size52003.1	-1.65	4.16E-02	NA	NA
1 / Ctrl	Non-common	evm.TU.scaffold5707size57206.1	-1.65	2.84E-02	CHICK	*EMC1*
1 / Ctrl	Non-common	evm.TU.scaffold1121size199104.8	-1.65	4.30E-02	NA	NA
1 / Ctrl	Non-common	evm.TU.scaffold5009size125620.1	-1.64	2.23E-02	HUMAN	*SSNA1*
1 / Ctrl	Non-common	evm.TU.scaffold850size206783.7	-1.63	2.35E-03	NA	NA
1 / Ctrl	Non-common	evm.TU.scaffold12690size49544.1	-1.62	3.99E-02	HUMAN	*HELZ2*
1 / Ctrl	Non-common	evm.TU.scaffold6209size89422.1	-1.61	4.91E-03	HUMAN	*ZMY12*
1 / Ctrl	Non-common	evm.TU.scaffold2802size169182.3	-1.61	1.85E-02	NA	NA
1 / Ctrl	Non-common	evm.TU.scaffold2026size102104.8	-1.60	2.79E-02	HUMAN	*ANR63*
1 / Ctrl	Non-common	evm.TU.scaffold11744size25915.3	-1.60	1.59E-02	NA	NA
1 / Ctrl	Non-common	evm.TU.scaffold1471size234825.3	-1.59	3.38E-02	RAT	*TBA1A*
1 / Ctrl	Common	evm.TU.scaffold486size164273.5	-1.59	5.00E-06	NA	NA

Table S3 (*continued*)

1 / Ctrl	Non-common	evm.TU.scaffold1444size196405.7	-1.59	4.66E-02	BOMMO	*EXD1*
1 / Ctrl	Non-common	evm.TU.scaffold7924size79650.2	-1.56	3.19E-02	RAT	*TBA1A*
1 / Ctrl	Non-common	evm.TU.scaffold112size675390.27	-1.55	3.78E-02	NA	NA
1 / Ctrl	Non-common	evm.TU.scaffold6949size137242.7	-1.54	4.84E-02	NA	NA
1 / Ctrl	Common	evm.TU.scaffold1174size268520.11	-1.52	5.19E-03	NA	NA
1 / Ctrl	Non-common	evm.TU.scaffold4367size111109.1	-1.52	3.67E-02	NA	NA
1 / Ctrl	Non-common	evm.TU.scaffold1866size105213.8	-1.52	3.00E-02	MOUSE	*FHAD1*
1 / Ctrl	Non-common	evm.TU.scaffold9784size33764.1	-1.51	9.67E-03	HUMAN	*ANR66*
1 / Ctrl	Non-common	evm.TU.scaffold4626size149477.4	-1.51	9.07E-03	MOUSE	*STPG3*
1 / Ctrl	Non-common	evm.TU.scaffold2627size90695.3	-1.50	3.00E-02	DROME	*CANB*
1 / Ctrl	Non-common	evm.TU.scaffold1802size107121.5	-1.50	1.47E-02	NA	NA
1 / Ctrl	Non-common	evm.TU.scaffold7961size42695.1	-1.49	2.10E-02	MACFA	*AXDN1*
1 / Ctrl	Non-common	evm.TU.scaffold12729size22574.1	-1.49	4.79E-02	MOUSE	*KITH*
1 / Ctrl	Non-common	evm.TU.scaffold5921size55650.4	-1.48	4.22E-02	DANRE	*CF161*
1 / Ctrl	Non-common	evm.TU.scaffold1298size186980.4	-1.47	2.56E-02	HUMAN	*M21D2*
1 / Ctrl	Non-common	evm.TU.scaffold11369size27302.2	-1.46	1.74E-02	HUMAN	*ACHA3*
1 / Ctrl	Non-common	evm.TU.scaffold10308size55656.6	-1.44	3.99E-02	HUMAN	*ENKUR*
1 / Ctrl	Non-common	evm.TU.scaffold8267size41080.3	-1.43	1.44E-02	MOUSE	*PTPRM*
1 / Ctrl	Common	evm.TU.scaffold410size171622.1	-1.43	5.00E-03	DROME	*GC76C*
1 / Ctrl	Non-common	evm.TU.scaffold1430size117431.3	-1.43	3.78E-03	HUMAN	*ABCA1*
1 / Ctrl	Non-common	evm.TU.scaffold46size318859.15	-1.43	4.32E-02	NA	NA
1 / Ctrl	Non-common	evm.TU.scaffold5634size57725.1	-1.43	2.57E-02	HUMAN	*SACS*
1 / Ctrl	Non-common	evm.TU.scaffold789size245146.23	-1.42	4.04E-02	XENTR	*ODF3A*
1 / Ctrl	Non-common	evm.TU.scaffold4384size136806.1	-1.42	2.76E-02	STRPU	*TBB*
1 / Ctrl	Non-common	evm.TU.scaffold1472size116207.2	-1.41	4.27E-02	LUMRU	*CALM*
1 / Ctrl	Non-common	evm.TU.scaffold2326size392610.8	-1.41	4.46E-02	DANRE	*CP135*
1 / Ctrl	Non-common	evm.TU.scaffold6655size50433.2	-1.41	1.77E-02	HUMAN	*CI135*
1 / Ctrl	Non-common	evm.TU.scaffold5563size58257.2	-1.40	3.19E-02	HUMAN	*EFHC1*
1 / Ctrl	Non-common	evm.TU.scaffold4431size68472.3	-1.40	4.11E-02	DANRE	*EFHC2*
1 / Ctrl	Non-common	evm.TU.scaffold5171size61321.2	-1.40	4.46E-02	HUMAN	*CC173*
1 / Ctrl	Non-common	evm.TU.scaffold1089size185187.1	-1.39	1.41E-02	PIG	*SUCB2*
1 / Ctrl	Non-common	evm.TU.scaffold10980size28775.1	-1.39	2.56E-02	HUMAN	*STKL1*
1 / Ctrl	Non-common	evm.TU.scaffold10710size29754.5	-1.39	3.69E-02	RAT	*F13A*
1 / Ctrl	Non-common	evm.TU.scaffold4384size136806.2	-1.38	3.29E-02	LYTPI	*TBB*
1 / Ctrl	Common	evm.TU.scaffold1523size134303.2	-1.38	1.93E-03	MOUSE	*RSPO2*
1 / Ctrl	Non-common	evm.TU.scaffold815size266289.1	-1.38	4.91E-03	MOUSE	*ZAN*
1 / Ctrl	Non-common	evm.TU.scaffold2578size177840.3	-1.38	1.36E-02	NA	NA
1 / Ctrl	Non-common	evm.TU.scaffold518size431291.5	-1.37	3.99E-02	RICFE	*Y580*
1 / Ctrl	Non-common	evm.TU.scaffold1319size120382.1	-1.37	4.61E-02	MOUSE	*KIF9*
1 / Ctrl	Common	evm.TU.scaffold2120size147150.8	-1.36	4.86E-03	NA	NA
1 / Ctrl	Non-common	evm.TU.scaffold637size177620.4	-1.36	8.74E-04	STRPU	*FBP3*
1 / Ctrl	Non-common	evm.TU.scaffold432size238846.15	-1.36	4.05E-02	MOUSE	*GPV*
1 / Ctrl	Non-common	evm.TU.scaffold2743size200640.4	-1.34	4.05E-02	NA	NA

Table S3 (*continued*)

1 / Ctrl	Non-common	evm.TU.scaffold11133size58585.6	-1.34	3.33E-02	NA	NA
1 / Ctrl	Non-common	evm.TU.scaffold304size184890.1	-1.33	3.70E-02	SCHAM	*ANNU*
1 / Ctrl	Non-common	evm.TU.scaffold2300size96173.4	-1.33	9.31E-03	NA	NA
1 / Ctrl	Non-common	evm.TU.scaffold5659size115446.3	-1.32	4.57E-02	HUMAN	*TEKT1*
1 / Ctrl	Non-common	evm.TU.scaffold125size413603.34	-1.32	9.07E-03	CVHN1	*R1A*
1 / Ctrl	Non-common	evm.TU.scaffold8336size101972.4	-1.31	4.48E-02	RAT	*K895L*
1 / Ctrl	Non-common	evm.TU.scaffold11274size27659.1	-1.31	4.78E-02	HUMAN	*PTPRT*
1 / Ctrl	Non-common	evm.TU.scaffold17134size9437.1	-1.31	3.98E-02	HUMAN	*IQCG*
1 / Ctrl	Non-common	evm.TU.scaffold5701size57243.3	-1.29	4.51E-02	NA	NA
1 / Ctrl	Non-common	evm.TU.scaffold6382size52386.1	-1.29	5.58E-03	RAT	*LEXM*
1 / Ctrl	Non-common	evm.TU.scaffold682size148060.6	-1.28	3.48E-02	DANRE	*C2512*
1 / Ctrl	Non-common	evm.TU.scaffold2202size278870.8	-1.28	4.31E-02	NA	NA
1 / Ctrl	Non-common	evm.TU.scaffold2610size137834.5	-1.27	4.44E-02	MACFA	*IQUB*
1 / Ctrl	Non-common	evm.TU.scaffold3189size104933.3	-1.27	4.38E-02	HUMAN	*SPAS1*
1 / Ctrl	Non-common	evm.TU.scaffold720size228729.12	-1.26	1.68E-02	MOUSE	*GRAN*
1 / Ctrl	Non-common	evm.TU.scaffold4710size123841.1	-1.25	4.84E-02	NA	NA
1 / Ctrl	Non-common	evm.TU.scaffold4505size150176.5	-1.25	4.05E-02	MOUSE	*RSH3B*
1 / Ctrl	Non-common	evm.TU.scaffold14275size36645.2	-1.25	2.34E-02	MOUSE	*CFA58*
1 / Ctrl	Non-common	evm.TU.scaffold1617size112222.5	-1.25	1.44E-02	HUMAN	*VWA3B*
1 / Ctrl	Non-common	evm.TU.scaffold2605size181081.8	-1.24	2.62E-02	HUMAN	*ARMC3*
1 / Ctrl	Non-common	evm.TU.scaffold1147size838866.2	-1.23	2.41E-02	NA	NA
1 / Ctrl	Non-common	evm.TU.scaffold198size204315.2	-1.23	4.06E-02	MOUSE	*TEX26*
1 / Ctrl	Non-common	evm.TU.scaffold1031size131350.6	-1.21	3.99E-02	RAT	*LR74A*
1 / Ctrl	Non-common	evm.TU.scaffold175size299376.1	-1.21	5.00E-03	HUMAN	*WSB1*
1 / Ctrl	Non-common	evm.TU.scaffold7783size43717.1	-1.21	3.43E-02	HUMAN	*GRAN*
1 / Ctrl	Non-common	evm.TU.scaffold2756size88728.1	-1.20	4.16E-02	HUMAN	*LRC72*
1 / Ctrl	Non-common	evm.TU.scaffold6780size235009.14	-1.20	5.12E-04	HUMAN	*PGFS*
1 / Ctrl	Non-common	evm.TU.scaffold1437size117226.3	-1.20	4.76E-02	CHLRE	*DYH1B*
1 / Ctrl	Non-common	evm.TU.scaffold1205size150501.3	-1.19	3.59E-02	NA	NA
1 / Ctrl	Non-common	evm.TU.scaffold8352size63603.2	-1.18	3.78E-02	HUMAN	*MYO3A*
1 / Ctrl	Non-common	evm.TU.scaffold1131size175864.3	-1.18	3.78E-02	HUMAN	*KAD9*
1 / Ctrl	Non-common	evm.TU.scaffold796size284195.5	-1.18	4.04E-02	DANRE	*LARG2*
1 / Ctrl	Non-common	evm.TU.scaffold1718size205308.5	-1.17	3.53E-02	NA	NA
1 / Ctrl	Common	evm.TU.scaffold1280size446155.31	-1.16	3.29E-02	XENLA	*CE152*
1 / Ctrl	Non-common	evm.TU.scaffold3867size409801.10	-1.16	2.75E-02	XENLA	*CCNF*
1 / Ctrl	Non-common	evm.TU.scaffold1184size197641.11	-1.16	4.04E-02	BOVIN	*TPMT*
1 / Ctrl	Non-common	evm.TU.scaffold1794size145318.5	-1.16	4.73E-02	MACFA	*CCD96*
1 / Ctrl	Non-common	evm.TU.scaffold1704size161865.4	-1.15	2.40E-02	HUMAN	*FA47E*
1 / Ctrl	Non-common	evm.TU.scaffold1617size112222.6	-1.15	2.76E-02	HUMAN	*VWA3B*
1 / Ctrl	Non-common	evm.TU.scaffold6730size147307.1	-1.13	3.89E-02	SAGLB	*ASPM*
1 / Ctrl	Non-common	evm.TU.scaffold46size318859.11	-1.10	6.35E-03	MOUSE	*CO6A6*
1 / Ctrl	Non-common	evm.TU.scaffold11086size92184.1	-1.09	3.03E-02	NA	NA
1 / Ctrl	Non-common	evm.TU.scaffold2157size244387.4	-1.08	3.97E-02	DROME	*DLL*

Table S3 (*continued*)

1 / Ctrl	Non-common	evm.TU.scaffold2400size294214.10	-1.08	4.46E-02	BOVIN	*ANXA6*
1 / Ctrl	Non-common	evm.TU.scaffold3834size181686.2	-1.07	3.99E-02	NA	NA
1 / Ctrl	Non-common	evm.TU.scaffold1947size217951.13	-1.06	4.27E-02	NA	NA
1 / Ctrl	Non-common	evm.TU.scaffold6051size132328.4	-1.06	4.11E-02	XENLA	*NOCT*
1 / Ctrl	Non-common	evm.TU.scaffold13839size19094.1	-1.06	4.05E-02	MOUSE	*DCLK1*
1 / Ctrl	Non-common	evm.TU.scaffold1303size315076.16	-1.05	3.26E-02	XENLA	*PGS1*
1 / Ctrl	Non-common	evm.TU.scaffold14823size27136.1	-1.05	4.91E-02	HUMAN	*IQCA1*
1 / Ctrl	Non-common	evm.TU.scaffold4133size128356.1	-1.02	4.85E-02	HUMAN	*PNKP*
1 / Ctrl	Non-common	evm.TU.scaffold8881size78301.3	-1.02	1.51E-03	CHICK	*5NTC*
1 / Ctrl	Common	evm.TU.scaffold4715size154169.2	-1.00	4.30E-02	MOUSE	*NIM1*
1 / Ctrl	Non-common	evm.TU.scaffold7948size42762.3	-1.00	5.24E-04	MOUSE	*TRIM2*
● Blue module						
0.025 / Ctrl	Non-common	evm.TU.scaffold7986size42548.1	2.04	4.73E-02	ARATH	*USPAL*
0.025 / Ctrl	Common	evm.TU.scaffold211size252336.1	1.41	4.13E-02	RAT	*MRC2*
1 / Ctrl	Common	evm.TU.scaffold211size252336.1	1.28	3.99E-02	RAT	*MRC2*
1 / Ctrl	Non-common	evm.TU.scaffold2212size97855.2	-1.03	4.04E-02	HUMAN	*FAT4*
1 / Ctrl	Non-common	evm.TU.scaffold11857size74220.2	-1.06	4.05E-02	NA	NA
1 / Ctrl	Non-common	evm.TU.scaffold6770size108272.1	-1.23	4.19E-02	DICDI	*MKCD*
1 / Ctrl	Non-common	evm.TU.scaffold2313size96057.1	-1.32	4.31E-02	DROME	*DUOX*
1 / Ctrl	Non-common	evm.TU.scaffold1577size270204.4	-1.46	4.63E-02	NA	NA
1 / Ctrl	Non-common	evm.TU.scaffold15032size15714.1	-1.58	1.21E-02	NA	NA
1 / Ctrl	Non-common	evm.TU.scaffold908size168178.1	-1.69	2.46E-04	NA	NA
1 / Ctrl	Non-common	evm.TU.scaffold8527size135830.4	-1.90	1.03E-03	MOUSE	*GCH1*
1 / Ctrl	Non-common	evm.TU.scaffold264size320753.24	-1.96	1.10E-02	NA	NA
1 / Ctrl	Non-common	evm.TU.scaffold9119size116109.8	-1.97	4.78E-02	MOUSE	*LGR6*
1 / Ctrl	Non-common	evm.TU.scaffold264size320753.25	-1.98	4.31E-02	CRIGR	*TLR2*
1 / Ctrl	Non-common	evm.TU.scaffold815size266289.2	-2.15	4.27E-02	MOUSE	*KCP*
1 / Ctrl	Non-common	evm.TU.scaffold2082size139968.2	-2.27	3.19E-02	HUMAN	*ANGL7*
1 / Ctrl	Non-common	evm.TU.scaffold1068size322763.10	-2.33	4.67E-02	HUMAN	*FCGBP*
1 / Ctrl	Non-common	evm.TU.scaffold5648size169074.4	-4.27	1.98E-04	DROME	*TBH1*
● Darkturquoise module						
1 / Ctrl	Non-common	evm.TU.scaffold258size299806.9	-1.07	3.49E-02	NA	NA
● Darkgreen module						
0.025 / Ctrl	Common	evm.TU.scaffold2612size116661.2	-4.06	1.83E-05	NA	NA
0.025 / Ctrl	Common	evm.TU.scaffold2383size182244.4	-3.51	1.79E-02	HUMAN	*CELR2*
0.025 / Ctrl	Common	evm.TU.scaffold2108size145499.4	-3.06	7.98E-03	HUMAN	*FAT1*
0.025 / Ctrl	Common	evm.TU.scaffold5595size58030.2	-3.05	1.37E-02	NA	NA
0.025 / Ctrl	Non-common	evm.TU.scaffold5793size56674.1	-3.04	3.57E-02	HUMAN	*VWDE*
0.025 / Ctrl	Common	evm.TU.scaffold10747size58510.3	-2.99	1.09E-03	DANRE	*ODF3B*
0.025 / Ctrl	Non-common	evm.TU.scaffold240size211441.8	-2.97	3.19E-02	RAT	*WFD18*

Table S3 (*continued*)

0.025 / Ctrl	Common	evm.TU.scaffold16833size10418.1	-2.77	3.51E-02	DANRE	*CDHR1*
0.025 / Ctrl	Non-common	evm.TU.scaffold240size211441.7	-2.75	1.36E-02	HUMAN	*VWDE*
0.025 / Ctrl	Common	evm.TU.scaffold69size251715.7	-2.62	5.62E-03	DROME	*RYAR*
0.025 / Ctrl	Common	evm.TU.scaffold2944size186744.16	-2.45	9.73E-03	HUMAN	*PCDH9*
0.025 / Ctrl	Common	evm.TU.scaffold1047size340248.4	-1.90	3.49E-02	NA	NA
0.025 / Ctrl	Non-common	evm.TU.scaffold8293size79692.4	-1.75	4.53E-02	NA	NA
0.025 / Ctrl	Common	evm.TU.scaffold7160size101947.5	-1.66	3.20E-02	DANRE	*CDHR1*
0.025 / Ctrl	Non-common	evm.TU.scaffold3375size152648.8	-1.60	3.06E-02	DICDI	*CALM*
1 / Ctrl	Non-common	evm.TU.scaffold2108size145499.3	-4.70	1.98E-02	HUMAN	*FAT4*
1 / Ctrl	Common	evm.TU.scaffold2108size145499.4	-3.79	5.14E-05	HUMAN	*FAT1*
1 / Ctrl	Common	evm.TU.scaffold2612size116661.2	-3.68	9.85E-05	NA	NA
1 / Ctrl	Common	evm.TU.scaffold16833size10418.1	-3.61	3.09E-04	DANRE	*CDHR1*
1 / Ctrl	Non-common	evm.TU.scaffold1067size129500.1	-3.41	5.77E-03	NA	NA
1 / Ctrl	Non-common	evm.TU.scaffold984size332810.1	-3.39	4.80E-03	NA	NA
1 / Ctrl	Non-common	evm.TU.scaffold4421size170941.6	-3.30	7.85E-03	NA	NA
1 / Ctrl	Common	evm.TU.scaffold10747size58510.3	-3.30	5.14E-05	DANRE	*ODF3B*
1 / Ctrl	Non-common	evm.TU.scaffold10319size85128.6	-3.27	2.73E-02	NA	NA
1 / Ctrl	Common	evm.TU.scaffold2383size182244.4	-3.27	1.43E-02	HUMAN	*CELR2*
1 / Ctrl	Common	evm.TU.scaffold5595size58030.2	-3.13	3.39E-03	NA	NA
1 / Ctrl	Common	evm.TU.scaffold2944size186744.16	-2.98	1.03E-04	HUMAN	*PCDH9*
1 / Ctrl	Non-common	evm.TU.scaffold5775size102228.5	-2.49	2.23E-02	DROME	*GSC*
1 / Ctrl	Non-common	evm.TU.scaffold11346size27402.1	-2.49	2.12E-02	ORYSJ	*CALM2*
1 / Ctrl	Non-common	evm.TU.scaffold7164size47312.3	-2.38	3.33E-02	NA	NA
1 / Ctrl	Common	evm.TU.scaffold1047size340248.4	-2.07	5.19E-03	NA	NA
1 / Ctrl	Common	evm.TU.scaffold69size251715.7	-2.04	3.26E-02	DROME	*RYAR*
1 / Ctrl	Non-common	evm.TU.scaffold12250size24140.1	-1.80	1.08E-02	DROME	*ACH1*
1 / Ctrl	Non-common	evm.TU.scaffold2069size138995.8	-1.78	1.43E-02	NA	NA
1 / Ctrl	Non-common	evm.TU.scaffold8670size39024.1	-1.76	1.65E-02	NA	NA
1 / Ctrl	Common	evm.TU.scaffold7160size101947.5	-1.61	1.65E-02	DANRE	*CDHR1*
1 / Ctrl	Non-common	evm.TU.scaffold1190size145671.3	-1.60	4.90E-02	NA	NA
1 / Ctrl	Non-common	evm.TU.scaffold521size160855.1	-1.29	2.56E-02	MOUSE	*WNT6*
1 / Ctrl	Non-common	evm.TU.scaffold2625size211361.5	-1.09	9.50E-03	RAT	*LHX5*
● **Darkgrey module**						
0.025 / Ctrl	Common	evm.TU.scaffold5737size147992.4	-10.22	1.19E-13	PLAYO	*CSP*
0.025 / Ctrl	Common	evm.TU.scaffold2059size101583.8	-9.83	2.75E-12	NA	NA
0.025 / Ctrl	Common	evm.TU.scaffold3140size111674.1	-8.82	1.05E-08	NA	NA
0.025 / Ctrl	Common	evm.TU.scaffold1765size248259.2	-7.66	9.60E-06	NA	NA
0.025 / Ctrl	Common	evm.TU.scaffold12797size22360.1	-7.52	9.65E-07	NA	NA
0.025 / Ctrl	Common	evm.TU.scaffold200size231477.1	-6.87	6.89E-06	NA	NA
0.025 / Ctrl	Common	evm.TU.scaffold6483size290382.9	-6.17	3.25E-04	HUMAN	*LOXH1*
0.025 / Ctrl	Non-common	evm.TU.scaffold3140size111674.2	-5.23	2.52E-02	PINMA	*GRP3*
0.025 / Ctrl	Common	evm.TU.scaffold2106size257207.9	-5.19	3.96E-05	NA	NA

Table S3 (*continued*)

0.025 / Ctrl	Common	evm.TU.scaffold821size195697.10	-5.14	3.15E-04	NA	NA
0.025 / Ctrl	Common	evm.TU.scaffold50size263963.6	-5.10	2.53E-05	PINMG	*PLSP*
0.025 / Ctrl	Non-common	evm.TU.scaffold2330size266946.11	-3.60	3.70E-03	PINMG	*KCP2*
0.025 / Ctrl	Non-common	evm.TU.scaffold1181size313700.16	-2.24	1.84E-02	NA	NA
0.025 / Ctrl	Common	evm.TU.scaffold269size275974.15	-1.84	4.63E-02	HUMAN	*SNED1*
1 / Ctrl	Common	evm.TU.scaffold5737size147992.4	-9.92	3.31E-13	PLAYO	*CSP*
1 / Ctrl	Common	evm.TU.scaffold2059size101583.8	-9.19	5.61E-11	NA	NA
1 / Ctrl	Common	evm.TU.scaffold6483size290382.9	-6.44	5.14E-05	HUMAN	*LOXH1*
1 / Ctrl	Common	evm.TU.scaffold1765size248259.2	-6.13	7.28E-04	NA	NA
1 / Ctrl	Common	evm.TU.scaffold12797size22360.1	-5.51	8.64E-04	NA	NA
1 / Ctrl	Common	evm.TU.scaffold3140size111674.1	-4.73	1.64E-02	NA	NA
1 / Ctrl	Common	evm.TU.scaffold2106size257207.9	-4.54	3.86E-04	NA	NA
1 / Ctrl	Non-common	evm.TU.scaffold1310size120650.5	-4.39	4.86E-03	NA	NA
1 / Ctrl	Common	evm.TU.scaffold50size263963.6	-4.30	5.59E-04	PINMG	*PLSP*
1 / Ctrl	Common	evm.TU.scaffold200size231477.1	-3.97	3.49E-02	NA	NA
1 / Ctrl	Common	evm.TU.scaffold821size195697.10	-3.84	9.91E-03	NA	NA
1 / Ctrl	Non-common	evm.TU.scaffold8841size45349.2	-2.41	3.00E-02	HUMAN	*HIPL2*
1 / Ctrl	Non-common	evm.TU.scaffold602size184052.6	-2.37	2.91E-02	NA	NA
1 / Ctrl	Common	evm.TU.scaffold269size275974.15	-1.87	1.85E-02	HUMAN	*SNED1*
1 / Ctrl	Non-common	evm.TU.scaffold5152size61452.2	-1.79	3.09E-02	NA	NA
• **Brown module**						
0.025 / Ctrl	Common	evm.TU.scaffold43size421361.3	2.61	3.61E-02	NA	NA
0.025 / Ctrl	Common	evm.TU.scaffold7152size47383.1	2.32	3.38E-02	NA	NA
0.025 / Ctrl	Non-common	evm.TU.scaffold1886size104796.7	1.70	4.53E-03	MOUSE	*TIMP3*
0.025 / Ctrl	Common	evm.TU.scaffold2796size88200.2	1.39	4.18E-02	RAT	*SQSTM*
1 / Ctrl	Non-common	evm.TU.scaffold3135size191244.13	3.39	2.48E-03	NA	NA
1 / Ctrl	Non-common	evm.TU.scaffold4691size150772.6	3.26	3.00E-02	NA	NA
1 / Ctrl	Non-common	evm.TU.scaffold2520size198016.9	3.23	9.44E-03	NA	NA
1 / Ctrl	Non-common	evm.TU.scaffold195size421668.4	3.05	3.59E-02	DROME	*ORCT*
1 / Ctrl	Non-common	evm.TU.scaffold589size246915.7	2.88	3.99E-02	PINMG	*USP11*
1 / Ctrl	Non-common	evm.TU.scaffold4038size138132.1	2.68	4.05E-02	NA	NA
1 / Ctrl	Non-common	evm.TU.scaffold7389size103885.2	2.67	4.22E-02	NA	NA
1 / Ctrl	Non-common	evm.TU.scaffold9793size46053.1	2.61	4.32E-02	RENRE	*CALM*
1 / Ctrl	Non-common	evm.TU.scaffold4719size195833.2	2.39	4.78E-02	NA	NA
1 / Ctrl	Common	evm.TU.scaffold7152size47383.1	2.39	9.07E-03	NA	NA
1 / Ctrl	Common	evm.TU.scaffold43size421361.3	2.28	4.31E-02	NA	NA
1 / Ctrl	Non-common	evm.TU.scaffold15973size12996.1	2.13	3.69E-02	RAT	*S22A1*
1 / Ctrl	Non-common	evm.TU.scaffold954size354069.4	2.12	4.11E-02	DANRE	*CHSTB*
1 / Ctrl	Non-common	evm.TU.scaffold10557size30422.4	1.92	4.04E-02	NA	NA
1 / Ctrl	Non-common	evm.TU.scaffold14275size36645.1	1.91	4.46E-02	DANRE	*PPR3B*
1 / Ctrl	Non-common	evm.TU.scaffold9061size109501.3	1.89	5.92E-03	ARATH	*CNIF3*
1 / Ctrl	Non-common	evm.TU.scaffold1051size221401.11	1.88	9.44E-03	NA	NA

Table S3 (*continued*)

1 / Ctrl	Non-common	evm.TU.scaffold2334size95770.5	1.84	2.21E-03	NA	NA
1 / Ctrl	Non-common	evm.TU.scaffold17038size9778.1	1.79	2.10E-02	HUMAN	*CHK2*
1 / Ctrl	Non-common	evm.TU.scaffold7295size46532.3	1.77	5.24E-04	CRIGR	*ASNS*
1 / Ctrl	Non-common	evm.TU.scaffold1347size133901.9	1.77	4.39E-02	HUMAN	*TYSY*
1 / Ctrl	Non-common	evm.TU.scaffold2293size159229.6	1.65	3.69E-02	MOUSE	*ANPRA*
1 / Ctrl	Non-common	evm.TU.scaffold10540size30515.2	1.57	9.21E-06	NA	NA
1 / Ctrl	Non-common	evm.TU.scaffold331size210939.5	1.52	6.07E-03	NA	NA
1 / Ctrl	Common	evm.TU.scaffold2796size88200.2	1.49	9.07E-03	RAT	*SQSTM*
1 / Ctrl	Non-common	evm.TU.scaffold669size217235.14	1.48	3.35E-02	NA	NA
1 / Ctrl	Non-common	evm.TU.scaffold2289size96356.2	1.44	2.48E-03	RAT	*ACOX1*
1 / Ctrl	Non-common	evm.TU.scaffold331size210939.6	1.43	9.39E-03	NA	NA
1 / Ctrl	Non-common	evm.TU.scaffold331size210939.7	1.42	3.13E-02	NA	NA
1 / Ctrl	Non-common	evm.TU.scaffold804size228196.3	1.39	3.69E-02	DANRE	*CHST1*
1 / Ctrl	Non-common	evm.TU.scaffold10998size55334.1	1.33	3.78E-02	CHICK	*HENMT*
1 / Ctrl	Non-common	evm.TU.scaffold2763size110907.3	1.31	4.31E-02	PONAB	*GUAD*
1 / Ctrl	Non-common	evm.TU.scaffold20size301897.8	1.29	3.59E-02	MOUSE	*PTPRK*
1 / Ctrl	Non-common	evm.TU.scaffold3153size131015.3	1.27	3.25E-02	HUMAN	*NCKX4*
1 / Ctrl	Non-common	evm.TU.scaffold6202size53514.4	1.19	1.44E-02	HUMAN	*NCKX4*
1 / Ctrl	Non-common	evm.TU.scaffold5648size169074.2	1.15	4.78E-02	MOUSE	*CO6A4*
1 / Ctrl	Non-common	evm.TU.scaffold6645size79183.4	1.10	2.10E-02	NA	NA
1 / Ctrl	Non-common	evm.TU.scaffold5864size56104.1	1.07	4.05E-02	XENTR	*RN126*
1 / Ctrl	Non-common	evm.TU.scaffold6245size92827.2	1.06	3.53E-02	NA	NA
● **Tan module**						
0.025 / Ctrl	Common	evm.TU.scaffold7405size45879.10	5.12	3.19E-02	NA	NA
0.025 / Ctrl	Common	evm.TU.scaffold4668size197402.2	4.16	3.54E-02	HUMAN	*HDHD5*
0.025 / Ctrl	Common	evm.TU.scaffold547size159297.1	4.07	1.34E-02	PONAB	*CRYAB*
0.025 / Ctrl	Common	evm.TU.scaffold8768size38583.2	3.44	4.13E-02	HUMAN	*HDHD5*
0.025 / Ctrl	Common	evm.TU.scaffold3144size225807.5	2.74	3.06E-02	METMA	*Y045*
0.025 / Ctrl	Common	evm.TU.scaffold4142size191490.2	2.28	3.49E-02	DROVI	*TIM*
0.025 / Ctrl	Common	evm.TU.scaffold156size437243.7	1.80	2.77E-03	DROME	*RIM2*
1 / Ctrl	Common	evm.TU.scaffold7405size45879.10	5.98	1.32E-03	NA	NA
1 / Ctrl	Non-common	evm.TU.scaffold516size244129.2	5.54	1.03E-04	BIOOB	*ACTC*
1 / Ctrl	Non-common	evm.TU.scaffold423size170276.3	5.50	2.23E-06	ANOAL	*HSP74*
1 / Ctrl	Non-common	evm.TU.scaffold7405size45879.11	5.25	1.35E-03	NA	NA
1 / Ctrl	Common	evm.TU.scaffold4668size197402.2	5.18	7.02E-04	HUMAN	*HDHD5*
1 / Ctrl	Non-common	evm.TU.scaffold7304size63610.2	5.07	8.63E-04	ANOAL	*HSP71*
1 / Ctrl	Common	evm.TU.scaffold4142size191490.2	4.72	9.93E-13	DROVI	*TIM*
1 / Ctrl	Common	evm.TU.scaffold547size159297.1	4.55	8.63E-04	PONAB	*CRYAB*
1 / Ctrl	Common	evm.TU.scaffold8768size38583.2	4.36	7.02E-04	HUMAN	*HDHD5*
1 / Ctrl	Non-common	evm.TU.scaffold10008size45161.1	4.30	2.30E-03	MOUSE	*XIAP*
1 / Ctrl	Non-common	evm.TU.scaffold4507size80223.1	4.19	9.57E-08	HUMAN	*ST1B1*
1 / Ctrl	Common	evm.TU.scaffold156size437243.7	4.09	9.60E-23	DROME	*RIM2*

Table S3 (*continued*)

1 / Ctrl	Non-common	evm.TU.scaffold4142size191490.1	4.03	7.21E-13	NA	NA
1 / Ctrl	Non-common	evm.TU.scaffold15236size35086.2	3.99	1.02E-05	HUMAN	*CP2J2*
1 / Ctrl	Non-common	evm.TU.scaffold1977size112688.7	3.96	3.33E-06	HUMAN	*CP2C8*
1 / Ctrl	Non-common	evm.TU.scaffold4424size135461.1	3.86	1.39E-04	NA	NA
1 / Ctrl	Non-common	evm.TU.scaffold2381size136822.10	3.86	5.59E-04	STRPU	*SUREJ*
1 / Ctrl	Non-common	evm.TU.scaffold4914size63546.4	3.80	1.51E-02	MOUSE	*XIAP*
1 / Ctrl	Non-common	evm.TU.scaffold3992size72970.1	3.55	2.98E-05	LYTVA	*ERG*
1 / Ctrl	Non-common	evm.TU.scaffold3340size152636.6	3.29	6.20E-06	HUMAN	*BAG4*
1 / Ctrl	Non-common	evm.TU.scaffold8613size59507.2	3.22	1.28E-03	HUMAN	*CP2C8*
1 / Ctrl	Non-common	evm.TU.scaffold8613size59507.1	3.19	6.87E-06	HUMAN	*CP2C8*
1 / Ctrl	Non-common	evm.TU.scaffold6111size64662.2	3.17	2.18E-02	NA	NA
1 / Ctrl	Non-common	evm.TU.scaffold10769size29507.1	3.16	2.19E-04	XENTR	*CRBL2*
1 / Ctrl	Non-common	evm.TU.scaffold1859size193902.2	3.16	3.59E-02	NA	NA
1 / Ctrl	Non-common	evm.TU.scaffold1306size120932.1	3.08	5.96E-03	RAT	*TANC1*
1 / Ctrl	Non-common	evm.TU.scaffold923size253024.9	3.00	3.31E-13	MOUSE	*GLNA*
1 / Ctrl	Non-common	evm.TU.scaffold1402size289848.5	2.93	1.31E-03	CUPNH	*BDHA*
1 / Ctrl	Non-common	evm.TU.scaffold1232size123727.3	2.92	8.94E-06	NA	NA
1 / Ctrl	Non-common	evm.TU.scaffold2263size96786.2	2.91	1.42E-04	NA	NA
1 / Ctrl	Non-common	evm.TU.scaffold16572size11220.1	2.88	1.32E-03	NA	NA
1 / Ctrl	Non-common	evm.TU.scaffold6147size107483.2	2.79	1.32E-03	MOUSE	*DNJB4*
1 / Ctrl	Non-common	evm.TU.scaffold14314size34631.2	2.77	8.34E-04	NA	NA
1 / Ctrl	Non-common	evm.TU.scaffold4007size117063.6	2.75	2.64E-03	NA	NA
1 / Ctrl	Common	evm.TU.scaffold3144size225807.5	2.71	1.23E-02	METMA	*Y045*
1 / Ctrl	Non-common	evm.TU.scaffold4421size170941.3	2.65	7.46E-04	NA	NA
1 / Ctrl	Non-common	evm.TU.scaffold6705size50169.3	2.61	7.21E-13	NA	NA
1 / Ctrl	Non-common	evm.TU.scaffold911size301844.6	2.56	3.27E-03	NA	NA
1 / Ctrl	Non-common	evm.TU.scaffold1569size194665.2	2.50	1.23E-02	HUMAN	*S26A5*
1 / Ctrl	Non-common	evm.TU.scaffold8459size104388.2	2.48	4.54E-03	NA	NA
1 / Ctrl	Non-common	evm.TU.scaffold4500size109838.9	2.41	2.30E-02	NA	NA
1 / Ctrl	Non-common	evm.TU.scaffold6782size89013.6	2.37	1.44E-02	EMENI	*AOX*
1 / Ctrl	Non-common	evm.TU.scaffold2268size120505.4	2.35	2.42E-02	HUMAN	*PERT*
1 / Ctrl	Non-common	evm.TU.scaffold1569size194665.3	2.25	2.31E-02	MOUSE	*S26A5*
1 / Ctrl	Non-common	evm.TU.scaffold4354size153558.3	2.17	9.35E-04	NA	NA
1 / Ctrl	Non-common	evm.TU.scaffold4799size148529.5	2.15	4.05E-02	NA	NA
1 / Ctrl	Non-common	evm.TU.scaffold2268size120505.3	2.15	3.34E-02	AEDAE	*PERC*
1 / Ctrl	Non-common	evm.TU.scaffold52size326587.11	2.11	5.29E-03	DROME	*CRERF*
1 / Ctrl	Non-common	evm.TU.scaffold2920size86078.3	2.10	6.87E-06	RAT	*RUNX1*
1 / Ctrl	Non-common	evm.TU.scaffold2571size175983.3	2.08	5.17E-03	BOVIN	*GA45G*
1 / Ctrl	Non-common	evm.TU.scaffold3054size84299.8	2.05	1.54E-03	RAT	*GA45G*
1 / Ctrl	Non-common	evm.TU.scaffold10893size29080.1	2.03	2.30E-03	HUMAN	*SC6A5*
1 / Ctrl	Non-common	evm.TU.scaffold566size390051.15	1.99	5.61E-06	DROME	*HR4*
1 / Ctrl	Non-common	evm.TU.scaffold3108size104591.9	1.98	9.07E-03	DROME	*TOLL8*
1 / Ctrl	Non-common	evm.TU.scaffold9443size112071.3	1.89	6.65E-06	MOUSE	*GLNA*

Table S3 (*continued*)

1 / Ctrl	Non-common	evm.TU.scaffold2size410065.8	1.87	1.03E-03	URECA	*PAPSS*
1 / Ctrl	Non-common	evm.TU.scaffold1232size123727.5	1.78	2.01E-02	NA	NA
1 / Ctrl	Non-common	evm.TU.scaffold3850size100891.3	1.77	3.99E-02	MOUSE	*PHKG2*
1 / Ctrl	Non-common	evm.TU.scaffold11014size28661.1	1.76	3.49E-02	NA	NA
1 / Ctrl	Non-common	evm.TU.scaffold2595size215894.2	1.75	2.30E-03	NA	NA
1 / Ctrl	Non-common	evm.TU.scaffold91size419679.12	1.74	2.18E-02	NA	NA
1 / Ctrl	Non-common	evm.TU.scaffold10028size32743.1	1.72	1.75E-04	NA	NA
1 / Ctrl	Non-common	evm.TU.scaffold3469size173103.3	1.71	1.20E-02	DROME	*GBS76*
1 / Ctrl	Non-common	evm.TU.scaffold1217size124397.2	1.67	1.08E-02	RAT	*RAD*
1 / Ctrl	Non-common	evm.TU.scaffold1975size160888.6	1.61	2.18E-02	MOUSE	*OTUD4*
1 / Ctrl	Non-common	evm.TU.scaffold2754size425210.25	1.61	3.89E-02	DROME	*GBS76*
1 / Ctrl	Non-common	evm.TU.scaffold284size239466.4	1.56	5.24E-04	CANLF	*CREM*
1 / Ctrl	Non-common	evm.TU.scaffold2243size120663.1	1.55	9.07E-03	NA	NA
1 / Ctrl	Non-common	evm.TU.scaffold2230size106613.2	1.52	1.65E-02	MOUSE	*LICH*
1 / Ctrl	Non-common	evm.TU.scaffold8726size38766.3	1.50	9.29E-03	NA	NA
1 / Ctrl	Non-common	evm.TU.scaffold1073size243907.6	1.50	4.06E-02	HUMAN	*ZF64A*
1 / Ctrl	Non-common	evm.TU.scaffold4865size132635.2	1.44	1.83E-02	NA	NA
1 / Ctrl	Non-common	evm.TU.scaffold6537size128148.3	1.43	4.57E-02	PONAB	*KCNJ6*
1 / Ctrl	Non-common	evm.TU.scaffold2595size215894.3	1.39	9.30E-03	HUMAN	*S12A2*
1 / Ctrl	Non-common	evm.TU.scaffold4865size132635.8	1.38	3.62E-02	NA	NA
1 / Ctrl	Non-common	evm.TU.scaffold4355size182761.1	1.23	3.15E-03	DROME	*TIPT*
1 / Ctrl	Non-common	evm.TU.scaffold988size360591.6	1.16	4.94E-02	HUMAN	*MOT9*
1 / Ctrl	Non-common	evm.TU.scaffold9548size76407.1	1.15	4.78E-02	NA	NA
1 / Ctrl	Non-common	evm.TU.scaffold1657size298101.24	1.09	4.02E-02	MOUSE	*SOX9*
1 / Ctrl	Non-common	evm.TU.scaffold2138size251389.4	1.07	2.76E-02	RAT	*FAXC*
1 / Ctrl	Non-common	evm.TU.scaffold2375size239988.1	1.05	6.30E-04	NA	NA
1 / Ctrl	Non-common	evm.TU.scaffold487size301406.5	1.01	2.40E-02	HUMAN	*BMX*
• **Other modules**						
0.025 / Ctrl	Common	evm.TU.scaffold1962size430023.11	4.97	2.34E-03	FOAMV	*POL*
0.025 / Ctrl	Non-common	evm.TU.scaffold311size184142.4	2.75	4.18E-02	HUMAN	*MRC1*
0.025 / Ctrl	Common	evm.TU.scaffold5998size98449.3	2.31	2.34E-03	RAT	*T53I1*
0.025 / Ctrl	Non-common	evm.TU.scaffold363size555997.8	2.04	2.87E-02	XENLA	*LSM11*
0.025 / Ctrl	Common	evm.TU.scaffold9632size86143.8	1.67	5.67E-03	HUMAN	*C1QT6*
0.025 / Ctrl	Common	evm.TU.scaffold821size195697.6	1.67	4.55E-02	NA	NA
0.025 / Ctrl	Common	evm.TU.scaffold2074size101205.4	1.34	3.51E-02	NA	NA
0.025 / Ctrl	Non-common	evm.TU.scaffold4780size84937.2	1.24	2.90E-02	HUMAN	*NALD2*
0.025 / Ctrl	Non-common	evm.TU.scaffold3988size84221.2	1.11	3.61E-02	NA	NA
0.025 / Ctrl	Non-common	evm.TU.scaffold7882size77958.3	1.11	8.30E-03	HUMAN	*ZN704*
0.025 / Ctrl	Non-common	evm.TU.scaffold1879size416184.6	1.06	3.97E-02	NA	NA
0.025 / Ctrl	Common	evm.TU.scaffold8273size41043.2	-1.83	3.49E-02	NA	NA
0.025 / Ctrl	Non-common	evm.TU.scaffold7920size91439.1	-2.78	3.49E-02	NA	NA
1 / Ctrl	Non-common	evm.TU.scaffold1001size193257.4	4.21	2.56E-02	NA	NA

Table S3 (*continued*)

1 / Ctrl	Non-common	evm.TU.scaffold4248size70342.2	4.10	2.05E-03	RAT	*SVEP1*
1 / Ctrl	Common	evm.TU.scaffold1962size430023.11	3.47	4.44E-02	FOAMV	*POL*
1 / Ctrl	Non-common	evm.TU.scaffold2659size90145.1	3.20	4.04E-02	NA	NA
1 / Ctrl	Non-common	evm.TU.scaffold1865size145351.3	2.99	1.65E-02	MYCUA	*PHMT1*
1 / Ctrl	Non-common	evm.TU.scaffold530size229996.12	2.83	3.99E-02	NA	NA
1 / Ctrl	Non-common	evm.TU.scaffold8832size38300.1	2.80	3.49E-02	NA	NA
1 / Ctrl	Non-common	evm.TU.scaffold7495size74862.7	2.73	4.90E-02	CRAGI	*GIGA3*
1 / Ctrl	Non-common	evm.TU.scaffold5528size58456.2	2.47	3.13E-02	HUMAN	*MMEL1*
1 / Ctrl	Non-common	evm.TU.scaffold11073size57721.2	2.43	2.35E-02	BOVIN	*PPBT*
1 / Ctrl	Non-common	evm.TU.scaffold538size272809.1	2.39	4.46E-02	NA	NA
1 / Ctrl	Non-common	evm.TU.scaffold11862size25470.1	2.34	2.91E-02	CHICK	*PCKGC*
1 / Ctrl	Non-common	evm.TU.scaffold4199size70737.3	2.17	4.61E-02	NA	NA
1 / Ctrl	Non-common	evm.TU.scaffold6329size140121.4	2.06	4.62E-02	NA	NA
1 / Ctrl	Non-common	evm.TU.scaffold1672size179538.1	2.04	3.78E-02	NA	NA
1 / Ctrl	Non-common	evm.TU.scaffold9910size82706.2	1.88	1.18E-02	RAT	*ATPD*
1 / Ctrl	Non-common	evm.TU.scaffold4679size173293.8	1.87	5.31E-03	CHICK	*CP2H2*
1 / Ctrl	Non-common	evm.TU.scaffold2355size147709.9	1.85	3.25E-02	NA	NA
1 / Ctrl	Common	evm.TU.scaffold5998size98449.3	1.67	4.05E-02	RAT	*T53I1*
1 / Ctrl	Non-common	evm.TU.scaffold2431size306300.17	1.64	4.23E-02	NA	NA
1 / Ctrl	Common	evm.TU.scaffold9632size86143.8	1.64	2.42E-03	HUMAN	*C1QT6*
1 / Ctrl	Non-common	evm.TU.scaffold8802size110191.3	1.62	3.59E-02	NA	NA
1 / Ctrl	Non-common	evm.TU.scaffold2431size306300.16	1.60	1.64E-02	NA	NA
1 / Ctrl	Non-common	evm.TU.scaffold2939size141835.1	1.59	9.44E-03	RAT	*RAD*
1 / Ctrl	Common	evm.TU.scaffold821size195697.6	1.53	3.99E-02	NA	NA
1 / Ctrl	Non-common	evm.TU.scaffold8size399332.9	1.53	7.85E-03	NA	NA
1 / Ctrl	Non-common	evm.TU.scaffold1860size168990.7	1.51	4.31E-02	NA	NA
1 / Ctrl	Non-common	evm.TU.scaffold12246size24154.1	1.44	4.04E-02	CHICK	*TSN*
1 / Ctrl	Non-common	evm.TU.scaffold4614size66670.1	1.43	4.19E-02	HUMAN	*NAA25*
1 / Ctrl	Common	evm.TU.scaffold2074size101205.4	1.39	9.28E-03	NA	NA
1 / Ctrl	Non-common	evm.TU.scaffold13683size19512.2	1.36	3.49E-02	MOUSE	*AP2A*
1 / Ctrl	Non-common	evm.TU.scaffold2259size212231.7	1.35	2.53E-02	CHICK	*SSPO*
1 / Ctrl	Non-common	evm.TU.scaffold9364size86438.2	1.19	2.31E-02	NA	NA
1 / Ctrl	Non-common	evm.TU.scaffold9293size58634.2	1.15	4.05E-02	SHEEP	*LYAM3*
1 / Ctrl	Non-common	evm.TU.scaffold1567size137386.7	1.13	3.96E-02	NA	NA
1 / Ctrl	Non-common	evm.TU.scaffold2112size310749.7	1.04	7.00E-03	NA	NA
1 / Ctrl	Non-common	evm.TU.scaffold3440size326921.3	1.02	3.25E-02	XENLA	*SESN1*
1 / Ctrl	Non-common	evm.TU.scaffold1933size142028.6	-1.03	2.14E-02	NA	NA
1 / Ctrl	Non-common	evm.TU.scaffold1695size255123.7	-1.06	4.06E-02	NA	NA
1 / Ctrl	Non-common	evm.TU.scaffold276size362962.24	-1.52	3.63E-02	HUMAN	*PC11X*
1 / Ctrl	Common	evm.TU.scaffold8273size41043.2	-1.59	4.16E-02	NA	NA
1 / Ctrl	Non-common	evm.TU.scaffold2434size116401.5	-2.12	3.96E-02	MOUSE	*ST1B1*

Table S4. Gene Ontology (GO) enrichments in molecular function (MF) and biological process (BP) of module genes of interest (magenta, pink, and red modules) identified in hemocyte samples from WGCNA.

GO ID	GO term	Level	Nseqs	P_{adj}
● Magenta module				
MF				
GO:0003735	structural constituent of ribosome	2	166	< 0.001
GO:0005198	structural molecule activity	1	499	< 0.001
GO:0019843	rRNA binding	2	73	< 0.001
GO:0070180	large ribosomal subunit rRNA binding	3	6	< 0.001
GO:0003746	translation elongation factor activity	2	30	< 0.001
GO:0016427	tRNA (cytosine) methyltransferase activity	2	10	< 0.001
GO:0008186	RNA-dependent ATPase activity	3	6	< 0.001
GO:0140098	catalytic activity, acting on RNA	2	561	< 0.001
GO:0004549	tRNA-specific ribonuclease activity	3	14	< 0.001
GO:0001091	RNA polymerase II general transcription initiation factor binding	2	10	< 0.001
GO:0017176	phosphatidylinositol N-acetylglucosaminyltransferase activity	2	5	< 0.001
GO:0008173	RNA methyltransferase activity	3	81	< 0.001
GO:0140101	catalytic activity, acting on a tRNA	2	168	< 0.001
GO:0045182	translation regulator activity	1	180	0.0013
GO:0008097	5S rRNA binding	4	12	0.0015
GO:0016428	tRNA (cytosine-5-)-methyltransferase activity	6	6	0.0025
GO:0106029	tRNA pseudouridine synthase activity	2	6	0.0026
GO:0000049	tRNA binding	3	106	0.0027
GO:0030621	U4 snRNA binding	2	6	0.0027
GO:0008172	S-methyltransferase activity	5	14	0.0077
GO:0001094	TFIID-class transcription factor complex binding	4	7	0.0093
GO:0016635	oxidoreductase activity, acting on the CH-CH group of donors, quinone or related compound as acceptor	2	7	0.0097
GO:0001968	fibronectin binding	2	7	0.0115
GO:0015450	P-P-bond-hydrolysis-driven protein transmembrane transporter activity	2	8	0.0212
GO:0016892	endoribonuclease activity, producing 3'-phosphomonoesters	5	8	0.0290
GO:0004888	transmembrane signaling receptor activity	3	530	0.0381
GO:0030515	snoRNA binding	2	40	0.0381
GO:0003743	translation initiation factor activity	2	69	0.0411
GO:0004745	retinol dehydrogenase activity	4	17	0.0424
GO:0008175	tRNA methyltransferase activity	2	40	0.0425
BP				
GO:0000027	ribosomal large subunit assembly	3	31	< 0.001
GO:0000028	ribosomal small subunit assembly	3	11	< 0.001

Table S4 (*continued*)

GO:0000463	maturation of LSU-rRNA from tricistronic rRNA transcript (SSU-rRNA, 5.8S rRNA, LSU-rRNA)	4	20	< 0.001
GO:0000470	maturation of LSU-rRNA	3	35	< 0.001
GO:0002181	cytoplasmic translation	4	33	< 0.001
GO:0006396	RNA processing	2	949	< 0.001
GO:0006518	peptide metabolic process	4	356	< 0.001
GO:0034470	ncRNA processing	2	460	< 0.001
GO:0034660	ncRNA metabolic process	5	615	< 0.001
GO:0043603	cellular amide metabolic process	4	575	< 0.001
GO:0043604	amide biosynthetic process	2	320	< 0.001
GO:0043628	ncRNA 3'-end processing	3	54	< 0.001
GO:0044271	cellular nitrogen compound biosynthetic process	2	1186	< 0.001
GO:1901566	organonitrogen compound biosynthetic process	2	813	< 0.001
GO:0031123	RNA 3'-end processing	2	113	0.0026
GO:0016071	mRNA metabolic process	2	618	0.0050
GO:0006399	tRNA metabolic process	2	245	0.0058
GO:0006414	translational elongation	3	51	0.0060
GO:0034472	snRNA 3'-end processing	2	33	0.0065
GO:0034622	cellular protein-containing complex assembly	6	670	0.0068
GO:0070972	protein localization to endoplasmic reticulum	2	49	0.0200
GO:0001732	formation of cytoplasmic translation initiation complex	7	25	0.0203
GO:0071025	RNA surveillance	2	21	0.0210
GO:0071051	polyadenylation-dependent snoRNA 3'-end processing	2	7	0.0235
GO:0006413	translational initiation	3	52	0.0286
GO:0006401	RNA catabolic process	2	191	0.0458
Pink module				
MF				
GO:0002151	G-quadruplex RNA binding	2	8	< 0.001
GO:0051010	microtubule plus-end binding	2	20	< 0.001
GO:0004534	5'-3' exoribonuclease activity	3	7	< 0.001
GO:0106018	phosphatidylinositol-3,5-bisphosphate phosphatase activity	7	7	< 0.001
GO:0034593	phosphatidylinositol bisphosphate phosphatase activity	2	23	< 0.001
GO:0016308	1-phosphatidylinositol-4-phosphate 5-kinase activity	2	5	< 0.001
GO:0015924	mannosyl-oligosaccharide mannosidase activity	2	15	< 0.001
GO:0034595	phosphatidylinositol phosphate 5-phosphatase activity	6	15	< 0.001
GO:0003700	DNA-binding transcription factor activity	2	532	< 0.001
GO:0035197	siRNA binding	2	7	< 0.001
GO:0052866	phosphatidylinositol phosphate phosphatase activity	2	31	< 0.001
GO:0050291	sphingosine N-acyltransferase activity	2	7	< 0.001
GO:0005096	GTPase activator activity	4	218	< 0.001
GO:0016964	alpha-2 macroglobulin receptor activity	2	8	< 0.001
GO:0004572	mannosyl-oligosaccharide 1,3-1,6-alpha-mannosidase activity	4	8	< 0.001

Table S4 (*continued*)

GO:0008392	arachidonic acid epoxygenase activity	2	19	0.0011
GO:0140110	transcription regulator activity	1	887	0.0011
GO:0003831	beta-N-acetylglucosaminylglycopeptide beta-1,4-galactosyltransferase activity	2	9	0.0014
GO:0016491	oxidoreductase activity	2	1073	0.0018
GO:0032051	clathrin light chain binding	3	9	0.0028
GO:0015026	coreceptor activity	2	23	0.0036
GO:0035091	phosphatidylinositol binding	4	227	0.0036
GO:1990380	Lys48-specific deubiquitinase activity	4	16	0.0042
GO:0015183	L-aspartate transmembrane transporter activity	2	5	0.0071
GO:0070728	leucine binding	2	5	0.0071
GO:0005543	phospholipid binding	2	352	0.0072
GO:0043515	kinetochore binding	2	10	0.0072
GO:0008289	lipid binding	2	590	0.0075
GO:0008047	enzyme activator activity	3	355	0.0097
GO:0016404	15-hydroxyprostaglandin dehydrogenase (NAD+) activity	3	5	0.0106
GO:0030276	clathrin binding	2	43	0.0108
GO:0015095	magnesium ion transmembrane transporter activity	2	11	0.0146
GO:0043422	protein kinase B binding	5	11	0.0151
GO:0003707	steroid hormone receptor activity	2	45	0.0158
GO:0043325	phosphatidylinositol-3,4-bisphosphate binding	2	18	0.0180
GO:0004652	polynucleotide adenylyltransferase activity	5	6	0.0198
GO:0016884	carbon-nitrogen ligase activity, with glutamine as amido-N-donor	3	18	0.0209
GO:0005522	profilin binding	3	12	0.0237
GO:0051721	protein phosphatase 2A binding	2	37	0.0264
GO:0046966	thyroid hormone receptor binding	2	20	0.0284
GO:1901981	phosphatidylinositol phosphate binding	5	130	0.0284
GO:0004715	non-membrane spanning protein tyrosine kinase activity	5	48	0.0301
GO:0008391	arachidonic acid monooxygenase activity	2	27	0.0301
GO:0015296	anion:cation symporter activity	5	13	0.0388
GO:0071889	14-3-3 protein binding	2	20	0.0388
GO:0034452	dynactin binding	3	13	0.0391
GO:0000340	RNA 7-methylguanosine cap binding	2	13	0.0400
GO:0005545	1-phosphatidylinositol binding	5	14	0.0482
GO:0005159	insulin-like growth factor receptor binding	3	7	0.0490
BP				
GO:0030509	BMP signaling pathway	2	29	< 0.001
GO:0035304	regulation of protein dephosphorylation	3	71	< 0.001
GO:0070647	protein modification by small protein conjugation or removal	2	1017	< 0.001
GO:1903146	regulation of autophagy of mitochondrion	2	52	< 0.001
GO:0035303	regulation of dephosphorylation	2	137	0.0038
GO:0008286	insulin receptor signaling pathway	6	67	0.0063
GO:0016241	regulation of macroautophagy	5	125	0.0071
GO:1902667	regulation of axon guidance	3	19	0.0088

Table S4 (*continued*)

GO:0061912	selective autophagy	5	38	0.0119
GO:1901524	regulation of mitophagy	2	32	0.0125
GO:0045732	positive regulation of protein catabolic process	2	154	0.0130
GO:1904562	phosphatidylinositol 5-phosphate metabolic process	5	5	0.0139
GO:0048584	positive regulation of response to stimulus	2	1298	0.0143
GO:0016458	gene silencing	3	118	0.0146
GO:0006508	proteolysis	3	1101	0.0148
GO:0099003	vesicle-mediated transport in synapse	4	69	0.0154
GO:0048609	multicellular organismal reproductive process	2	490	0.0217
GO:0022603	regulation of anatomical structure morphogenesis	3	640	0.0226
GO:0010628	positive regulation of gene expression	4	1376	0.0258
GO:0031047	gene silencing by RNA	2	75	0.0386
GO:0060341	regulation of cellular localization	2	686	0.0408
GO:0022604	regulation of cell morphogenesis	5	232	0.0419
GO:1903599	positive regulation of autophagy of mitochondrion	4	32	0.0431
● **Red module**				
MF				
GO:0004497	monooxygenase activity	2	167	< 0.001
GO:0005506	iron ion binding	4	231	< 0.001
GO:0003964	RNA-directed DNA polymerase activity	3	94	< 0.001
GO:0015293	symporter activity	5	220	< 0.001
GO:0005343	organic acid:sodium symporter activity	4	56	< 0.001
GO:0008395	steroid hydroxylase activity	3	69	< 0.001
GO:0008028	monocarboxylic acid transmembrane transporter activity	2	84	< 0.001
GO:0016705	oxidoreductase activity, acting on paired donors, with incorporation or reduction of molecular oxygen	3	240	< 0.001
GO:0004930	G protein-coupled receptor activity	2	276	< 0.001
GO:0033781	cholesterol 24-hydroxylase activity	5	5	< 0.001
GO:0016491	oxidoreductase activity	2	1073	< 0.001
GO:0004062	aryl sulfotransferase activity	2	21	< 0.001
GO:0101021	estrogen 2-hydroxylase activity	4	14	< 0.001
GO:0016709	oxidoreductase activity, acting on paired donors, with incorporation or reduction of molecular oxygen, NAD(P)H as one donor, and incorporation of one atom of oxygen	2	52	< 0.001
GO:0008146	sulfotransferase activity	2	53	< 0.001
GO:0016798	hydrolase activity, acting on glycosyl bonds	2	269	< 0.001
GO:0004132	dCMP deaminase activity	2	7	< 0.001
GO:0004888	transmembrane signaling receptor activity	2	530	< 0.001
GO:0015081	sodium ion transmembrane transporter activity	2	166	< 0.001
GO:0004499	N,N-dimethylaniline monooxygenase activity	2	10	< 0.001
GO:0015171	amino acid transmembrane transporter activity	2	90	< 0.001
GO:0101020	estrogen 16-alpha-hydroxylase activity	2	23	< 0.001

Table S4 (*continued*)

GO:0001758	retinal dehydrogenase activity	5	11	< 0.001
GO:0016887	ATPase activity	3	688	< 0.001
GO:0034061	DNA polymerase activity	2	136	< 0.001
GO:1990935	splicing factor binding	2	5	< 0.001
GO:0046914	transition metal ion binding	3	1373	< 0.001
GO:0031628	opioid receptor binding	4	8	< 0.001
GO:0003943	N-acetylgalactosamine-4-sulfatase activity	4	8	< 0.001
GO:0008453	alanine-glyoxylate transaminase activity	2	5	< 0.001
GO:0042165	neurotransmitter binding	2	13	0.0010
GO:0015291	secondary active transmembrane transporter activity	4	295	0.0013
GO:0050649	testosterone 6-beta-hydroxylase activity	4	12	0.0013
GO:0050051	leukotriene-B4 20-monooxygenase activity	2	8	0.0014
GO:0030274	LIM domain binding	3	9	0.0022
GO:0016782	transferase activity, transferring sulfur-containing groups	3	84	0.0028
GO:0043237	laminin-1 binding	2	6	0.0029
GO:0008391	arachidonic acid monooxygenase activity	2	27	0.0030
GO:0008532	N-acetyllactosaminide beta-1,3-N-acetylglucosaminyltransferase activity	2	6	0.0030
GO:0004553	hydrolase activity, hydrolyzing O-glycosyl compounds	4	183	0.0034
GO:0015631	tubulin binding	2	361	0.0039
GO:0003774	motor activity	4	200	0.0046
GO:0046920	alpha-(1->3)-fucosyltransferase activity	2	14	0.0046
GO:0015926	glucosidase activity	2	36	0.0053
GO:0030246	carbohydrate binding	2	276	0.0066
GO:0070410	co-SMAD binding	3	25	0.0077
GO:0008422	beta-glucosidase activity	3	10	0.0078
GO:0050840	extracellular matrix binding	2	39	0.0100
GO:0008227	G protein-coupled amine receptor activity	2	16	0.0108
GO:0046974	histone methyltransferase activity (H3-K9 specific)	6	12	0.0108
GO:0017017	MAP kinase tyrosine/serine/threonine phosphatase activity	4	7	0.0112
GO:0018685	alkane 1-monooxygenase activity	2	6	0.0122
GO:0008417	fucosyltransferase activity	4	33	0.0137
GO:0008195	phosphatidate phosphatase activity	2	7	0.0145
GO:0043236	laminin binding	2	17	0.0163
GO:0003777	microtubule motor activity	2	125	0.0163
GO:0004065	arylsulfatase activity	5	16	0.0175
GO:0015245	fatty acid transmembrane transporter activity	3	34	0.0175
GO:0008484	sulfuric ester hydrolase activity	3	22	0.0218
GO:0005540	hyaluronic acid binding	4	24	0.0249
GO:0070412	R-SMAD binding	3	34	0.0251
GO:0005096	GTPase activator activity	2	218	0.0290
GO:0030234	enzyme regulator activity	2	838	0.0334
GO:0003682	chromatin binding	2	481	0.0338
GO:0005328	neurotransmitter:sodium symporter activity	4	17	0.0338

Table S4 (*continued*)

GO:0098772	molecular function regulator	1	1334	0.0338
GO:0008047	enzyme activator activity	2	355	0.0349
GO:0008017	microtubule binding	2	263	0.0368
GO:0008514	organic anion transmembrane transporter activity	2	175	0.0387
BP				
GO:0007186	G protein-coupled receptor signaling pathway	2	347	< 0.001
GO:0007530	sex determination	2	11	< 0.001
GO:0008202	steroid metabolic process	2	258	< 0.001
GO:0015074	DNA integration	5	89	< 0.001
GO:0030238	male sex determination	2	7	< 0.001
GO:0034308	primary alcohol metabolic process	2	80	< 0.001
GO:0042445	hormone metabolic process	3	162	< 0.001
GO:0006720	isoprenoid metabolic process	3	112	0.0019
GO:0060134	prepulse inhibition	6	13	0.0020
GO:0110053	regulation of actin filament organization	2	199	0.0021
GO:0032102	negative regulation of response to external stimulus	2	230	0.0022
GO:0042572	retinol metabolic process	3	34	0.0023
GO:0030855	epithelial cell differentiation	4	196	0.0024
GO:0006805	xenobiotic metabolic process	3	79	0.0026
GO:0006066	alcohol metabolic process	2	335	0.0028
GO:0044282	small molecule catabolic process	3	412	0.0033
GO:0034035	purine ribonucleoside bisphosphate metabolic process	2	26	0.0036
GO:0110110	positive regulation of animal organ morphogenesis	5	7	0.0038
GO:1901615	organic hydroxy compound metabolic process	3	478	0.0042
GO:0034754	cellular hormone metabolic process	2	85	0.0045
GO:0030155	regulation of cell adhesion	2	407	0.0047
GO:0050878	regulation of body fluid levels	3	146	0.0048
GO:0050807	regulation of synapse organization	3	207	0.0052
GO:0031333	negative regulation of protein-containing complex assembly	2	114	0.0054
GO:0019935	cyclic-nucleotide-mediated signaling	5	108	0.0056
GO:0120254	olefinic compound metabolic process	2	75	0.0108
GO:0015800	acidic amino acid transport	6	41	0.0114
GO:0010817	regulation of hormone levels	3	383	0.0118
GO:0050907	detection of chemical stimulus involved in sensory perception	2	16	0.0132
GO:0060049	regulation of protein glycosylation	4	20	0.0134
GO:0071425	hematopoietic stem cell proliferation	2	7	0.0137
GO:0042472	inner ear morphogenesis	4	28	0.0140
GO:0019932	second-messenger-mediated signaling	2	210	0.0141
GO:0045058	T cell selection	2	7	0.0144
GO:0007218	neuropeptide signaling pathway	2	64	0.0146
GO:0048935	peripheral nervous system neuron development	2	10	0.0148
GO:0021537	telencephalon development	2	21	0.0149
GO:1902903	regulation of supramolecular fiber organization	2	304	0.0151

Table S4 (*continued*)

GO:0031532	actin cytoskeleton reorganization	2	49	0.0158
GO:0045216	cell-cell junction organization	3	126	0.0192
GO:0022407	regulation of cell-cell adhesion	2	189	0.0195
GO:0009653	anatomical structure morphogenesis	2	1205	0.0210
GO:0060070	canonical Wnt signaling pathway	6	33	0.0222
GO:0030834	regulation of actin filament depolymerization	3	36	0.0262
GO:0034110	regulation of homotypic cell-cell adhesion	3	30	0.0269
GO:1900016	negative regulation of cytokine production involved in inflammatory response	2	7	0.0272
GO:0009247	glycolipid biosynthetic process	2	63	0.0273
GO:0007160	cell-matrix adhesion	3	78	0.0307
GO:0060124	positive regulation of growth hormone secretion	2	6	0.0312
GO:0090183	regulation of kidney development	4	8	0.0317
GO:0070371	ERK1 and ERK2 cascade	6	10	0.0322
GO:0060485	mesenchyme development	4	22	0.0349
GO:0007162	negative regulation of cell adhesion	2	167	0.0353
GO:0060563	neuroepithelial cell differentiation	6	6	0.0370
GO:1905332	positive regulation of morphogenesis of an epithelium	2	9	0.0450
GO:0015849	organic acid transport	7	202	0.0457
GO:0007610	behavior	1	504	0.0470
GO:0051241	negative regulation of multicellular organismal process	4	526	0.0488
GO:0006694	steroid biosynthetic process	2	123	0.0489
GO:0034330	cell junction organization	2	331	0.0494
GO:0022408	negative regulation of cell-cell adhesion	2	76	0.0494

Table S3. Differentially expressed genes (DEGs) across MNP conditions (0.025 and 1 µg L^{-1}) compared with the control condition identified in modules of interest from WGCNA performed on hemocyte samples sequencing dataset.

MNP condition	Sharing DEG	Sequencing gene ID	Log_2FC	P_{adj}	Uniprot *sp.*	Uniprot ID
● Magenta module						
0.025 / Ctrl	Common	evm.TU.scaffold7393size256918.12	-5.24	1.60E-03	NA	NA
0.025 / Ctrl	Non-common	evm.TU.scaffold2333size276275.9	-3.96	3.95E-03	CAEEL	*TYR1*
0.025 / Ctrl	Common	evm.TU.scaffold7711size59887.2	-3.55	3.45E-03	ARATH	*ARI4*
0.025 / Ctrl	Common	evm.TU.scaffold3049size175038.8	-3.31	2.41E-03	HUMAN	*KLH35*
0.025 / Ctrl	Common	evm.TU.scaffold4074size126334.5	-3.17	1.12E-02	HUMAN	*KLH35*
0.025 / Ctrl	Common	evm.TU.scaffold5110size61824.5	-3.08	3.99E-02	RAT	*RAB1A*
0.025 / Ctrl	Common	evm.TU.scaffold16265size12078.1	-2.78	4.89E-03	PONAB	*NUDT4*
0.025 / Ctrl	Common	evm.TU.scaffold2538size306768.10	-2.46	3.41E-02	XENLA	*UBC12*
0.025 / Ctrl	Non-common	evm.TU.scaffold13744size19329.1	-2.39	3.69E-02	MACFA	*GRIK3*
0.025 / Ctrl	Common	evm.TU.scaffold5948size109308.5	-2.38	1.45E-03	MOUSE	*LENG9*
0.025 / Ctrl	Common	evm.TU.scaffold361size559435.11	-2.26	3.52E-02	TETFL	*FOS*
0.025 / Ctrl	Common	evm.TU.scaffold1983size149908.5	-2.11	6.64E-03	MOUSE	*RASM*
0.025 / Ctrl	Non-common	evm.TU.scaffold13157size21177.1	-1.89	3.71E-02	CAEEL	*LACT2*
0.025 / Ctrl	Non-common	evm.TU.scaffold3050size175475.11	-1.85	1.90E-02	HUMAN	*PAR12*
0.025 / Ctrl	Non-common	evm.TU.scaffold8752size38646.1	-1.75	1.12E-02	NA	NA
0.025 / Ctrl	Common	evm.TU.scaffold2938size139678.6	-1.63	1.42E-02	NA	NA
0.025 / Ctrl	Non-common	evm.TU.scaffold3884size204650.3	-1.44	1.12E-02	PONAB	*T2EA*
0.025 / Ctrl	Common	evm.TU.scaffold12639size22886.1	-1.22	4.55E-02	HUMAN	*STX16*
0.025 / Ctrl	Common	evm.TU.scaffold297size379208.5	-1.18	8.80E-03	BOVIN	*WDR55*
0.025 / Ctrl	Non-common	evm.TU.scaffold7115size64842.1	-1.17	1.12E-02	BACSU	*YDAC*
0.025 / Ctrl	Non-common	evm.TU.scaffold5111size79043.2	-1.10	1.58E-02	HUMAN	*TBCD4*
1 / Ctrl	Non-common	evm.TU.scaffold9515size85861.4	-5.12	4.66E-06	ASHGO	*ARF*
1 / Ctrl	Common	evm.TU.scaffold5110size61824.5	-5.05	5.06E-06	RAT	*RAB1A*
1 / Ctrl	Non-common	evm.TU.scaffold6666size83753.9	-4.82	2.70E-03	DROME	*RHO1*
1 / Ctrl	Common	evm.TU.scaffold4074size126334.5	-4.57	5.06E-06	HUMAN	*KLH35*
1 / Ctrl	Non-common	evm.TU.scaffold3375size152648.1	-4.26	5.63E-03	RAT	*BATF3*
1 / Ctrl	Common	evm.TU.scaffold7393size256918.12	-4.07	2.80E-02	NA	NA
1 / Ctrl	Common	evm.TU.scaffold3049size175038.8	-3.94	1.62E-05	HUMAN	*KLH35*
1 / Ctrl	Common	evm.TU.scaffold7711size59887.2	-3.91	1.42E-04	ARATH	*ARI4*
1 / Ctrl	Non-common	evm.TU.scaffold950size134745.6	-3.61	2.93E-02	DIPOM	*RAB1*
1 / Ctrl	Common	evm.TU.scaffold2538size306768.10	-3.29	4.04E-04	XENLA	*UBC12*
1 / Ctrl	Non-common	evm.TU.scaffold4572size145658.10	-3.19	3.26E-02	RHIFE	*MET*
1 / Ctrl	Common	evm.TU.scaffold16265size12078.1	-2.83	1.44E-03	PONAB	*NUDT4*
1 / Ctrl	Common	evm.TU.scaffold1983size149908.5	-2.81	5.06E-06	MOUSE	*RASM*
1 / Ctrl	Common	evm.TU.scaffold5948size109308.5	-2.38	4.04E-04	MOUSE	*LENG9*
1 / Ctrl	Common	evm.TU.scaffold361size559435.11	-2.35	2.81E-02	TETFL	*FOS*

Table S5 (*continued*)

1 / Ctrl	Non-common	evm.TU.scaffold4254size144808.2	-2.27	1.27E-04	HUMAN	*GRHPR*
1 / Ctrl	Common	evm.TU.scaffold2938size139678.6	-1.84	2.43E-03	NA	NA
1 / Ctrl	Common	evm.TU.scaffold12639size22886.1	-1.47	5.64E-03	HUMAN	*STX16*
1 / Ctrl	Non-common	evm.TU.scaffold950size134745.10	-1.24	4.44E-02	XENLA	*RNF8B*
1 / Ctrl	Common	evm.TU.scaffold297size379208.5	-1.15	8.05E-03	BOVIN	*WDR55*
1 / Ctrl	Non-common	evm.TU.scaffold7344size46251.4	-1.00	2.80E-02	HUMAN	*AAMP*
Pink module						
1 / Ctrl	Non-common	evm.TU.scaffold15236size35086.2	5.63	4.34E-05	HUMAN	*CP2J2*
1 / Ctrl	Non-common	evm.TU.scaffold8613size59507.1	4.99	4.35E-05	HUMAN	*CP2C8*
1 / Ctrl	Non-common	evm.TU.scaffold4507size80223.1	3.90	1.27E-04	HUMAN	*ST1B1*
1 / Ctrl	Non-common	evm.TU.scaffold7855size43288.1	3.72	4.02E-02	RAT	*APJ*
1 / Ctrl	Non-common	evm.TU.scaffold208size201665.19	2.97	2.81E-02	HUMAN	*FEM1B*
1 / Ctrl	Non-common	evm.TU.scaffold3917size111660.3	1.89	2.70E-02	NA	NA
1 / Ctrl	Non-common	evm.TU.scaffold8043size64624.1	1.36	4.04E-04	MOUSE	*ZNT1*
1 / Ctrl	Non-common	evm.TU.scaffold1363size181262.6	1.36	3.89E-02	MOUSE	*ZNT10*
Red module						
0.025 / Ctrl	Common	evm.TU.scaffold16787size10633.1	-2.97	1.12E-02	ARATH	*ARI4*
0.025 / Ctrl	Non-common	evm.TU.scaffold309size232637.11	-2.83	3.34E-02	CAEEL	*YRD6*
0.025 / Ctrl	Common	evm.TU.scaffold919size193053.2	-2.78	5.06E-05	HUMAN	*RN126*
0.025 / Ctrl	Common	evm.TU.scaffold13945size18790.1	-2.60	4.17E-02	ARATH	*ARI1*
0.025 / Ctrl	Non-common	evm.TU.scaffold12218size40870.3	-2.34	9.55E-03	MOUSE	*SIAE*
0.025 / Ctrl	Non-common	evm.TU.scaffold7564size139168.1	-2.15	4.17E-02	DANRE	*JAG1A*
0.025 / Ctrl	Non-common	evm.TU.scaffold7356size111678.5	-2.01	4.99E-02	XENLA	*RO60*
0.025 / Ctrl	Non-common	evm.TU.scaffold7549size111641.1	-1.99	1.29E-02	BOVIN	*OXDD*
0.025 / Ctrl	Non-common	evm.TU.scaffold15230size15130.1	-1.96	3.62E-02	DICDI	*VWKA*
0.025 / Ctrl	Non-common	evm.TU.scaffold3615size291024.22	-1.88	1.88E-02	XENLA	*BECN1*
0.025 / Ctrl	Non-common	evm.TU.scaffold2076size120888.4	-1.66	1.12E-02	HUMAN	*CEBPG*
0.025 / Ctrl	Non-common	evm.TU.scaffold2571size175983.7	-1.48	1.51E-02	RAT	*GA45A*
0.025 / Ctrl	Non-common	evm.TU.scaffold320size404118.4	-1.06	3.62E-02	NA	NA
1 / Ctrl	Non-common	evm.TU.scaffold9515size85861.2	-5.14	1.38E-04	ASHGO	*ARF*
1 / Ctrl	Non-common	evm.TU.scaffold950size134745.7	-4.33	4.04E-04	DIPOM	*RAB1*
1 / Ctrl	Non-common	evm.TU.scaffold5110size61824.6	-3.81	1.60E-03	DIPOM	*RAB1*
1 / Ctrl	Non-common	evm.TU.scaffold1131size175864.5	-3.39	2.84E-04	DICDI	*AAC4*
1 / Ctrl	Non-common	evm.TU.scaffold5902size97825.3	-3.28	2.00E-02	NA	NA
1 / Ctrl	Non-common	evm.TU.scaffold4897size63734.4	-3.15	7.82E-05	DROME	*RHO1*
1 / Ctrl	Common	evm.TU.scaffold13945size18790.1	-3.12	5.52E-03	ARATH	*ARI1*
1 / Ctrl	Common	evm.TU.scaffold16787size10633.1	-3.10	5.52E-03	ARATH	*ARI4*
1 / Ctrl	Non-common	evm.TU.scaffold13307size20673.1	-2.59	1.81E-02	NA	NA
1 / Ctrl	Non-common	evm.TU.scaffold14583size16930.1	-2.49	2.49E-03	HUMAN	*GRHPR*
1 / Ctrl	Common	evm.TU.scaffold919size193053.2	-2.43	2.16E-04	HUMAN	*RN126*
1 / Ctrl	Non-common	evm.TU.scaffold2007size114573.3	-2.38	4.45E-02	MOUSE	*COCA1*

Table S5 (*continued*)

1 / Ctrl	Non-common	evm.TU.scaffold4760size205847.8	-2.35	2.97E-02	MOUSE	*EAA2*
1 / Ctrl	Non-common	evm.TU.scaffold11219size78477.2	-2.29	3.93E-03	MIMIV	*YR811*
1 / Ctrl	Non-common	evm.TU.scaffold812size140740.3	-2.04	3.32E-02	XENLA	*EGR1B*
1 / Ctrl	Non-common	evm.TU.scaffold2964size95999.5	-1.21	2.88E-02	CHICK	*PGGHG*
1 / Ctrl	Non-common	evm.TU.scaffold8467size62171.3	-1.11	1.73E-03	HUMAN	*PIR*
• **Other modules**						
0.025 / Ctrl	Common	evm.TU.scaffold11837size49671.2	7.90	7.58E-03	MOUSE	*RSP14*
0.025 / Ctrl	Common	evm.TU.scaffold221size240150.25	6.47	2.05E-02	NA	NA
0.025 / Ctrl	Non-common	evm.TU.scaffold222size381503.2	6.12	1.29E-02	NA	NA
0.025 / Ctrl	Common	evm.TU.scaffold2404size94544.2	6.02	9.72E-03	DROME	*Y3556*
0.025 / Ctrl	Non-common	evm.TU.scaffold4647size66183.6	5.99	1.12E-02	DANRE	*CFA53*
0.025 / Ctrl	Non-common	evm.TU.scaffold681size258651.11	5.94	3.92E-02	MOUSE	*BAI1*
0.025 / Ctrl	Non-common	evm.TU.scaffold12294size23998.1	5.91	7.52E-03	NA	NA
0.025 / Ctrl	Non-common	evm.TU.scaffold463size180809.1	5.86	4.34E-03	HUMAN	*IF*
0.025 / Ctrl	Non-common	evm.TU.scaffold7393size256918.3	5.78	2.90E-02	NA	NA
0.025 / Ctrl	Non-common	evm.TU.scaffold2610size137834.4	5.76	1.12E-02	MACFA	*IQUB*
0.025 / Ctrl	Non-common	evm.TU.scaffold850size206783.3	5.75	3.03E-02	NA	NA
0.025 / Ctrl	Non-common	evm.TU.scaffold5921size55650.4	5.72	1.12E-02	DANRE	*CF161*
0.025 / Ctrl	Non-common	evm.TU.scaffold6456size51796.1	5.71	4.55E-02	NA	NA
0.025 / Ctrl	Non-common	evm.TU.scaffold3546size132595.3	5.68	7.52E-03	HUMAN	*ANK3*
0.025 / Ctrl	Common	evm.TU.scaffold8940size68868.3	5.56	1.12E-02	XENTR	*CF157*
0.025 / Ctrl	Non-common	evm.TU.scaffold3321size121371.3	5.51	1.12E-02	DANRE	*PKD2*
0.025 / Ctrl	Non-common	evm.TU.scaffold12592size23029.1	5.50	6.64E-03	HUMAN	*DYH8*
0.025 / Ctrl	Common	evm.TU.scaffold4459size79009.8	5.26	6.64E-03	BOVIN	*PPR32*
0.025 / Ctrl	Non-common	evm.TU.scaffold806size231242.2	5.14	2.88E-02	NA	NA
0.025 / Ctrl	Non-common	evm.TU.scaffold4672size195439.9	5.05	1.55E-02	HUMAN	*CC113*
0.025 / Ctrl	Common	evm.TU.scaffold3517size464559.25	5.03	1.27E-02	MOUSE	*RSP14*
0.025 / Ctrl	Non-common	evm.TU.scaffold2197size98154.8	4.93	3.45E-03	NA	NA
0.025 / Ctrl	Non-common	evm.TU.scaffold3241size249433.15	4.91	1.12E-02	NA	NA
0.025 / Ctrl	Non-common	evm.TU.scaffold563size157350.3	4.88	1.12E-02	NA	NA
0.025 / Ctrl	Non-common	evm.TU.scaffold5174size81425.5	4.87	3.68E-02	NA	NA
0.025 / Ctrl	Non-common	evm.TU.scaffold992size143308.6	4.86	1.87E-02	XENTR	*MORN5*
0.025 / Ctrl	Common	evm.TU.scaffold146size219328.4	4.86	2.87E-02	DROME	*DCHS*
0.025 / Ctrl	Common	evm.TU.scaffold226size262146.9	4.86	1.51E-02	MOUSE	*CJ107*
0.025 / Ctrl	Non-common	evm.TU.scaffold4142size191490.3	4.80	1.12E-02	HUMAN	*IQCG*
0.025 / Ctrl	Common	evm.TU.scaffold4681size152784.13	4.77	1.12E-02	DANRE	*CA194*
0.025 / Ctrl	Non-common	evm.TU.scaffold3836size146814.7	4.73	1.88E-02	NA	NA
0.025 / Ctrl	Common	evm.TU.scaffold463size180809.4	4.63	2.08E-02	HUMAN	*IF*
0.025 / Ctrl	Non-common	evm.TU.scaffold9143size36786.1	4.59	4.24E-02	NA	NA
0.025 / Ctrl	Non-common	evm.TU.scaffold2529size92329.8	4.53	4.99E-02	MOUSE	*TTLL3*
0.025 / Ctrl	Common	evm.TU.scaffold1897size104575.3	4.46	1.90E-02	NA	NA
0.025 / Ctrl	Non-common	evm.TU.scaffold1829size129277.8	4.39	1.55E-02	DANRE	*RSPH9*

Table S5 (*continued*)

0.025 / Ctrl	Common	evm.TU.scaffold5577size58180.9	4.23	4.93E-02	NA	NA
0.025 / Ctrl	Non-common	evm.TU.scaffold9510size88084.1	4.02	1.28E-02	NA	NA
0.025 / Ctrl	Non-common	evm.TU.scaffold2595size215894.1	4.02	3.03E-02	NA	NA
0.025 / Ctrl	Non-common	evm.TU.scaffold4133size128356.4	4.02	1.75E-02	BOVIN	*CA228*
0.025 / Ctrl	Non-common	evm.TU.scaffold5653size69837.1	3.91	2.51E-02	XENLA	*STPG1*
0.025 / Ctrl	Non-common	evm.TU.scaffold221size240150.23	3.90	4.22E-02	NA	NA
0.025 / Ctrl	Non-common	evm.TU.scaffold1719size162498.5	3.76	4.01E-02	NA	NA
0.025 / Ctrl	Non-common	evm.TU.scaffold1436size266347.2	3.75	3.67E-02	HUMAN	*PPE2*
0.025 / Ctrl	Non-common	evm.TU.scaffold4185size140911.1	3.71	1.14E-02	NA	NA
0.025 / Ctrl	Non-common	evm.TU.scaffold4372size109182.3	3.61	3.41E-02	RAT	*ATS7*
0.025 / Ctrl	Non-common	evm.TU.scaffold7961size42695.2	3.46	2.36E-02	HUMAN	*AXDN1*
0.025 / Ctrl	Non-common	evm.TU.scaffold5998size98449.3	3.46	3.52E-02	RAT	*T53I1*
0.025 / Ctrl	Non-common	evm.TU.scaffold3088size183400.8	3.38	7.59E-03	CAEEL	*NU301*
0.025 / Ctrl	Non-common	evm.TU.scaffold5484size173863.14	3.37	1.12E-02	ANOGA	*ACT5C*
0.025 / Ctrl	Non-common	evm.TU.scaffold1685size218742.7	3.36	1.12E-02	NA	NA
0.025 / Ctrl	Non-common	evm.TU.scaffold533size312678.16	3.34	1.12E-02	MOUSE	*FRS1L*
0.025 / Ctrl	Non-common	evm.TU.scaffold8115size110444.6	3.22	4.99E-02	XENLA	*DRC1*
0.025 / Ctrl	Non-common	evm.TU.scaffold91size419679.4	3.09	4.99E-02	HUMAN	*DCST1*
0.025 / Ctrl	Non-common	evm.TU.scaffold1359size119114.5	3.07	4.75E-02	DROME	*ORCT*
0.025 / Ctrl	Non-common	evm.TU.scaffold4725size212881.2	3.06	2.45E-02	RAT	*PA216*
0.025 / Ctrl	Common	evm.TU.scaffold4142size191490.2	3.00	7.58E-03	DROVI	*TIM*
0.025 / Ctrl	Common	evm.TU.scaffold779size161378.9	2.93	3.00E-02	MOUSE	*ASGR1*
0.025 / Ctrl	Non-common	evm.TU.scaffold827size139563.7	2.83	4.55E-02	MOUSE	*THSD4*
0.025 / Ctrl	Non-common	evm.TU.scaffold8864size38164.3	2.83	1.12E-02	CAEEL	*SAR1*
0.025 / Ctrl	Non-common	evm.TU.scaffold4943size115742.4	2.58	1.81E-02	NA	NA
0.025 / Ctrl	Non-common	evm.TU.scaffold3170size128794.5	2.39	4.97E-02	PONAB	*DERL2*
0.025 / Ctrl	Common	evm.TU.scaffold4142size191490.1	2.35	1.12E-02	NA	NA
0.025 / Ctrl	Non-common	evm.TU.scaffold11862size25470.1	2.33	2.90E-02	CHICK	*PCKGC*
0.025 / Ctrl	Common	evm.TU.scaffold11383size52394.5	2.32	4.71E-02	RAT	*EXOC5*
0.025 / Ctrl	Non-common	evm.TU.scaffold630size420493.13	2.24	2.45E-02	ECOK1	*NEUO*
0.025 / Ctrl	Non-common	evm.TU.scaffold9302size36091.2	2.22	1.25E-02	MOUSE	*I23O2*
0.025 / Ctrl	Non-common	evm.TU.scaffold42size538778.13	1.90	3.77E-02	HUMAN	*PLMN*
0.025 / Ctrl	Common	evm.TU.scaffold156size437243.7	1.59	1.55E-02	DROME	*RIM2*
0.025 / Ctrl	Non-common	evm.TU.scaffold2559size260802.11	1.48	2.45E-02	CAEEL	*UNC9*
0.025 / Ctrl	Non-common	evm.TU.scaffold12791size22372.1	1.35	3.62E-02	NA	NA
0.025 / Ctrl	Non-common	evm.TU.scaffold4076size181903.4	1.24	1.55E-02	HUMAN	*ANK1*
0.025 / Ctrl	Non-common	evm.TU.scaffold12116size42260.2	1.17	3.52E-02	SAIBB	*FUT1*
0.025 / Ctrl	Non-common	evm.TU.scaffold731size258772.7	-1.06	2.45E-02	MOUSE	*F10C1*
0.025 / Ctrl	Non-common	evm.TU.scaffold8669size39025.1	-1.22	4.93E-02	HUMAN	*TAF4*
0.025 / Ctrl	Non-common	evm.TU.scaffold68size278367.11	-1.34	9.72E-03	RAT	*ANM3*
0.025 / Ctrl	Non-common	evm.TU.scaffold11975size49011.2	-1.35	3.28E-02	MOUSE	*TMPS2*
0.025 / Ctrl	Non-common	evm.TU.scaffold2857size108847.1	-1.83	3.41E-02	MOUSE	*SIK2*
0.025 / Ctrl	Common	evm.TU.scaffold5172size117595.4	-1.98	4.90E-02	ORYSJ	*KNOS3*

Table S5 (*continued*)

0.025 / Ctrl	Non-common	evm.TU.scaffold10size363274.2	-2.18	4.55E-02	HUMAN	*FUT7*
0.025 / Ctrl	Common	evm.TU.scaffold957size414861.12	-2.21	2.64E-02	NA	NA
0.025 / Ctrl	Common	evm.TU.scaffold3726size140820.4	-2.26	9.49E-03	DIPOM	*RB11B*
0.025 / Ctrl	Common	evm.TU.scaffold5948size109308.4	-2.33	1.45E-03	NA	NA
0.025 / Ctrl	Non-common	evm.TU.scaffold17170size9325.1	-2.36	2.05E-02	NA	NA
0.025 / Ctrl	Non-common	evm.TU.scaffold787size141661.9	-2.58	4.84E-02	CAEEL	*NPR15*
0.025 / Ctrl	Non-common	evm.TU.scaffold3680size154855.9	-2.65	1.12E-02	NA	NA
0.025 / Ctrl	Non-common	evm.TU.scaffold8681size70456.2	-2.83	2.79E-02	DANRE	*WSCD2*
0.025 / Ctrl	Non-common	evm.TU.scaffold11219size78477.3	-3.06	1.17E-02	HUMAN	*BIRC2*
0.025 / Ctrl	Non-common	evm.TU.scaffold3164size130232.2	-3.13	2.48E-02	NA	NA
0.025 / Ctrl	Non-common	evm.TU.scaffold107size612490.55	-3.32	1.12E-02	NA	NA
0.025 / Ctrl	Non-common	evm.TU.scaffold9246size95691.2	-3.44	1.88E-02	HUMAN	*MET27*
0.025 / Ctrl	Non-common	evm.TU.scaffold3500size108302.4	-3.48	3.28E-02	NA	NA
0.025 / Ctrl	Non-common	evm.TU.scaffold1926size250250.4	-3.81	4.63E-04	XENLA	*BIR7A*
0.025 / Ctrl	Non-common	evm.TU.scaffold720size228729.1	-4.17	3.14E-02	NA	NA
0.025 / Ctrl	Non-common	evm.TU.scaffold8216size41291.3	-4.19	1.83E-02	NA	NA
0.025 / Ctrl	Common	evm.TU.scaffold2723size101665.4	-4.38	1.84E-04	HUMAN	*CO6A5*
0.025 / Ctrl	Non-common	evm.TU.scaffold5577size58180.7	-5.08	1.87E-02	NA	NA
0.025 / Ctrl	Non-common	evm.TU.scaffold5176size75793.4	-5.44	6.64E-03	HUMAN	*ZN862*
1 / Ctrl	Non-common	evm.TU.scaffold10457size30855.2	6.69	3.37E-06	STRPU	*FBP3*
1 / Ctrl	Common	evm.TU.scaffold11837size49671.2	6.48	4.80E-02	MOUSE	*RSP14*
1 / Ctrl	Common	evm.TU.scaffold221size240150.25	6.48	2.39E-02	NA	NA
1 / Ctrl	Non-common	evm.TU.scaffold5577size58180.8	6.36	2.52E-02	NA	NA
1 / Ctrl	Common	evm.TU.scaffold2404size94544.2	6.27	3.17E-03	DROME	*Y3556*
1 / Ctrl	Non-common	evm.TU.scaffold4341size142224.5	5.58	4.06E-03	NA	NA
1 / Ctrl	Common	evm.TU.scaffold463size180809.4	4.98	9.08E-03	HUMAN	*IF*
1 / Ctrl	Common	evm.TU.scaffold5577size58180.9	4.98	9.38E-03	NA	NA
1 / Ctrl	Common	evm.TU.scaffold8940size68868.3	4.88	4.08E-02	XENTR	*CF157*
1 / Ctrl	Common	evm.TU.scaffold146size219328.4	4.85	3.22E-02	DROME	*DCHS*
1 / Ctrl	Common	evm.TU.scaffold3517size464559.25	4.78	2.52E-02	MOUSE	*RSP14*
1 / Ctrl	Common	evm.TU.scaffold4681size152784.13	4.69	1.33E-02	DANRE	*CA194*
1 / Ctrl	Non-common	evm.TU.scaffold2628size90693.2	4.56	1.71E-02	HUMAN	*HYDIN*
1 / Ctrl	Common	evm.TU.scaffold226size262146.9	4.33	4.99E-02	MOUSE	*CJ107*
1 / Ctrl	Common	evm.TU.scaffold4459size79009.8	4.29	4.24E-02	BOVIN	*PPR32*
1 / Ctrl	Non-common	evm.TU.scaffold6774size130978.2	4.27	4.34E-02	NA	NA
1 / Ctrl	Non-common	evm.TU.scaffold2445size93778.1	4.25	3.90E-02	NA	NA
1 / Ctrl	Common	evm.TU.scaffold1897size104575.3	4.13	4.50E-02	NA	NA
1 / Ctrl	Non-common	evm.TU.scaffold9130size57754.1	3.83	2.09E-02	RAT	*CRFR1*
1 / Ctrl	Non-common	evm.TU.scaffold13701size19462.1	3.82	4.08E-02	XENLA	*LR2BP*
1 / Ctrl	Non-common	evm.TU.scaffold8613size59507.2	3.52	7.51E-03	HUMAN	*CP2C8*
1 / Ctrl	Non-common	evm.TU.scaffold8085size55599.1	3.50	4.08E-02	HUMAN	*BMX*
1 / Ctrl	Non-common	evm.TU.scaffold8043size64624.2	3.46	7.51E-03	NA	NA
1 / Ctrl	Common	evm.TU.scaffold4142size191490.2	3.37	4.04E-04	DROVI	*TIM*

Table S5 (*continued*)

1 / Ctrl	Common	evm.TU.scaffold779size161378.9	3.30	7.63E-03	MOUSE	*ASGR1*
1 / Ctrl	Non-common	evm.TU.scaffold2404size94544.3	3.17	9.38E-03	MOUSE	*IF*
1 / Ctrl	Non-common	evm.TU.scaffold3865size74240.7	2.88	2.85E-02	NA	NA
1 / Ctrl	Non-common	evm.TU.scaffold1977size112688.7	2.86	4.76E-02	HUMAN	*CP2C8*
1 / Ctrl	Common	evm.TU.scaffold156size437243.7	2.76	1.92E-08	DROME	*RIM2*
1 / Ctrl	Common	evm.TU.scaffold4142size191490.1	2.74	5.96E-04	NA	NA
1 / Ctrl	Non-common	evm.TU.scaffold3232size114449.5	2.70	3.35E-02	NA	NA
1 / Ctrl	Non-common	evm.TU.scaffold4865size132635.8	2.68	1.09E-02	NA	NA
1 / Ctrl	Non-common	evm.TU.scaffold566size390051.15	2.67	3.06E-05	DROME	*HR4*
1 / Ctrl	Common	evm.TU.scaffold11383size52394.5	2.48	2.81E-02	RAT	*EXOC5*
1 / Ctrl	Non-common	evm.TU.scaffold38size466805.16	2.45	2.52E-02	HUMAN	*FBX41*
1 / Ctrl	Non-common	evm.TU.scaffold1113size334742.4	2.39	4.08E-02	MOUSE	*ALK*
1 / Ctrl	Non-common	evm.TU.scaffold6370size96622.1	2.14	4.24E-02	DICDI	*DRKC*
1 / Ctrl	Non-common	evm.TU.scaffold5716size144689.4	2.11	2.80E-02	MOUSE	*KCNJ1*
1 / Ctrl	Non-common	evm.TU.scaffold6202size53514.4	1.96	3.73E-02	HUMAN	*NCKX4*
1 / Ctrl	Non-common	evm.TU.scaffold3957size93592.6	1.94	1.71E-02	HUMAN	*KNTC1*
1 / Ctrl	Non-common	evm.TU.scaffold8417size54106.2	1.65	4.08E-02	PONAB	*KCNK1*
1 / Ctrl	Non-common	evm.TU.scaffold2697size303698.3	1.63	7.80E-03	NA	NA
1 / Ctrl	Non-common	evm.TU.scaffold11491size26846.2	1.50	4.08E-02	NA	NA
1 / Ctrl	Non-common	evm.TU.scaffold331size210939.7	1.47	4.44E-02	NA	NA
1 / Ctrl	Non-common	evm.TU.scaffold9157size73761.1	1.36	4.23E-02	BOMMO	*AGO3*
1 / Ctrl	Non-common	evm.TU.scaffold331size210939.6	1.30	4.02E-02	NA	NA
1 / Ctrl	Non-common	evm.TU.scaffold2452size260681.5	1.05	2.26E-02	NA	NA
1 / Ctrl	Non-common	evm.TU.scaffold8874size38082.3	-1.00	2.20E-02	MOUSE	*TRXR2*
1 / Ctrl	Non-common	evm.TU.scaffold6654size66187.1	-1.11	3.90E-02	SYLBO	*CRY1*
1 / Ctrl	Non-common	evm.TU.scaffold154size320920.13	-1.22	3.67E-02	DROME	*POL3*
1 / Ctrl	Non-common	evm.TU.scaffold9826size33606.1	-1.33	2.26E-02	CAEEL	*UNC9*
1 / Ctrl	Non-common	evm.TU.scaffold2120size147150.7	-1.43	1.33E-02	NA	NA
1 / Ctrl	Non-common	evm.TU.scaffold102size233204.2	-1.45	1.33E-02	NA	NA
1 / Ctrl	Non-common	evm.TU.scaffold2726size89241.1	-1.90	8.05E-04	NA	NA
1 / Ctrl	Common	evm.TU.scaffold5172size117595.4	-2.05	3.90E-02	ORYSJ	*KNOS3*
1 / Ctrl	Non-common	evm.TU.scaffold9183size36649.2	-2.31	2.34E-02	NA	NA
1 / Ctrl	Common	evm.TU.scaffold957size414861.12	-2.40	1.07E-02	NA	NA
1 / Ctrl	Common	evm.TU.scaffold5948size109308.4	-2.44	1.27E-04	NA	NA
1 / Ctrl	Non-common	evm.TU.scaffold2938size139678.12	-2.55	4.06E-03	MIMIV	*YR811*
1 / Ctrl	Non-common	evm.TU.scaffold8767size92048.1	-2.69	3.40E-02	RAT	*PRAX*
1 / Ctrl	Non-common	evm.TU.scaffold6397size112829.3	-2.91	2.09E-02	NA	NA
1 / Ctrl	Common	evm.TU.scaffold3726size140820.4	-3.04	8.40E-06	DIPOM	*RB11B*
1 / Ctrl	Common	evm.TU.scaffold2723size101665.4	-3.58	2.49E-03	HUMAN	*CO6A5*
1 / Ctrl	Non-common	evm.TU.scaffold7359size46131.3	-4.52	2.89E-02	NA	NA

Table S4. Differentially expressed genes (DEGs) across MNP conditions (0.025 and 1 μg L^{-1}) compared with the control condition in pearl sac samples.

MNP condition	Sharing DEG	Sequencing gene ID	Log_2FC	P_{adj}	Uniprot *sp.*	Uniprot ID
0.025 / Ctrl	Common	evm.TU.scaffold7405size45879.10	4.74	8.66E-03	NA	NA
0.025 / Ctrl	Non-common	evm.TU.scaffold9393size35692.1	3.97	4.73E-02	NA	NA
0.025 / Ctrl	Non-common	evm.TU.scaffold4903size63670.1	3.93	6.60E-04	NA	NA
0.025 / Ctrl	Non-common	evm.TU.scaffold2435size262771.5	3.40	4.02E-03	BOVIN	*PHLD*
0.025 / Ctrl	Non-common	evm.TU.scaffold12241size24179.1	3.11	8.66E-03	NA	NA
0.025 / Ctrl	Non-common	evm.TU.scaffold547size159297.1	2.90	2.97E-02	PONAB	*CRYAB*
0.025 / Ctrl	Non-common	evm.TU.scaffold4162size71203.4	2.87	2.97E-02	NA	NA
0.025 / Ctrl	Non-common	evm.TU.scaffold3145size187703.3	2.68	2.31E-02	MOUSE	*XLRS1*
0.025 / Ctrl	Non-common	evm.TU.scaffold1275size122086.11	2.67	1.11E-04	HUMAN	*FGL2*
0.025 / Ctrl	Non-common	evm.TU.scaffold311size184142.4	2.58	2.08E-02	HUMAN	*MRC1*
0.025 / Ctrl	Non-common	evm.TU.scaffold645size150701.3	2.44	1.15E-02	RAT	*MRP1*
0.025 / Ctrl	Non-common	evm.TU.scaffold104size934493.2	2.19	2.97E-02	NA	NA
0.025 / Ctrl	Non-common	evm.TU.scaffold2052size135315.9	2.09	2.08E-02	NA	NA
0.025 / Ctrl	Non-common	evm.TU.scaffold2436size218809.4	2.05	1.16E-02	NA	NA
0.025 / Ctrl	Non-common	evm.TU.scaffold1034size318021.7	2.02	1.15E-02	NA	NA
0.025 / Ctrl	Non-common	evm.TU.scaffold2388size190213.3	1.93	3.51E-02	CELJU	*MANA*
0.025 / Ctrl	Non-common	evm.TU.scaffold2074size101205.4	1.62	4.10E-02	NA	NA
0.025 / Ctrl	Non-common	evm.TU.scaffold10097size32462.1	1.52	4.98E-02	MOUSE	*RU2A*
0.025 / Ctrl	Non-common	evm.TU.scaffold6718size110288.2	1.41	3.51E-02	CAEEL	*YT66*
0.025 / Ctrl	Non-common	evm.TU.scaffold363size555997.8	1.28	2.63E-02	XENLA	*LSM11*
0.025 / Ctrl	Non-common	evm.TU.scaffold8574size39536.1	1.26	2.63E-02	MOUSE	*SLD5*
0.025 / Ctrl	Non-common	evm.TU.scaffold4177size70991.1	1.25	4.02E-03	HUMAN	*DAPLE*
0.025 / Ctrl	Non-common	evm.TU.scaffold580size251751.7	-1.11	8.66E-03	NA	NA
0.025 / Ctrl	Common	evm.TU.scaffold7564size139168.1	-1.30	1.52E-02	DANRE	*JAG1A*
0.025 / Ctrl	Non-common	evm.TU.scaffold12667size22784.1	-1.43	4.10E-02	THEMA	*FABG*
0.025 / Ctrl	Non-common	evm.TU.scaffold9784size33764.1	-1.44	4.73E-02	HUMAN	*ANR66*
0.025 / Ctrl	Common	evm.TU.scaffold4314size145107.7	-1.45	2.63E-02	NA	NA
0.025 / Ctrl	Non-common	evm.TU.scaffold5446size199412.6	-1.58	4.21E-02	XENLA	*TM145*
0.025 / Ctrl	Non-common	evm.TU.scaffold8273size41043.2	-1.62	3.51E-02	NA	*NA*
0.025 / Ctrl	Non-common	evm.TU.scaffold8309size80043.3	-1.76	3.51E-02	DANRE	*AOF*
0.025 / Ctrl	Non-common	evm.TU.scaffold5027size97772.4	-1.78	4.73E-02	ACRMI	*MLRP2*
0.025 / Ctrl	Non-common	evm.TU.scaffold6385size101604.2	-1.82	3.58E-02	NA	NA
0.025 / Ctrl	Non-common	evm.TU.scaffold6157size72139.1	-1.83	2.93E-02	NA	NA
0.025 / Ctrl	Non-common	evm.TU.scaffold164size248782.21	-1.85	1.84E-02	MOUSE	*NID1*
0.025 / Ctrl	Non-common	evm.TU.scaffold812size140740.3	-1.87	2.97E-02	XENLA	*EGR1B*
0.025 / Ctrl	Non-common	evm.TU.scaffold1408size188276.17	-1.92	8.66E-03	MOUSE	*MARK2*
0.025 / Ctrl	Non-common	evm.TU.scaffold3260size138505.1	-2.09	3.88E-02	NA	NA
0.025 / Ctrl	Common	evm.TU.scaffold1544size237200.6	-2.11	4.10E-02	BOVIN	*AMPN*
0.025 / Ctrl	Non-common	evm.TU.scaffold12018size52989.2	-2.16	2.97E-02	NA	NA

Table S6 (*continued*)

0.025 / Ctrl	Non-common	evm.TU.scaffold2778size160406.2	-2.51	8.66E-03	NA	NA
0.025 / Ctrl	Non-common	evm.TU.scaffold13284size59462.3	-2.74	2.41E-02	XENLA	*ADA10*
0.025 / Ctrl	Non-common	evm.TU.scaffold7276size46712.1	-2.75	4.87E-02	MOUSE	*TIF1B*
0.025 / Ctrl	Non-common	evm.TU.scaffold538size272809.1	-2.83	2.63E-02	NA	NA
0.025 / Ctrl	Non-common	evm.TU.scaffold2106size257207.8	-2.90	3.88E-02	NA	NA
0.025 / Ctrl	Non-common	evm.TU.scaffold6071size54414.2	-2.94	2.97E-02	NA	NA
0.025 / Ctrl	Non-common	evm.TU.scaffold740size376897.13	-2.97	8.66E-03	MOUSE	*C1QL4*
0.025 / Ctrl	Non-common	evm.TU.scaffold3198size82302.8	-2.99	3.55E-02	MOUSE	*MFAP4*
0.025 / Ctrl	Common	evm.TU.scaffold1323size145704.4	-3.03	2.97E-03	NA	NA
0.025 / Ctrl	Non-common	evm.TU.scaffold14903size16010.2	-3.12	1.22E-02	MOUSE	*C1QL3*
0.025 / Ctrl	Non-common	evm.TU.scaffold1107size194094.9	-3.19	4.98E-02	MOUSE	*ST1C2*
0.025 / Ctrl	Non-common	evm.TU.scaffold16800size10565.1	-3.24	3.28E-02	XENLA	*S15A4*
0.025 / Ctrl	Non-common	evm.TU.scaffold11359size27355.1	-3.35	9.68E-03	NA	NA
0.025 / Ctrl	Non-common	evm.TU.scaffold7354size99212.1	-3.37	4.02E-03	HUMAN	*NOS1*
0.025 / Ctrl	Common	evm.TU.scaffold3440size326921.10	-3.42	4.73E-02	NA	NA
0.025 / Ctrl	Non-common	evm.TU.scaffold831size317030.14	-3.46	8.66E-03	NA	NA
0.025 / Ctrl	Non-common	evm.TU.scaffold2454size124454.1	-3.50	2.93E-02	PINMG	*KCP2*
0.025 / Ctrl	Non-common	evm.TU.scaffold2454size124454.3	-3.54	4.67E-03	PINMG	*KCP2*
0.025 / Ctrl	Non-common	evm.TU.scaffold113size299110.2	-3.56	4.05E-03	HUMAN	*QRIC2*
0.025 / Ctrl	Non-common	evm.TU.scaffold2095size529737.6	-3.57	8.66E-03	RHILO	*BETA*
0.025 / Ctrl	Non-common	evm.TU.scaffold7792size68911.4	-3.66	3.11E-06	MOUSE	*NCAM2*
0.025 / Ctrl	Non-common	evm.TU.scaffold11357size27364.3	-3.69	9.15E-03	NA	NA
0.025 / Ctrl	Non-common	evm.TU.scaffold9616size78232.4	-3.78	1.15E-02	NA	NA
0.025 / Ctrl	Non-common	evm.TU.scaffold1224size307968.2	-3.80	8.66E-03	NA	NA
0.025 / Ctrl	Non-common	evm.TU.scaffold3739size110585.1	-3.80	4.73E-02	NA	NA
0.025 / Ctrl	Non-common	evm.TU.scaffold7423size132347.6	-3.89	8.66E-03	MOUSE	*ANR17*
0.025 / Ctrl	Non-common	evm.TU.scaffold634size277710.2	-3.89	4.73E-02	MOUSE	*NQO2*
0.025 / Ctrl	Non-common	evm.TU.scaffold12851size36164.1	-3.91	1.84E-02	NA	NA
0.025 / Ctrl	Non-common	evm.TU.scaffold14337size55465.1	-3.97	8.66E-03	DROME	*CAD99*
0.025 / Ctrl	Common	evm.TU.scaffold6274size151240.1	-4.05	6.46E-04	PINMG	*PMN14*
0.025 / Ctrl	Non-common	evm.TU.scaffold8832size38300.1	-4.19	2.63E-02	NA	NA
0.025 / Ctrl	Non-common	evm.TU.scaffold5124size61716.4	-4.26	2.87E-02	MOUSE	*MOT9*
0.025 / Ctrl	Non-common	evm.TU.scaffold1748size108773.7	-4.32	2.97E-02	PINMA	*SLP2*
0.025 / Ctrl	Non-common	evm.TU.scaffold26size344546.7	-4.38	2.90E-02	STRPU	*SPAN*
0.025 / Ctrl	Non-common	evm.TU.scaffold1263size221832.6	-4.43	2.08E-02	STRPU	*SPAN*
0.025 / Ctrl	Non-common	evm.TU.scaffold2454size124454.2	-4.56	2.63E-02	PINMG	*KCP2*
0.025 / Ctrl	Non-common	evm.TU.scaffold15685size13759.1	-4.57	4.67E-03	PINMG	*NCP*
0.025 / Ctrl	Non-common	evm.TU.scaffold2099size100549.2	-4.70	3.73E-02	NA	NA
0.025 / Ctrl	Non-common	evm.TU.scaffold10285size61330.4	-4.71	4.02E-03	PINMA	*SLP3*
0.025 / Ctrl	Non-common	evm.TU.scaffold1748size108773.5	-5.61	3.51E-02	PINMA	*SLP3*
0.025 / Ctrl	Non-common	evm.TU.scaffold4288size69999.1	-5.98	2.66E-02	PINMA	*KCP1*
1 / Ctrl	Non-common	evm.TU.scaffold7304size63610.2	4.24	1.03E-02	ANOAL	*HSP71*
1 / Ctrl	Common	evm.TU.scaffold7405size45879.10	4.22	3.55E-02	NA	NA

Table S6 (*continued*)

1 / Ctrl	Non-common	evm.TU.scaffold15236size35086.2	4.08	1.36E-04	HUMAN	*CP2J2*
1 / Ctrl	Non-common	evm.TU.scaffold423size170276.3	4.07	8.75E-03	ANOAL	*HSP74*
1 / Ctrl	Non-common	evm.TU.scaffold7405size45879.11	4.06	1.41E-02	NA	NA
1 / Ctrl	Non-common	evm.TU.scaffold4914size63546.4	3.56	3.08E-02	MOUSE	*XIAP*
1 / Ctrl	Non-common	evm.TU.scaffold4424size135461.1	3.47	8.17E-05	NA	NA
1 / Ctrl	Non-common	evm.TU.scaffold10008size45161.1	3.28	4.59E-02	MOUSE	*XIAP*
1 / Ctrl	Non-common	evm.TU.scaffold8613size59507.1	3.21	2.02E-04	HUMAN	*CP2C8*
1 / Ctrl	Non-common	evm.TU.scaffold2995size85125.1	3.08	3.08E-02	NA	NA
1 / Ctrl	Non-common	evm.TU.scaffold4500size109838.9	2.87	1.03E-02	NA	NA
1 / Ctrl	Non-common	evm.TU.scaffold4507size80223.1	2.87	6.18E-04	HUMAN	*ST1B1*
1 / Ctrl	Non-common	evm.TU.scaffold4142size191490.2	2.65	1.24E-04	DROVI	*TIM*
1 / Ctrl	Non-common	evm.TU.scaffold156size437243.7	2.55	1.66E-10	DROME	*RIM2*
1 / Ctrl	Non-common	evm.TU.scaffold5544size66712.3	2.47	3.66E-02	SCYTO	*TIMP3*
1 / Ctrl	Non-common	evm.TU.scaffold4917size106096.5	2.46	4.71E-02	NA	NA
1 / Ctrl	Non-common	evm.TU.scaffold1402size289848.5	2.40	4.04E-02	CUPNH	*BDHA*
1 / Ctrl	Non-common	evm.TU.scaffold6207size71120.2	2.36	1.19E-02	NA	NA
1 / Ctrl	Non-common	evm.TU.scaffold4142size191490.1	2.25	2.41E-05	NA	NA
1 / Ctrl	Non-common	evm.TU.scaffold4679size173293.8	2.06	1.11E-02	CHICK	*CP2H2*
1 / Ctrl	Non-common	evm.TU.scaffold3385size80003.5	2.03	3.66E-02	NA	NA
1 / Ctrl	Non-common	evm.TU.scaffold2967size360768.11	1.88	9.79E-03	NA	NA
1 / Ctrl	Non-common	evm.TU.scaffold1232size123727.3	1.87	7.84E-04	NA	NA
1 / Ctrl	Non-common	evm.TU.scaffold2192size98314.3	1.86	4.59E-02	ARATH	*GAMT2*
1 / Ctrl	Non-common	evm.TU.scaffold463size180809.9	1.85	8.75E-03	NA	NA
1 / Ctrl	Non-common	evm.TU.scaffold334size341206.3	1.83	4.24E-02	XENLA	*UBIQP*
1 / Ctrl	Non-common	evm.TU.scaffold3340size152636.6	1.78	1.19E-02	HUMAN	*BAG4*
1 / Ctrl	Non-common	evm.TU.scaffold9271size36218.1	1.77	2.92E-02	MOUSE	*V1BR*
1 / Ctrl	Non-common	evm.TU.scaffold91size419679.12	1.75	3.08E-02	NA	NA
1 / Ctrl	Non-common	evm.TU.scaffold2263size96786.2	1.74	3.55E-02	NA	NA
1 / Ctrl	Non-common	evm.TU.scaffold3230size151995.1	1.73	2.92E-02	NA	NA
1 / Ctrl	Non-common	evm.TU.scaffold7032size48018.1	1.55	4.22E-03	STRPU	*BMPH*
1 / Ctrl	Non-common	evm.TU.scaffold923size253024.9	1.52	9.79E-03	MOUSE	*GLNA*
1 / Ctrl	Non-common	evm.TU.scaffold14782size16399.1	1.39	3.08E-02	MIMIV	*COLL7*
1 / Ctrl	Non-common	evm.TU.scaffold2796size88200.2	1.37	3.08E-02	RAT	*SQSTM*
1 / Ctrl	Non-common	evm.TU.scaffold9443size112071.3	1.36	4.59E-02	MOUSE	*GLNA*
1 / Ctrl	Non-common	evm.TU.scaffold566size390051.15	1.33	2.74E-04	DROME	*HR4*
1 / Ctrl	Non-common	evm.TU.scaffold7880size108515.1	1.31	3.53E-02	NA	NA
1 / Ctrl	Non-common	evm.TU.scaffold1962size430023.13	1.26	3.85E-02	XENLA	*TLL1*
1 / Ctrl	Non-common	evm.TU.scaffold6705size50169.3	1.22	7.84E-04	NA	NA
1 / Ctrl	Non-common	evm.TU.scaffold303size331505.6	1.16	4.24E-02	HUMAN	*MMP16*
1 / Ctrl	Non-common	evm.TU.scaffold10028size32743.1	1.08	2.29E-02	NA	NA
1 / Ctrl	Non-common	evm.TU.scaffold7554size95047.2	1.04	2.11E-02	MOUSE	*ATRX*
1 / Ctrl	Non-common	evm.TU.scaffold936size300356.3	1.02	3.53E-02	DANRE	*SBK1*
1 / Ctrl	Non-common	evm.TU.scaffold14668size16684.2	-1.08	4.59E-02	NA	NA

Table S6 (*continued*)

1 / Ctrl	Non-common	evm.TU.scaffold2120size147150.8	-1.21	1.19E-02	NA	NA
1 / Ctrl	Common	evm.TU.scaffold7564size139168.1	-1.25	3.08E-02	DANRE	*JAG1A*
1 / Ctrl	Non-common	evm.TU.scaffold2120size147150.9	-1.39	7.50E-03	DROYA	*PER*
1 / Ctrl	Non-common	evm.TU.scaffold2120size147150.7	-1.39	2.86E-04	NA	NA
1 / Ctrl	Common	evm.TU.scaffold4314size145107.7	-1.40	4.71E-02	NA	NA
1 / Ctrl	Non-common	evm.TU.scaffold7224size46994.4	-1.61	6.69E-05	HUMAN	*HEBP2*
1 / Ctrl	Non-common	evm.TU.scaffold8809size38378.3	-1.65	4.71E-02	APIME	*TREA*
1 / Ctrl	Non-common	evm.TU.scaffold10833size58035.4	-1.65	3.08E-02	CHICK	*ST1B1*
1 / Ctrl	Non-common	evm.TU.scaffold2627size90695.4	-1.93	1.19E-02	CHICK	*CAN3*
1 / Ctrl	Non-common	evm.TU.scaffold2328size202496.4	-1.94	3.47E-02	NA	NA
1 / Ctrl	Non-common	evm.TU.scaffold5381size147161.1	-2.10	3.08E-02	NA	NA
1 / Ctrl	Non-common	evm.TU.scaffold3392size79886.2	-2.34	8.75E-03	NA	NA
1 / Ctrl	Non-common	evm.TU.scaffold264size320753.24	-2.42	1.01E-02	NA	NA
1 / Ctrl	Common	evm.TU.scaffold1544size237200.6	-2.49	9.60E-03	BOVIN	*AMPN*
1 / Ctrl	Non-common	evm.TU.scaffold5957size328954.4	-2.55	3.02E-02	NA	NA
1 / Ctrl	Common	evm.TU.scaffold1323size145704.4	-2.72	1.00E-02	NA	NA
1 / Ctrl	Common	evm.TU.scaffold6274size151240.1	-3.04	3.62E-02	PINMG	*PMN14*
1 / Ctrl	Non-common	evm.TU.scaffold13924size18829.1	-3.18	1.07E-02	HUMAN	*CD109*
1 / Ctrl	Non-common	evm.TU.scaffold6363size103460.4	-3.18	4.53E-02	NA	NA
1 / Ctrl	Non-common	evm.TU.scaffold16332size27114.1	-3.30	4.40E-03	CAEEL	*BAT38*
1 / Ctrl	Non-common	evm.TU.scaffold891size137303.3	-3.36	3.83E-03	PIG	*PNMT*
1 / Ctrl	Common	evm.TU.scaffold3440size326921.10	-4.00	1.11E-02	NA	NA
1 / Ctrl	Non-common	evm.TU.scaffold7216size47029.4	-4.25	5.45E-03	NA	NA
1 / Ctrl	Non-common	evm.TU.scaffold8499size142240.4	-4.34	3.46E-03	NA	NA
1 / Ctrl	Non-common	evm.TU.scaffold2109size100372.3	-5.03	6.19E-03	MOUSE	*SRPX2*
1 / Ctrl	Non-common	evm.TU.scaffold14848size34703.1	-6.70	3.76E-02	NA	NA
1 / Ctrl	Non-common	evm.TU.scaffold12174size24356.2	-7.29	2.65E-03	NA	NA
1 / Ctrl	Non-common	evm.TU.scaffold12174size24356.1	-8.74	1.93E-02	HUMAN	*FBLN7*

References

(1) Linard, C.; Gueguen, Y.; Moriceau, J.; Soyez, C.; Hui, B.; Raoux, A.; Cuif, J. P.; Cochard, J.-C.; Le Pennec, M.; Le Moullac, G. Calcein Staining of Calcified Structures in Pearl Oyster *Pinctada Margaritifera* and the Effect of Food Resource Level on Shell Growth. *Aquaculture* **2011**, *313* (1), 149–155. https://doi.org/10.1016/j.aquaculture.2011.01.008.

(2) Le Moullac, G. L.; Schuck, L.; Chabrier, S.; Belliard, C.; Lyonnard, P.; Broustal, F.; Soyez, C.; Saulnier, D.; Brahmi, C.; Ky, C.-L.; Beliaeff, B. Influence of Temperature and Pearl Rotation on Biomineralization in the Pearl Oyster, *Pinctada Margaritifera*. *J. Exp. Biol.* **2018**, *221* (18). https://doi.org/10.1242/jeb.186858.

(3) Chávez-Villalba, J.; Soyez, C.; Aurentz, H.; Le Moullac, G. Physiological Responses of Female and Male Black-Lip Pearl Oysters *(Pinctada Margaritifera)* to Different Temperatures and Concentrations of Food. *Aquat. Living Resour.* **2013**, *26* (3), 263–271. https://doi.org/10.1051/alr/2013059.

(4) Savina, M.; Pouvreau, S. A Comparative Ecophysiological Study of Two Infaunal Filter-Feeding Bivalves: *Paphia Rhomboïdes* and *Glycymeris Glycymeris*. *Aquaculture* **2004**, *239* (1–4), 289–306. https://doi.org/10.1016/j.aquaculture.2004.05.029.

(5) Bayne, B. L.; Hawkins, A. J. S.; Navarro, E. Feeding and Digestion by the Mussel *Mytilus Edulis* L. (Bivalvia: Mollusca) in Mixtures of Silt and Algal Cells at Low Concentrations. *J. Exp. Mar. Biol. Ecol.* **1987**, *111* (1), 1–22. https://doi.org/10.1016/0022-0981(87)90017-7.

(6) Hermabessiere, L.; Himber, C.; Boricaud, B.; Kazour, M.; Amara, R.; Cassone, A.-L.; Laurentie, M.; Paul-Pont, I.; Soudant, P.; Dehaut, A.; Duflos, G. Optimization, Performance, and Application of a Pyrolysis-GC/MS Method for the Identification of Microplastics. *Anal. Bioanal. Chem.* **2018**, *410* (25), 6663–6676. https://doi.org/10.1007/s00216-018-1279-0.

(7) Djouina, M.; Vignal, C.; Dehaut, A.; Caboche, S.; Hirt, N.; Waxin, C.; Himber, C.; Beury, D.; Hot, D.; Dubuquoy, L.; Launay, D.; Duflos, G.; Body-Malapel, M. Oral Exposure to Polyethylene Microplastics Alters Gut Morphology, Immune Response, and Microbiota Composition in Mice. *Environ. Res.* **2022**, *212*, 113230. https://doi.org/10.1016/j.envres.2022.113230.